DANIEL **ŠEVČOVIČ**

DIRECT LAGRANGIAN METHODS FOR SOLVING CURVATURE DRIVEN FLOWS AND THEIR APPLICATIONS

IRIS

Direct Lagrangian Methods for Solving Curvature Driven Flows and their Applications

Daniel Ševčovič

2016

Published by
IRIS – Vydavateľstvo a tlač, s.r.o., Bratislava, Slovakia, 2016

Reviewers:
Prof. Katarína Cechlárová, P. J. Šafárik University, Košice,
Prof. Vít Dolejší, Charles University, Prague,
Prof. Pavel Drábek, University of West Bohemia, Pilsen
Prof. Otmar Scherzer, University of Vienna

web page: www.iam.fmph.uniba.sk/institute/sevcovic
email: sevcovic@fmph.uniba.sk

ISBN 978-80-89726-75-2

Contents

Foreword

The main goal of this survey paper is to investigate qualitative and numerical issues related to the evolution of plane curves and surfaces evolving in the normal direction by the velocity which may depend on the main curvature, position and the orientation of the normal vector. In the case of evolution of planar curves we assume that the normal velocity is a function of the curvature, tangential angle and the position vector of an evolving curve in the plane. As for the evolution of two dimensional manifolds we assume that they are evolving in the normal direction by the mean curvature and given external force.

We follow the direct Lagrangian approach and we analyze the so-called intrinsic heat equation governing the motion of plane curves obeying such a geometric equation. We show how to reduce the geometric problem to a solution of fully nonlinear parabolic equation for important geometric quantities. Using the theory of fully nonlinear parabolic equations we present results on local time existence of classical solutions. We investigate the stability of stationary curves and network of curves. We discuss numerical approximation schemes for computing curvature driven flows and we present various examples of applications of theoretical results in practical problems.

The paper is organized as follows. In the introductory Chapter 1 we briefly recall typical applications of curvature driven flows. We review various applications in interface dynamics, edge detection problems arising in image segmentation, geodesic flows, dislocation dynamics, spiral motions of open curves as well as flows driven by non-locally dependent normal velocities arising in conserved and gradient geometric flows. In Chapter 2 we present the basic ideas of the direct Lagrangian approach of description of curvature driven evolution of

curves and surfaces. We recall the system of governing equations for the relevant geometric quantities like the curvature and position vector. We show how a nontrivial tangential velocity can be incorporated in the governing equations. We also mention and discuss other methods for computing curvature driven flows like, e.g. level set methods. The next Chapter 3 is devoted to theoretical results on existence, uniqueness and continuation of the classical solution of the parabolic system of governing equations. The methodology is based on the theory of fully nonlinear parabolic equations. In Chapter 4 we focus on the numerical aspects of the direct Lagrangian approach. We discuss the role of a nontrivial tangential velocity for the construction of efficient numerical scheme. Special attention is put on analysis of the so-called curvature adjusted tangential velocity. Chapter 5 is devoted to various applications of the direct Lagrangian approach. Several computational examples are presented in order to illustrate the enhancement of numerical results of the direct approach combined with a suitably chosen tangential velocity. Furthermore, we show how the geodesic curvature driven flow of curves on a given surface can be solved by the direct approach. We also present applications of the direct approach in edge detection problems in segmentation of images. The direct approach has been also applied to stability analysis of a flow of network open curves forming a triple junction. Furthermore, we show how the idea tangential redistribution can be generalized to mean curvature driven flows of surfaces. In the last part of the chapter we focus our attention to applications of conserved and gradient geometric flows. In more detail, we investigate and analyze the area and length preserving flows as well as gradient flows minimizing the isoperimetric ratio in the Euclidean and relative Finsler geometry. We end this chapter by analysis of the inverse Wulff problem enabling us to construct an underlying anisotropy by minimizing the anisoperimetric ratio for a given planar curve or interface. The last Chapter 6 consists of nine selected papers by the author.

Finally, I want to express my sincere gratitude and highest respect to all co-authors and collaborators. Many of them contributed to my research in the field of analysis of geometric equations. I thank Karol Mikula who always had very positive influence during all my research carrier and life. It was a great pleasure for me to work with him and follow his enthusiasm for applied mathematics and everything in life. I appreciate very much collaboration with Harald Garcke and Yoshihito Kohsaka from whom I learned a lot on how the mathemat-

ical preciseness is really important in analyzing applied problems. I very much appreciate joint work with Michal Beneš who revealed me many important applications of direct approach in the field of material science. I thank Shigetoshi Yazaki for his long-term fruitful and friendly collaboration, broadening my scope of knowledge in related fields of research and suggestions leading to improvements in this paper. Special thanks go to Mariana Remešíková who made it possible to push forward our tangential redistribution ideas to higher space dimensions enabling us to deal with the motion of surfaces. Last, but not the least, I am thankful Mária Trnovská who motivated my recent interests to the field of nonlinear optimization and its applications, and who gave me new inspiration for future research.

Daniel Ševčovič,
January 2016

Chapter 1

Introduction

In this section, we are concerned with the time evolution of curves and surfaces driven in the normal direction by a function of the mean curvature. As for the evolution of one dimensional curves we will assume the normal velocity to be a function of the curvature k, the tangent angle ν and the position vector x of the plane curve Γ, i.e.

$$v = \beta(k, x, \nu), \tag{1.1}$$

where v is the normal velocity at the point $x \in \Gamma^t$ of an evolving family $\{\Gamma^t, t \geq 0\}$ of planar closed or open curves. As for the evolution of two dimensional surfaces with or without boundary we investigate the flows of surfaces $\{\mathcal{M}^t, t \geq 0\}$ in the Euclidean space $\mathbb{R}^3$ driven in the normal direction with the speed v

$$v = H + F, \tag{1.2}$$

where H is the mean curvature and F is a given external force.

Geometric equations of the form (1.1) and (1.2) can be often found in variety of applied problems like, e.g. material science, dynamics of phase boundaries in thermo-mechanics, in modeling of flame front propagation, in combustion, in computations of first arrival times of seismic waves, in computational geometry, robotics, semiconductors industry, etc. They also have a special conceptual importance in image processing and computer vision theories.

One of the pioneer works in the field of curvature driven flows is due to Mullins [95]. He studied the two-dimensional motion of idealized grain boundaries. Geometrical or Lagrangian approach to

crystal growth can be found in subsequent works by Mullins, Sekerka, J.Taylor, Brower, Kessler, Koplik, Levine and many others.

In Nature, there are no substances of curves, surfaces or boundaries which are mathematical functions or sets. In this sense, the motion of curves and surfaces is an idealized object. On the other hand, it accurately approximates physical phenomena.

A typical case in which the normal velocity v may depend on the position vector x can be found in image segmentation [26, 64] or dislocation dynamics [70]. For a comprehensive overview of other important applications of the geometric equation (1.1) we refer to books by Sethian, Sapiro and Osher and Fedkiw [116, 107, 98] or to the review paper [113] by Ševčovič.

The aim of this section is to present various application of the mean curvature flows of curves and interfaces with special focus on the direct Lagrangian approach. Direct Lagrangian methods have been developed and studied by many authors especially in the last thirty years, as well as indirect approaches such as level set methods and phase-field approaches.

1.1 Mathematical models leading to curvature driven flows of planar curves

1.1.1 Interface dynamics

If a solid phase occupies a subset $\Omega_s^t \subset \Omega$ and a liquid phase - a subset $\Omega_l^t \subset \Omega$, $\Omega \subset \mathbb{R}^2$, at a time t, then the phase interface is the set $\Gamma^t = \partial\Omega_s^t \cap \partial\Omega_l^t$, which is assumed to be a closed smooth embedded curve. The sharp-interface description of the solidification process is then described by the Stefan problem with a surface tension

$$\begin{aligned} \rho c \partial_t U &= \lambda \Delta U \qquad \text{in } \Omega_s^t \text{ and } \Omega_l^t, \\ [\lambda \partial_n U]_s^l &= -Lv \qquad \text{on } \Gamma^t, \qquad (1.3) \\ \frac{\delta e}{\sigma}(U - U^*) &= -\delta_2(\nu)k + \delta_1(\nu)v \text{ on } \Gamma^t, \qquad (1.4) \end{aligned}$$

subject to initial and boundary conditions for the temperature field U and initial position of the interface Γ (see, e.g. [12]). The constants ρ, c, λ represent material characteristics (density, specific heat and thermal conductivity), L is the latent heat per unit volume, U^* is

a melting point and v is the normal velocity of an interface. Discontinuity in the heat flux on the interface Γ^t is described by the Stefan condition (1.3). The relationship (1.4) is referred to as the Gibbs – Thomson law on the interface Γ^t, where δe is the difference in entropy per unit volume between liquid and solid phases, σ is a constant surface tension, δ_1 is a coefficient of attachment kinetics and the dimensionless function δ_2 describes anisotropy of the interface. One can see that the Gibbs–Thomson condition can be viewed as a geometric equation having the form (1.1). In this application the normal velocity $v = \beta(k, \nu, x)$ has a special form

$$\beta = \beta(k, \nu) = \delta(\nu)k + F.$$

In the theory of phase interfaces separating solid and liquid phases, the geometric equation (1.1) with $\beta(k, \nu, x) = \delta(\nu)k + F$ corresponds to the so-called Gibbs–Thomson law governing the crystal growth in an under-cooled liquid [51, 14]. Angenent and Gurtin in the series of papers [1, 2, 3] studied motion of phase interfaces. They proposed to study the equation of the form

$$\mu(\nu, v)v = h(\nu)k - g,$$

where μ is the kinetic coefficient and quantities h, g arise from constitutive description of the phase boundary. The dependence of the normal velocity v on the curvature k is related to the surface tension effects on the interface, whereas the dependence on ν (orientation of interface) introduces anisotropic effects into the model. In general, the kinetic coefficient μ may also depend on the velocity v itself giving rise to a nonlinear dependence of the function $v = \beta(k, \nu)$ on k and ν. If the motion of an interface is very slow, then $\beta(k, \nu, x)$ is linear in k (cf. [1]) and (1.1) corresponds to the classical mean curvature flow studied extensively from both the mathematical (see [40, 4, 5, 50]) and the numerical point of view (see [34, 31, 83, 96, 99]).

In the papers [1, 3], Angenent and Gurtin studied perfect conductors where the problem can be reduced to a single equation on the interface. Following their approach and assuming a constant kinetic coefficient one obtains the equation

$$v = \beta(k, \nu) \equiv \delta(\nu)k + F$$

describing the interface dynamics. It is often referred to as the *anisotropic curve shortening equation* with a constant driving force

F (energy difference between bulk phases) and a given anisotropy function δ.

The direct Lagrangian approach taking into account topological changes has been applied in the modeling of forest fire front propagation by Balažovjech *et al.* in [9].

In [43, 44, 42] Garcke *et al.* studied evolution of a network of open plane curves driven by the curvature or surface diffusion (Laplace-Beltrami operator of the curvature) (see also [76]).

1.1.2 Image segmentation

A similar equation to (1.1) arises from the theory of image segmentation in which detection of object boundaries in the analyzed image plays an important role. A given black and white image can be represented by its intensity function $I : \mathbb{R}^2 \to [0, 255]$. The aim is to detect edges of the image, i.e. closed planar curves on which the gradient ∇I is large (see [62]). The idea behind the so-called *active contour models* is to construct an evolving family of plane curves converging to an edge (see [63]). One can construct a family of curves evolved by the normal velocity $v = \beta(k, \nu, x)$ of the form

$$\beta(k, \nu, x) = \delta(x, \nu)k + c(x, \nu),$$

where $c(x, \nu)$ is a driving force and $\delta(x, \nu) > 0$ is a smoothing coefficient. These functions depend on the position vector x as well as orientation angle ν of a curve. Evolution starts from an initial curve, which is a suitable approximation of the edge and then it converges to the edge provided that δ, c are suitable chosen functions.

In the context of level set methods, edge detection techniques based on this idea were first discussed by Caselles *et al.* and Malladi *et al.* in [25, 75]. Later on, they have been revisited and improved in [26, 27, 64]. Recently, Mikula *et al.* applied level set techniques in image segmentation and lineage tracking of embryo-genesis (cf. [91, 126]). The direct Lagrangian approach has been also applied by Mikula and Urbán [92] to evolution of open curves in $\mathbb{R}^3$ with application in the virtual colonoscopy.

A case with special importance in image segmentation and filtering is the so-called affine scale space flow in which the normal velocity is given by

$$\beta = k^{1/3}$$

analyzed by Angenent, Shapiro and Tannenbaum in [7] and [106]. The flow is invariant with respect to affine transformations. Since ellipses are invariant with respect to affine transformations they are self-similar solutions of this flow (see also [84]).

In [118, 119] Srikrishnan, Chaudhuri, Dutta Roy and Ševčovič applied the direct approach in tracking moving boundaries in sequences of images.

1.1.3 Geodesic curvature driven flow of curves on a surface

Another interesting application of the geometric equation (1.1) arises from differential geometry. The purpose is to investigate the evolution of curves on a given surface driven by the geodesic curvature and prescribed external force. We restrict our attention to the case when the normal velocity $\mathcal{V}$ is a linear function of the geodesic curvature $\mathcal{K}_g$ and external force $\mathcal{F}$, i.e.

$$\mathcal{V} = \mathcal{K}_g + \mathcal{F}$$

and the surface $\mathcal{M}$ in $\mathbb{R}^3$ can be represented by a smooth graph. The idea how to analyze a flow of curves on a surface $\mathcal{M}$ consists in the vertical projection of surface curves into the plane. This allows for reducing the problem to the analysis of the evolution of planar curves instead of surface ones. Although the geometric equation $\mathcal{V} = \mathcal{K}_g + \mathcal{F}$ is simple the description of the normal velocity v of the family of projected planar curves is rather involved. Nevertheless, it can be written in the form of equation (1.1).

It is interesting to note that the geodesic flow can be related to edge detection problems in image segmentation.

1.1.4 Evolution of open curves and dislocation dynamics

All real crystals contain some imperfections, which locally disturb the regular arrangements of the atoms. These imperfections may have point, line, surface or volume character and they occur in nanoscale. However, their presence can significantly influence the physical and mechanical properties of crystalline solids. Dislocations are defects of the crystalline lattice. They act in such a way that the crystallographic

arrangement of atoms is disturbed along a so-called dislocation line. From the mathematical point of view, dislocations can be represented as closed curves (acting inside the crystal) or open curves (ending on a surface of the crystal), which can, under certain physical conditions, evolve in time and space and even interact with each other. At certain physical conditions, e.g., at low homologous temperature, the motion is only two-dimensional and dislocations can move only along the so-called slip planes, i.e., some crystallographic planes with the highest density of atoms. We can describe the motion by means of the mean curvature flow of the form:

$$\beta(k, \nu, x) = k + F,$$

where $F = F_{app} + F_{wall} + F_{int} - F_{fr}$ is the external force, which can be decomposed into the following acting forces: F_{app} caused by the resolved shear stress, F_{wall} caused by the stress from the walls of the channel, force F_{int} caused by the mutual interaction stress between the dislocations in the channel and the force F_{fr} caused by the crystalline lattice resistance. The reader is refereed for details to papers by Kratochvíl *et al.* [70, 13, 72, 71]. In this application the fixed end boundary condition were prescribed for evolution of open curves representing dislocation lines. Recently, Pauš *et al.* [101] constructed exact solutions for dislocation bowing and developed a new numerical technique for dislocation touching-splitting.

There are other important application of curvature driven flows of open curves. For example, in [92] Mikula and Urbán studied curvature driven evolution of open curves in $\mathbb{R}^3$ having applications in the virtual colonoscopy. In this application Mikula and Urbán derived a law for movement of end-points of a curve representing a virtual camera in a gut.

Another possible application of curvature driven evolution of open curves arises from modeling spiral motion of pattern formations observed in various nonlinear phenomena such like, e.g. Belousov-Zhabotinsky reaction, crystal growth of some materials. In [97] Osaki *et al.* proposed a simple evolution law for the motion of open curves with the boundary conditions towards realizing spiral growth. The model is based on the well-known model established by Davydov, Mikhailov and Zykov [81]. Similarly to the application in virtual colonoscopy, the tangential velocity at end-points have to be prescribed by following the model derived in [81].

Open curves evolution has been also studied in the context of optimal design of a truss of network curves on a given surfaces studied recently by Remešíková, Mikula, Sarkoci and šSevčovič in [102]. The goal was to design a network of curves minimizing the discrepancy of lengths of truss elements.

1.1.5 Nonlocal flows and variational problems

In this section we discuss the role and importance of geometric equation (1.1) with a non-local term F_Γ depending the entire curve Γ. The normal velocity is given by $\beta(x,k,\nu) \equiv \tilde\beta(x,k,\nu) + F_\Gamma$, where $\tilde\beta(x,k,\nu) : \mathbb{R}^2 \times \mathbb{R} \times \mathbb{R} \to \mathbb{R}$ is the local part of the normal velocity and $F_\Gamma = F(L,A,\mathcal{E})$ represents its non-local part depending on the global quantities like, e.g. the total length L, the enclosed area A, or the elastic energy $\mathcal{E} = \int_\Gamma k^2 ds$ computed over the entire curve Γ.

Our first example is the area-preserving flow having the normal velocity of the form:

$$v = k - \frac{2\pi}{L}. \tag{1.5}$$

For such a normal velocity one can derive that the enclosed area A of the evolved curve Γ is preserved. This geometric flow was investigated by Gage [41]. This geometric law originates in the theory of phase transitions for crystalline materials and describes the evolution of closed embedded curves with constant enclosed area. The area preserving mean curvature flow usually appears in applications where physical systems like cell structures, soap films and bubbles evolve to minimize its surface energy while preserving mass. In [103] Rubinstein and Sternberg studied the mean-curvature flow with the constraint of constant area enclosed by the evolving curve (see, e.g. [24, 38, 78] and references therein). In particular, problem (1.5) was studied by Beneš *et al.* [20] in the context of a non-local modification of the Allen-Cahn equation. The area preserving flow has been recently investigated by Sakakibara and Yazaki [104, 125] in the context of the Hele-Shaw flow.

The area preserving flow can be also viewed as a gradient flow for the following variational problem with a constraint:

$$\begin{aligned} &\min_\Gamma L(\Gamma) \\ &\text{s.t. } A(\Gamma) = const. \end{aligned}$$

Another important non-local geometric flow is the total length preserving flow. Recently, Yazaki and Ševčovič [110] investigated the gradient flow for the isoperimetric ratio in which the normal velocity has the form

$$v = k - \frac{L}{2A}. \tag{1.6}$$

Such flow minimizes the isoperimetric ratio $\Pi = L^2/(4\pi A)$ and $\Pi^t \to 1$ as $t \to \infty$. It means that it is a gradient flow for the following variational problem:

$$\min_{\Gamma} \frac{L(\Gamma)^2}{4\pi A(\Gamma)}.$$

In [114] Yazaki and Ševčovič generalized the gradient flow (1.6) to the case of minimization of the isoperimetric ratio in the relative Finsler geometry described by the Finsler metric (cf [39]). In this case, the normal velocity has the form

$$v = k_\sigma - \frac{L_\sigma}{2A}, \tag{1.7}$$

where k_σ and L_σ are the curvature and length in the corresponding Finsler geometry defined through the anisotropy function σ. Again, this is a gradient flow for the following variational problem:

$$\min_{\Gamma} \frac{L_\sigma(\Gamma)^2}{4|W_\sigma|A(\Gamma)},$$

where $|W_\sigma|$ is the area of the Wulff shape W_σ (see Chapter 5 for details).

The inverse variational problem for finding the optimal anisotropy function σ

$$\min_{\sigma} \frac{L_\sigma(\Gamma)^2}{4|W_\sigma|A(\Gamma)}$$

has been recently addressed and investigated by Trnovská and Ševčovič in [111, 112, 121].

Chapter 2

Preliminaries and description of the direct Lagrangian approach

The purpose of this chapter is to review basic facts and results concerning the curvature driven flow of planar curves. We will focus our attention on the so-called direct (or Lagrangian) description of a moving curve in which we follow the evolution of point positions of the curve. This is also referred to as a direct approach in the context of curvature driven flows of planar curves. We refer the reader to papers by Abresch and Langer [4], Angenent, Sapiro and Tannenbaum [7], [33, 34], Deckelnick [31], Mikula and Kačur [83], Mikula and Ševčovič [84, 85, 88, 87] and other papers referred therein.

First, we recall some basic facts and elements of differential geometry. Then, we derive a system of equations for important geometric quantities like, e.g. a curvature, local length and tangential angle. With help of these equations we will be able to derive equations describing evolution of the total length, enclosed area of an evolving curve and transport of a scalar function quantity.

2.1 Notations and elements of differential geometry

An embedded regular plane curve (a Jordan curve) Γ is a closed C^1 smooth one dimensional non-self-intersecting curve in the plane $\mathbb{R}^2$. It can be parametrized by a smooth function $x : S^1 \to \mathbb{R}^2$. It means that $\Gamma = \mathrm{Img}(x) := \{x(u), u \in S^1\}$ and $g = |\partial_u x| > 0$. Taking into

account the periodic boundary conditions at $u = 0, 1$ we can hereafter identify the unit circle S^1 with the interval $[0, 1]$. The unit arc-length parametrization of a curve $\Gamma = \mathrm{Img}(x)$ is denoted by s and it satisfies $|\partial_s x(s)| = 1$ for any s. Furthermore, the arc-length parametrization is related to the original parametrization u via the equality $ds = g\,du$. Notice that the interval of values of the arc-length parameter depends on the curve Γ. More precisely, $s \in [0, L(\Gamma)]$, where $L(\Gamma)$ is the length of the curve Γ. Since s is the arc-length parametrization the tangent vector $\vec{T}$ of a curve Γ is given by $\vec{T} = \partial_s x = g^{-1}\partial_u x$. We choose the orientation of the unit inward normal vector $\vec{N}$ in such a way that $\det(\vec{T}, \vec{N}) = 1$ where $\det(\vec{a}, \vec{b})$ is the determinant of the 2×2 matrix with column vectors $\vec{a}, \vec{b}$. In what follows, $a \cdot b$ denotes the standard Euclidean scalar product in $\mathbb{R}^2$ and $|a| = \sqrt{a \cdot a}$ the Euclidean norm. Notice that $1 = |\vec{T}|^2 = \vec{T} \cdot \vec{T}$. Therefore, $0 = \partial_s(\vec{T} \cdot \vec{T}) = 2(\vec{T} \cdot \partial_s \vec{T})$. Thus, the direction of the normal vector $\vec{N}$ must be proportional to $\partial_s \vec{T}$. It means that there is a real number $k \in \mathbb{R}$ such that $\vec{N} = k\partial_s \vec{T}$. Similarly, as $1 = |\vec{N}|^2 = (\vec{N} \cdot \vec{N})$ we have $0 = \partial_s(\vec{N} \cdot \vec{N}) = 2(\vec{N} \cdot \partial_s \vec{N})$ and so $\partial_s \vec{N}$ is collinear to the vector $\vec{T}$. Since $\vec{N} \cdot \vec{T} = 0$ we have $0 = \partial_s(\vec{N} \cdot \vec{T}) = \partial_s \vec{N} \cdot \vec{T} + \vec{N} \cdot \partial_s \vec{T}$. Therefore, $\partial_s \vec{N} = -k\vec{T}$. In summary, for the arc-length derivative of the unit tangent and normal vectors to a curve Γ we have

$$\partial_s \vec{T} = k\vec{N}, \qquad \partial_s \vec{N} = -k\vec{T}, \tag{2.1}$$

where the scalar quantity $k \in \mathbb{R}$ is called the curvature of the curve Γ at a point $x \in \Gamma$. In the literature, equations (2.1) are referred to as Frenét formulae. The quantity k fulfilling (2.1) is indeed a curvature in the sense that it is a reciprocal value of the radius of a circle having C^2 smooth contact with Γ point at a point $x(s)$. Since $\partial_s \vec{T} = \partial_s^2 x$ we obtain a formula for the signed curvature

$$k = \det(\partial_s x, \partial_s^2 x) = g^{-3} \det(\partial_u x, \partial_u^2 x)\,. \tag{2.2}$$

Notice that, according to our notation, the curvature k is positive on the convex side of a curve Γ whereas it is negative on its concave part (see Fig. 2.1). By ν we denote the tangent angle to Γ, i.e. $\nu = \arg(\vec{T})$ and $\vec{T} = (\cos\nu, \sin\nu)^T$. Then, by Frenét's formulae, we have

$$k(-\sin\nu, \cos\nu)^T = k\vec{N} = \partial_s \vec{T} = \partial_s \nu(-\sin\nu, \cos\nu)^T$$

and therefore $\partial_s \nu = k$. For an embedded planar curve Γ, its tangential angle ν varies from 0 to 2π and so we have $2\pi = \nu(1) - \nu(0) =$

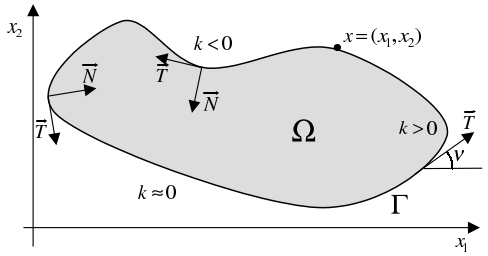

Figure 2.1: Description of a planar curve Γ enclosing a domain Ω, its signed curvature k, unit inward normal $\vec{N}$ and tangent vector $\vec{T}$, position vector x. Source: Ševčovič [113].

$\int_0^1 \partial_u \nu \, du = \int_0^1 kg \, du = \int_\Gamma k \, ds$ and hence the total curvature of an embedded curve satisfies the following equality:

$$\int_\Gamma k ds = 2\pi \, . \tag{2.3}$$

This equality can be generalized to the case when a closed non-selfintersecting smooth curve Γ belongs to an orientable two dimensional surface $\mathcal{M}$. According to the Gauss-Bonnet formula we have

$$\int_{int(\Gamma)} K dx + \int_\Gamma k \, ds = 2\pi \, \chi(\mathcal{M}),$$

where K is the Gaussian curvature of a orientable two dimensional surface $\mathcal{M}$ and $\chi(\mathcal{M})$ is the Euler characteristics of the surface $\mathcal{M}$. In the trivial case when $\mathcal{M} = \mathbb{R}^2$ we have $K \equiv 0$ and $\chi(\mathcal{M}) = 1$ and so the equality (2.3) is a consequence of the Gauss-Bonnet formula.

2.2 Methodology based on the Lagrangian direct approach

Our methodology on how to solve (1.1) is based on the so-called direct approach investigated by Dziuk, Deckelnick, Gage and Hamilton, Grayson, Mikula and Ševčovič and other authors (see, e.g. [31, 34, 35, 40, 50, 83, 82, 84, 85, 86, 87] and references therein). The main idea is to use the so-called Lagrangian description of motion and to represent the flow of planar curves by a position vector x,

which is a solution to the geometric equation

$$\partial_t x = \beta \vec{N} + \alpha \vec{T},$$

where $\vec{N}, \vec{T}$ are the unit inward normal and tangent vectors, respectively. It turns out that one can construct a closed system of parabolic-ordinary differential equations for the relevant geometric quantities: the curvature, tangential angle, local length and position vector. Other well-known techniques, like, e.g. level-set method due to Osher and Sethian [116, 98] (see also Giga [45]) or phase-field approximations (see e.g. Caginalp, Nochetto *et al.*, Beneš [23, 96, 12]) treat the geometric equation (1.1) by means of a solution of a higher dimensional parabolic problem. In the direct approach one space dimensional evolutionary problems are solved only. Notice that the direct approach for solving (1.1) can be accompanied by a proper choice of tangential velocity α significantly improving and stabilizing numerical computations as it was documented in many papers (see, e.g. [31, 56, 55, 66, 84, 85, 86, 87]).

2.3 Governing equations

We will assume that the normal velocity v of an evolving family of plane curves $\{\Gamma^t, t \geq 0\}$, is equal to a function β of the curvature k, tangential angle ν and position vector $x \in \Gamma^t$,

$$v = \beta(k, \nu, x)$$

(see (1.1)). Hereafter, we will suppose that the function $\beta(k, \nu, x)$ is a smooth function, which is increasing in the k variable, i.e.

$$\beta'_k(k, x, \nu) > 0\,.$$

The idea behind the direct approach consists of representation of a family of embedded curves Γ^t by the position vector $x \in \mathbb{R}^2$, i.e.

$$\Gamma^t = \mathrm{Img}(x(\cdot, t)) = \{x(u, t),\ u \in [0, 1]\},$$

where x is a solution to the geometric equation

$$\partial_t x = \beta \vec{N} + \alpha \vec{T}, \tag{2.4}$$

where $\beta = \beta(k, \nu, x)$, $\vec{N} = (-\sin\nu, \cos\nu)^T$ and $\vec{T} = (\cos\nu, \sin\nu)^T$ are the unit inward normal and tangent vectors, respectively. For

the normal velocity $v = \partial_t x \cdot \vec{N}$ we have $v = \beta(k, \nu, x)$. Notice that the presence of the arbitrary tangential velocity functional α has no impact on the shape of the evolving closed curves.

The goal of this section is to derive a system of PDEs governing the evolution of the curvature k of $\Gamma^t = \text{Img}(x(\cdot, t)), t \in [0, T)$, and some other geometric quantities where the family of regular plane curves where $x = x(u, t)$ is a solution to the position vector equation (2.4). These equations will be used in order to derive *a-priori* estimates of solutions. Notice that such an equation for the curvature is well known for the case when $\alpha = 0$, and it reads as follows: $\partial_t k = \partial_s^2 \beta + k^2 \beta$ (cf. [40, 1]). Here, we present a brief sketch of the derivation of the corresponding equations for the case of a nontrivial tangential velocity α.

Differentiating the curvature expression (2.2) and taking into account the governing equation (2.4) for the position vector x one can derive the second-order nonlinear parabolic equation for the curvature:

$$\partial_t k = \partial_s^2 \beta + \alpha \partial_s k + k^2 \beta \,. \tag{2.5}$$

The Frenét identities (2.1) can be used in order to derive an evolutionary equation for the local length $|\partial_u x|$. Indeed, $\partial_t |\partial_u x| = (\partial_u x \,.\, \partial_u \partial_t x)/|\partial_u x| = (\vec{p} \,.\, \partial_t \vec{p})/|\partial_u x|$. By (2.1) we have the

$$\partial_t |\partial_u x| = -|\partial_u x| \, k\beta \; + \partial_u \alpha, \tag{2.6}$$

where $(u, t) \in Q_T = [0, 1] \times [0, T)$. In other words, $\partial_t ds = (-k\beta + \partial_s \alpha) ds$. It yields the commutation relation

$$\partial_t \partial_s - \partial_s \partial_t = (k\beta - \partial_s \alpha) \partial_s. \tag{2.7}$$

Next, we derive equations for the time derivative of the unit tangent vector $\vec{T}$ and tangent angle ν. Using the above commutation relation and Frenét formulae we obtain

$$\begin{aligned} \partial_t \vec{T} &= \partial_t \partial_s x = \partial_s \partial_t x + (k\beta - \partial_s \alpha) \partial_s x \,, \\ &= \partial_s (\beta \vec{N} + \alpha \vec{T}) + (k\beta - \partial_s \alpha) \vec{T} \,, \\ &= (\partial_s \beta + \alpha k) \vec{N} \,. \end{aligned}$$

Since $\vec{T} = (\cos \nu, \sin \nu)^T$ and $\vec{N} = (-\sin \nu, \cos \nu)^T$ we conclude that $\partial_t \nu = \partial_s \beta + \alpha k$. Summarizing, we end up with evolutionary equations

for the unit tangent and normal vectors $\vec{T}, \vec{N}$ and the tangent angle ν

$$\begin{aligned} \partial_t \vec{T} &= (\partial_s \beta + \alpha k)\vec{N}\,, \\ \partial_t \vec{N} &= -(\partial_s \beta + \alpha k)\vec{T}\,, \\ \partial_t \nu &= \partial_s \beta + \alpha k\,. \end{aligned} \tag{2.8}$$

Since $\partial_s \nu = k$ and $\partial_s \beta = \beta'_k \partial_s k + \beta'_\nu k + \nabla_x \beta \cdot \vec{T}$ we obtain the following closed system of parabolic-ordinary differential equations:

$$\partial_t k = \partial_s^2 \beta + \alpha \partial_s k + k^2 \beta\,, \tag{2.9}$$

$$\partial_t \nu = \beta'_k \partial_s^2 \nu + (\alpha + \beta'_\nu)\partial_s \nu + \nabla_x \beta \cdot \vec{T}\,, \tag{2.10}$$

$$\partial_t g = -gk\beta + \partial_u \alpha\,, \tag{2.11}$$

$$\partial_t x = \beta \vec{N} + \alpha \vec{T}\,, \tag{2.12}$$

where $(u,t) \in Q_T = [0,1] \times (0,T)$, $ds = g\,du$ and $\vec{T} = \partial_s x = (\cos\nu, \sin\nu)^T, \vec{N} = \vec{T}^\perp = (-\sin\nu,\, \cos\nu)^T$. The functional α may depend on the variables k, ν, g, x. A solution (k, ν, g, x) to (2.9) – (2.12) is subject to initial conditions

$$k(\cdot,0) = k_0\,, \quad \nu(\cdot,0) = \nu_0\,, \quad g(\cdot,0) = g_0\,, \quad x(\cdot,0) = x_0(.)\,,$$

and periodic boundary conditions at $u = 0, 1$, except of the tangent angle ν for which we require that the tangent vector $\vec{T}(u,t) = (\cos(\nu(u,t)), \sin(\nu(u,t)))^T$ is 1-periodic in the u variable, i.e. $\nu(1,t) = \nu(0,t) + 2\pi$. Notice that the initial conditions for k_0, ν_0, g_0 and x_0 (the curvature, tangent angle, local length element and position vector of the initial curve Γ_0) must satisfy the following compatibility constraints:

$$g_0 = |\partial_u x_0| > 0\,, \quad k_0 = \det(g_0^{-3}\partial_u x_0, \partial_u^2 x_0)\,, \quad \partial_u \nu_0 = g_0 k_0\,.$$

2.4 First, integrals for geometric quantities

The aim of this section is derivation of basic identities for various geometric quantities like, e.g. the length of a closed curve and the area enclosed by a Jordan curve in the plane. These identities (first integrals) will be used later in the analysis of the governing system of equations.

2.4.1 The total length equation

By integrating (2.6) over the interval $[0,1]$ and taking into account that α satisfies periodic boundary conditions, we obtain the total length equation

$$\frac{d}{dt}L^t + \int_{\Gamma^t} k\beta ds = 0, \tag{2.13}$$

where $L^t = L(\Gamma^t)$ is the total length of the curve Γ^t, $L^t = \int_{\Gamma^t} ds = \int_0^1 |\partial_u x(u,t)|\, du$. If $k\beta \geq 0$, then the evolution of the planar curves parametrized by a solution of (1.1) represents a curve shortening flow, i.e., $L^{t_2} \leq L^{t_1} \leq L^0$ for any $0 \leq t_1 \leq t_2 \leq T$. The condition $k\beta \geq 0$ is obviously satisfied in the case $\beta(k,\nu) = \gamma(\nu)|k|^{m-1}k$, where $m > 0$ and γ is a non-negative anisotropy function. In particular, the Euclidean curvature driven flow ($\beta = k$) is curve shortening flow.

2.4.2 The area equation

Let us denote by $A = A^t$ the area of the domain Ω^t enclosed by a Jordan curve Γ^t. Then, by using Green's formula we obtain, for $P = -x_2/2, Q = x_1/2$,

$$\begin{aligned} A^t &= \iint_{\Omega_t} dx = \iint_{\Omega_t} \frac{\partial Q}{\partial x_1} - \frac{\partial P}{\partial x_2} dx = \oint_{\Gamma^t} P dx_1 + Q dx_2 \\ &= \frac{1}{2}\oint_{\Gamma^t} -x_2 dx_1 + x_1 dx_2\,. \end{aligned}$$

Since $dx_i = \partial_u x_i du, u \in [0,1]$, we have

$$A^t = \frac{1}{2}\int_0^1 \det(x, \partial_u x)\, du\,.$$

Clearly, integration of the derivative of a quantity along a closed curve yields zero. Therefore $0 = \int_0^1 \partial_u \det(x, \partial_t x) du = \int_0^1 \det(\partial_u x, \partial_t x) + \det(x, \partial_u \partial_t x) du$, and so $\int_0^1 \det(x, \partial_u \partial_t x) du = \int_0^1 \det(\partial_t x, \partial_u x) du$ because $\det(\partial_u x, \partial_t x) = -\det(\partial_t x, \partial_u x)$. As $\partial_t x = \beta\vec{N} + \alpha\vec{T}$, $\partial_u x du = \vec{T} ds$ and $\frac{d}{dt}A^t = \frac{1}{2}\int_0^1 2\det(\partial_t x, \partial_u x) du$ we can conclude that

$$\frac{d}{dt}A^t + \int_{\Gamma^t} \beta ds = 0. \tag{2.14}$$

Remark. In the case when a curve is evolving according to the curvature, i.e. $\beta = k$, then it follows from (2.3) and (2.14) that $\frac{d}{dt}A^t = -2\pi$

and so

$$A^t = A^0 - 2\pi t\,.$$

It means that the curve Γ^t does not exist for $t = T_{max} = \frac{A^0}{2\pi}$, i.e. the lifespan of the curve evolution with $\beta = k$ is finite.

2.5 Gage-Hamilton and Grayson's theorems

Assume that a smooth, closed, and embedded curve evolves by the normal velocity proportional to its curvature, i.e. $\beta = k$. This curve evolution is known as the Euclidean curve shortening flow. Since the curvature is positive on the convex side and it is negative on the concave side one may expect that the evolving curve becomes more convex and less concave as time t increases. Finally, it becomes a convex shape and it shrinks to a circular point in finite time. This natural observation has been rigorously proven by Grayson in [50]. He used already known result due to Gage and Hamilton. They considered the evolution of convex curves in the plane and proved that evolved curves shrink to a circular point in finite time.

Theorem 2.1 *(Gage and Hamilton [40]) Any smooth closed convex curve embedded in $\mathbb{R}^2$ evolved by the curvature converges to a point with asymptotic circular shape in finite time.*

What Grayson added to this proof was the statement that any embedded smooth planar curve (not necessarily convex) when evolving according to the curvature becomes convex in finite time, stays embedded and then it shrinks to a circular point in finite time.

Theorem 2.2 *(Grayson [50]) Any smooth closed curve embedded in $\mathbb{R}^2$ evolved by the curvature becomes convex in finite time and then it converges to a point in finite time with asymptotically circular shape.*

In Fig. 2.2 we show computational results of curvature driven evolution of two initial planar curve evolved with the normal velocity $v = k$ and $v = k^{1/3}$.

Although we will not go into the details of proofs of the above theorems it is worthwhile to note that the proof of Grayson's theorem consists of several steps. First, one needs to prove that an embedded initial curve Γ^0 when evolved according to the curvature stays embedded for $t > 0,$ i.e. self-intersections cannot occur for $t > 0$. Then, it is

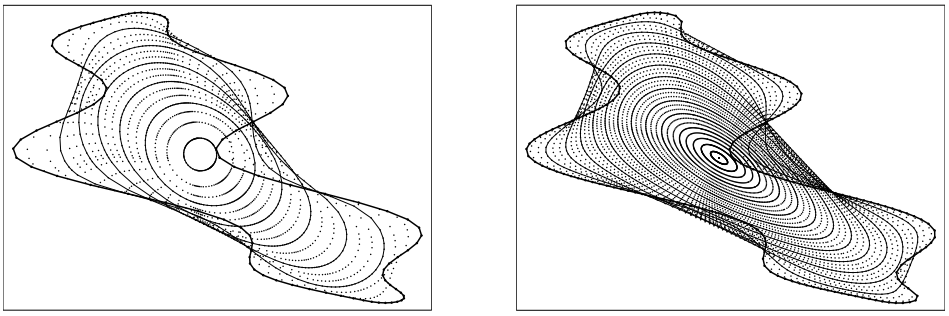

Figure 2.2: An example of evolution of planar curves evolved by the normal velocity $v = k$ (left) and power-like velocity $v = k^{1/3}$. Source: Ševčovič [85].

necessary to prove that eventual concave parts of the curve decrease their length. To this end, one can construct a partition a curve into its convex and concave part and show that concave parts are vanishing when time increases. The curve eventually becomes convex. Then, Grayson applied the previous result due to Gage and Hamilton. Their result says that any initial convex curve asymptotically approaches a circle when $t \to T_{max}$ where T_{max} is finite. To interpret their result in the language of parabolic partial differential equations we notice that the solution to (2.9) with $\beta = k$ remains positive provided that the initial value k^0 was non-negative. This is a direct consequence of the maximum principle for parabolic equations.

2.5.1 Asymptotic profile of shrinking curves for other normal velocities

There are some partial results in this direction. If $\beta = k^{1/3}$ then the corresponding flow of planar curves is called affine space scale flow. It has been studied and analyzed by Angenent, Shapiro and Tannenbaum in [7] and [106]. In this case, the limiting profile of a shrinking family of curves is an ellipse. Self-similar property of shrinking ellipses in the case $\beta = k^{1/3}$ has been also addressed in [84]. In Fig. 2.2 (right) we present a computational result of evolution of shrinking ellipses in which the curve is evolved with velocity $v = k^{1/3}$. Notice that the normal velocity of form $\beta(k) = k^p$ has been investigated by Ushijima and Yazaki in [122] in the context of crystalline curvature numerical approximation of the flow. It can be

shown that $p = 1/(n^2-1), n = 2, 3, \cdots$, are bifurcation values for which one can prove the existence of local branches of self-similar solutions of evolving curves shrinking to a point as a rounded polygon with n facets.

2.6 Failure of the Grayson theorem for evolution of closed surface by the mean curvature

In Fig. 2.3 we present evolution of a two dimensional dumb-bell like surface, which is evolved by the mean curvature. Since the mean curvature for a two dimensional surface is the sum of two principal cross-sectional curvatures one can conclude that the mean curvature at the bottle-neck of the surface is positive because of the dominating principal curvature of the section plane perpendicular to the axis of the rotational symmetry of the dumb-bell. Thus the flow of a surface tends to shrink the bottle-neck. Notice that this is a purely three dimensional feature and can not be observed in two dimensions. Furthermore, we can see from Fig. 2.3 that dumb-bell's bottle-neck shrinks to a pinching point in a finite time. After that time evolution continues in two separate sphere–like surfaces, which shrink to two points in finite time. This observation enables us to conclude that a three dimensional generalization of Grayson's theorem (see Section 2) is false.

Another intuitive explanation for the failure of the Grayson theorem in three dimensions comes from the description of the mean curvature flow of two dimensional embedded surfaces in $\mathbb{R}^3$. According to Huisken [57] the mean curvature H of the surface is a solution of the following system of nonlinear parabolic equations

$$\begin{aligned} \partial_t H &= \Delta_{\mathcal{M}} H + |A|^2 H\,, \\ \partial_t |A|^2 &= \Delta_{\mathcal{M}} |A|^2 - 2|\nabla_{\mathcal{M}} A|^2 + 2|A|^4, \end{aligned}$$

where $|A|^2$ is the second trace (Frobenius norm) of the second fundamental form of the embedded manifold $\mathcal{M}$. Here, $\Delta_{\mathcal{M}}$ is the Laplace-Beltrami operator with respect to the surface $\mathcal{M}$. The above system of equations is a two dimensional generalization of the simple one dimensional parabolic equation $\partial_t k = \partial_s^2 k + k^3$ describing the Euclidean

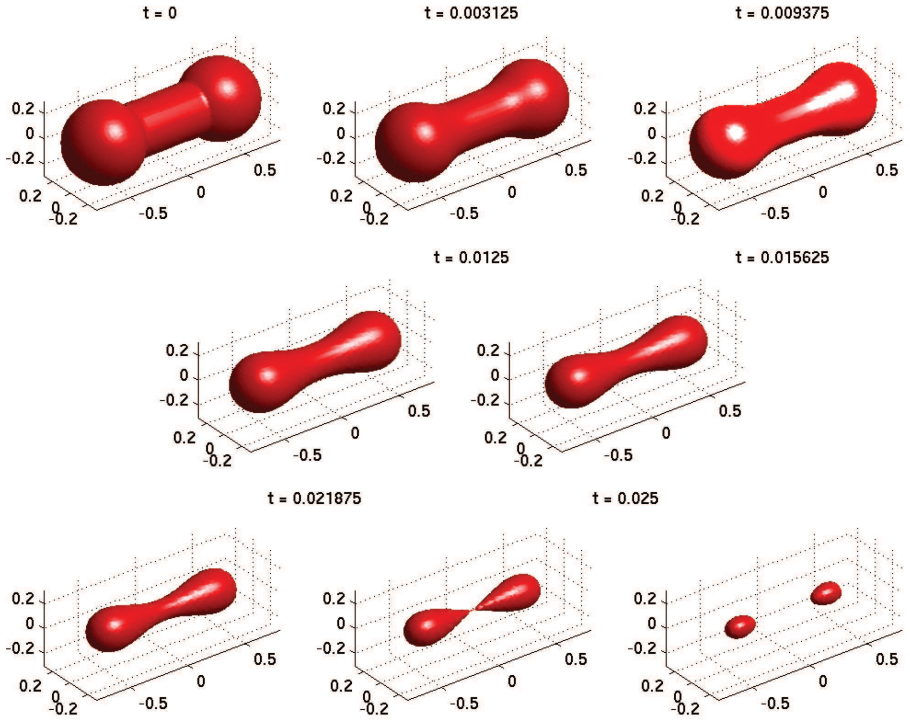

Figure 2.3: Time evolution of a dumb-bell initial surface driven by the mean curvature. Source for computation: I. Mitchell, ToolboxLS, available at: `www.cs.ubc.ca/m̃itchell`.

flow of planar curves evolving by the curvature. Now, one can interpret Grayson's theorem for embedded curves in terms of non-increase of nodal points of the curvature k. This result is known in the case of a scalar reaction diffusion equation and is referred to as Sturm's theorem or non-increase of lap number theorem due to Zelenyak [127] and Matano [77]. However, in the case of a system of two dimensional equations for the mean curvature H and the second trace $|A|^2$ one cannot expect similar result, which is known to be an intrinsic property of scalar parabolic equations and cannot be extended for systems of parabolic equations.

2.7 Level set methods for curvature driven flows of planar curves and comparison to the direct Lagrangian approach

By contrast to the direct approach, *level set methods* are based on introducing an auxiliary shape function whose zero level sets represent a family of planar curves, which evolves according to the geometric equation (1.1) as well as to (1.2) (see, e.g. [99, 115, 116, 117, 45]). The level set approach handles implicitly the curvature-driven motion, passing the problem to higher dimensional space. One can deal with splitting and/or merging of evolving curves in a robust way. However, from the computational point of view, level set methods are much more computationally expensive than methods based on the direct approach. The purpose of this section is to present basic ideas and results concerning the level set approach in curvature driven flows of planar curves.

2.7.1 Level set representation of Jordan curves in the plane

In the level set method the evolving family of planar curves $\{\Gamma^t, t \geq 0\}$, is represented by the zero level set of the so-called shape function $\phi : \Omega \times [0,T] \to \mathbb{R}$ where $\Omega \subset \mathbb{R}^2$ is a simply connected domain containing the whole family of evolving curves $\{\Gamma^t, t \in [0,T]\}$. We adopt a notation according to which the interior of a curve is described as: $int(\Gamma^t) = \{x \in \mathbb{R}^2, \phi(x,t) < 0\}$ and, consequently, $ext(\Gamma^t) = \{x \in \mathbb{R}^2, \phi(x,t) > 0\}$ and $\Gamma^t = \{x \in \mathbb{R}^2, \phi(x,t) = 0\}$ (see

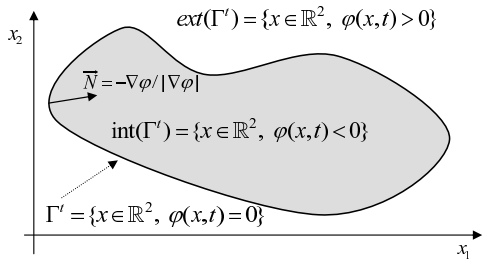

Figure 2.4: Description of the level set representation of a planar embedded curve by a shape function $\phi : \mathbb{R}^2 \times [0, T) \to \mathbb{R}$. Source: Ševčovič [113].

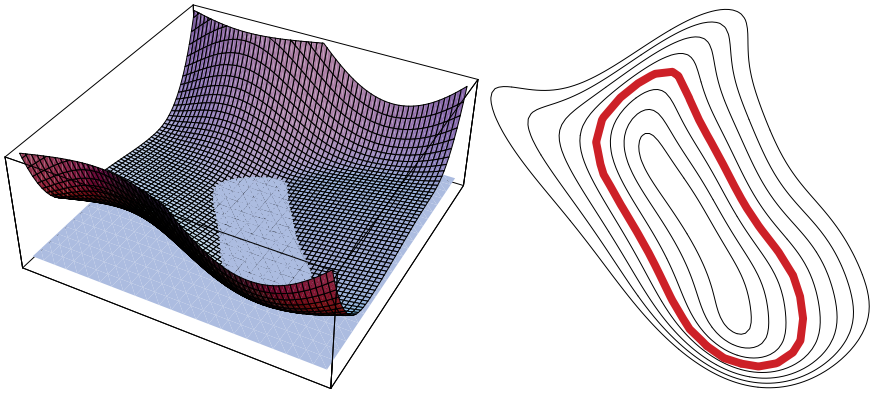

Figure 2.5: Representation of a planar embedded curve by the level set of a function $\phi : \mathbb{R}^2 \to \mathbb{R}$. The level set function (left) and its level cross-sections (right). Source: Ševčovič [113].

Fig. 2.4). With this convection, the unit inward normal vector $\vec{N}$ can be expressed as

$$\vec{N} = -\nabla\phi/|\nabla\phi|\,.$$

In order to express the signed curvature k of the curve Γ^t we make use of the identity $\phi(x(s,t),t) = 0$. Differentiating this identity with respect to the arc-length parameter s we obtain $0 = \nabla\phi\cdot\partial_s x = \nabla\phi\cdot\vec{T}$. Differentiating the latter identity with respect to s again and using the Frenét formula $\partial_s\vec{T} = k\vec{N}$ we obtain $0 = k(\nabla\phi\cdot\vec{N}) + \vec{T}^{\perp}\nabla^2\phi\vec{T}$. Since $\vec{N} = -\nabla\phi/|\nabla\phi|$ we have

$$k = \frac{1}{|\nabla\phi|}\vec{T}^T\nabla^2\phi\vec{T}\,. \tag{2.15}$$

It is a straightforward computation to verify the identity

$$|\nabla\phi|\mathrm{div}\left(\frac{\nabla\phi}{|\nabla\phi|}\right) = \vec{T}^{\perp}\nabla^2\phi\vec{T}\,.$$

Hence the signed curvature k is given by the formula

$$k = \mathrm{div}\left(\frac{\nabla\phi}{|\nabla\phi|}\right)\,.$$

In other words, the curvature k is just minus the divergence of the normal vector $\vec{N} = \nabla\phi/|\nabla\phi|$, i.e. $k = -\mathrm{div}\vec{N}$.

Let us differentiate the equation $\phi(x(s,t),t) = 0$ with respect to time. We obtain $\partial_t\phi + \nabla\phi\cdot\partial_t x = 0$. Since the normal velocity of x is $\beta = \partial_t x\cdot\vec{N}$ and $\vec{N} = -\nabla\phi/|\nabla\phi|$ we obtain

$$\partial_t\phi = |\nabla\phi|\beta\,.$$

Combining the above identities for $\partial_t\phi, \vec{N}$, and k we conclude that the geometric equation (1.1) can be reformulated in terms of the evolution of the shape function $\phi = \phi(x,t)$ satisfying the following fully nonlinear parabolic equation:

$$\partial_t\phi = |\nabla\phi|\beta\left(\mathrm{div}\left(\nabla\phi/|\nabla\phi|\right), x, -\nabla\phi/|\nabla\phi|\right), \qquad x\in\Omega,\ t\in(0,T)\,. \tag{2.16}$$

Here, we assume that the normal velocity β may depend on the curvature k, the position vector x and the tangent angle ν expressed through the unit inward normal vector $\vec{N}$, i.e. $\beta = \beta(k,x,\vec{N})$. Since the behavior of the shape function ϕ in a far distance from the set of

evolving curves $\{\Gamma^t, t \in [0,T]\}$, does not influence their evolution, it is usual in the context of the level set equation to prescribe homogeneous Neumann boundary conditions at the boundary $\partial\Omega$ of the computational domain Ω, i.e.

$$\phi(x,t) = 0 \;\text{ for } x \in \partial\Omega\,. \tag{2.17}$$

The initial condition for the level set shape function ϕ can be constructed as the signed distance function measuring the signed distance of a point $x \in \mathbb{R}^2$ and the initial curve Γ^0, i.e.

$$\phi(x,0) = \text{dist}(x,\Gamma^0), \tag{2.18}$$

where $\text{dist}(x,\Gamma^0)$ is a signed distance function defined as

$$\begin{aligned}
\text{dist}(x,\Gamma^0) &= \inf_{y\in\Gamma^0} |x-y|, \qquad \text{for } x \in ext(\Gamma^0)\,,\\
\text{dist}(x,\Gamma^0) &= -\inf_{y\in\Gamma^0} |x-y|, \qquad \text{for } x \in int(\Gamma^0)\,,\\
\text{dist}(x,\Gamma^0) &= 0, \qquad \text{for } x \in \Gamma^0\,.
\end{aligned}$$

If we assume that the normal velocity of an evolving curve Γ^t is an affine function in the k variable, i.e.

$$\beta = \mu k + f,$$

where $\mu = \mu(x,\vec{N})$ is a coefficient describing dependence of the velocity speed on the position vector x and the orientation of the curve Γ^t expressed through the unit inward normal vector $\vec{N}$ and $f = f(x,\vec{N})$ is an external forcing term.

$$\partial_t\phi = \mu\,|\nabla\phi|\,\text{div}\,\left(\frac{\nabla\phi}{|\nabla\phi|}\right) + f|\nabla\phi|, \qquad x \in \Omega, t \in (0,T)\,. \tag{2.19}$$

2.7.2 Pros and cons of the Level set method and the direct Lagrangian approach

By contrast to the direct approach, *level set methods* are based on introducing an auxiliary function whose zero level sets represent an evolving family of planar curves undergoing the geometric equation (1.1) (see, e.g., [99, 115, 116, 117, 53]). Another indirect method is based on the phase-field formulations (see, e.g., [23, 96, 37, 14]).

The level set approach handles implicitly the curvature-driven motion, passing the problem to a higher dimensional space. One can deal with splitting and/or merging of evolving curves in a robust way. However, from the computational point of view, level set methods are much more expensive than methods based on the direct approach. For some non-local flows, open curves evolution and/or evolution of curves in $\mathbb{R}^3$ application of the level set method might be unclear or even impossible.

The advantage of the direct approach consists mainly in the fact that the corresponding governing equations are one dimensional in the spatial variable (for the evolution of curves). They can handle open curves as well as curves in $\mathbb{R}^3$. A certain disadvantage of the direct approach consists in handling of topological changes. This drawback can be however overcome by a fast algorithm recently proposed by Mikula and Urbán [92].

Chapter 3

Results on existence and qualitative behavior of solutions

In this chapter we focus our attention on mathematical analysis and qualitative behavior of curvature driven flows of planar curves. We present a functional analytic method for the proof of the local time existence of a smooth family of curves evolving with the normal velocity given by a general function $\beta = \beta(k, \nu, x)$ depending on the curvature k, position vector x as well as the tangential angle ν. The main idea is to transform the geometric problem into the language of a time depending solution to an evolutionary partial differential equation like, e.g. (2.9)–(2.12). First, we present an approach due to Angenent describing the evolution of an initial curve by a fully nonlinear parabolic equation for the distance function measuring the normal distance of the initial curve tΓ^0 the evolved curve Γ^t for small values of $t > 0$. The second approach presented in this chapter is based on the solution of the system of nonlinear parabolic-ordinary differential equations (2.9)–(2.12) also proposed by Angenent and Gurtin [1, 2] and further analyzed and applied by Mikula and Ševčovič in the series of papers [85, 86, 87] (see also Ševčovič and Yazaki [110]). Both approaches are based on the solution to a certain fully nonlinear parabolic equation or system of equations. To prove a local existence and continuation result we apply the theory of nonlinear analytic semi-flows due to Da Prato and Grisvard, Lunardi [29, 30, 73] and Angenent [5, 6].

3.1 Local existence of smooth solutions

The idea of the proof of the local existence of an evolving family of closed embedded curves is to transform solution of the geometric equation (1.1) into a solution of a fully nonlinear parabolic equation for the distance $\phi(u,t)$ of a point $x(u,t) \in \Gamma^t$ from its initial value position $x^0(u) = x(u,0) \in \Gamma^0$. This idea is due to Angenent [6] who derived the fully nonlinear parabolic equation for ϕ and proved local existence of smooth solutions by the method of abstract nonlinear evolutionary equations in Banach spaces [6].

3.1.1 Local representation of an embedded curve

Let $\Gamma^0 = \text{Img}(x^0)$ be a smooth initial Jordan curve embedded in $\mathbb{R}^2$. Because of its smoothness and embeddednes one can construct a local parametrization of any smooth curve $\Gamma^t = \text{Img}(x(\cdot,t))$ lying in the thin tubular neighborhood along Γ^0, i.e. $\text{dist}_H(\Gamma^t, \Gamma^0) < \varepsilon$ where dist_H is the Hausdorff set distance function. This is why there exists a small number $0 < \varepsilon \ll 1$ and a smooth immersion function $\sigma : S^1 \times (-\varepsilon, \varepsilon) \to \mathbb{R}^2$ such that

- $x^0(u) = \sigma(u,0)$ for any $u \in S^1$,
- for any $u \in S^1$ there exists a unique $\phi = \phi(u,t) \in (-\varepsilon, \varepsilon)$ such that $\sigma(u, \phi(u,t)) = x(u,t)$,
- the implicitly defined function $\phi = \phi(u,t)$ is smooth in its variables provided the function $x = x(u,t)$ is smooth.

It is easy to verify that the function $\sigma(u,\phi) = x^0(u) + \phi \vec{N}^0(u)$ is the immersion having the above properties. Here, $\vec{N}^0(u)$ is the unit inward vector to the curve Γ^0 at the point $x^0(u)$ (see Fig. 3.1).

Now we can evaluate $\partial_t x, \partial_u x, \partial_u^2 x$ and $|\partial_u x|$ as follows:

$$\begin{aligned}
\partial_t x &= \sigma'_\phi \partial_t \phi \,, \\
\partial_u x &= \sigma'_u + \sigma'_\phi \partial_u \phi \,, \\
\partial_u^2 x &= \sigma''_{uu} + 2\sigma''_{u\phi} \partial_u \phi + \sigma''_{\phi\phi} (\partial_u \phi)^2 + \sigma'_\phi \partial_u^2 \phi \,, \\
g = |\partial_u x| &= \left(|\sigma'_u|^2 + 2(\sigma'_u . \sigma'_\phi) \partial_u \phi + |\sigma'_\phi|^2 (\partial_u \phi)^2 \right)^{\frac{1}{2}} \,.
\end{aligned}$$

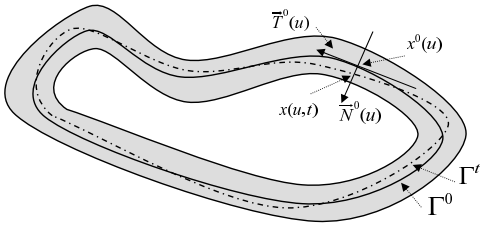

Figure 3.1: Description of a local parametrization of an embedded curve Γ^t in the neighborhood of the initial curve Γ^0. Source: Ševčovič [113].

Hence we can express the curvature $k = \det(\partial_u x, \partial_u^2 x)/|\partial_u x|^3$ as follows:

$$\begin{aligned} g^3 k &= \det(\partial_u x, \partial_u^2 x) = \partial_u^2\phi\partial_u\phi\det(\sigma'_\phi,\sigma'_\phi) + \partial_u^2\phi\det(\sigma'_u,\sigma'_\phi) \\ &+ (\partial_u\phi)^2\left[\det(\sigma'_u,\sigma''_{\phi\phi}) + \partial_u\phi\det(\sigma'_\phi,\sigma''_{\phi\phi})\right] + 2\partial_u\phi\det(\sigma'_u,\sigma''_{u\phi}) \\ &+ 2(\partial_u\phi)^2\det(\sigma'_\phi,\sigma''_{u\phi}) + \det(\sigma'_u,\sigma''_{uu}) + \partial_u\phi\det(\sigma'_\phi,\sigma''_{uu})\,. \end{aligned}$$

Clearly, $\det(\sigma'_\phi,\sigma'_\phi) = 0$. Since $\sigma'_\phi = \vec{N}^0$ and $\sigma'_u = \partial_u x^0 + \phi\partial_u\vec{N}^0 = g^0(1-k^0\phi)\vec{T}^0$ we have $\det(\sigma'_u,\sigma'_\phi) = g^0(1-k^0\phi)$ and $(\sigma'_u.\sigma'_\phi) = 0$. Therefore the local length $g = |\partial_u x|$ and the curvature k can be expressed as

$$\begin{aligned} g &= |\partial_u x| = \left((g^0(1-k^0\phi))^2 + (\partial_u\phi)^2\right)^{\frac{1}{2}}\,, \\ k &= \frac{g^0(1-k^0\phi)}{g^3}\partial_u^2\phi + R(u,\phi,\partial_u\phi), \end{aligned}$$

where $R(u,\phi,\partial_u\phi)$ is a smooth function.

We proceed with evaluation of the time derivative $\partial_t x$. Since $\partial_u x = \sigma'_u + \sigma'_\phi\partial_u\phi$ we have $\vec{T} = \frac{1}{g}(\sigma'_u + \sigma'_\phi\partial_u\phi)$. The vectors $\vec{N}$ and $\vec{T}$ are perpendicular to each other. Thus

$$\partial_t x\cdot\vec{N} = -\det(\partial_t x,\vec{T}) = \frac{1}{g}\det(\sigma'_u,\sigma'_\phi)\partial_t\phi = \frac{g^0(1-k^0\phi)}{g}\partial_t\phi$$

because $\det(\sigma'_\phi,\sigma'_\phi) = 0$. Hence, a family of embedded curves $\{\Gamma^t, t\in[0,T)\}$ evolves according to the normal velocity

$$\beta = \mu k + c$$

if and only if the function $\phi = \phi(u,t)$ is a solution to the nonlinear parabolic equation

$$\partial_t\phi = \frac{\mu}{g^2}\partial_u^2\phi + \frac{g}{g^0(1-k^0\phi)}(\mu R(u,\phi,\partial_u\phi) + c),$$

where

$$g = \left(|g^0|^2(1-k^0\phi)^2 + (\partial_u\phi)^2\right)^{\frac{1}{2}} .$$

In a general case when the normal velocity $\beta = \beta(k, x, \vec{N})$ is a function of curvature k, position vector x and the inward unit normal vector $\vec{N}$, ϕ is a solution to a fully nonlinear parabolic equation of the form:

$$\partial_t\phi = F(\partial_u^2\phi, \partial_u\phi, \phi, u), \quad u \in S^1, t \in (0,T) . \tag{3.1}$$

The right-hand side function $F = F(q,p,\phi,u)$ is C^1 is a smooth function of its variables and

$$\frac{\partial F}{\partial q} = \frac{\beta_k'}{g^2} > 0$$

and so equation (3.1) is a nonlinear strictly parabolic equation. Equation (3.1) is subject to an initial condition

$$\phi(u,0) = \phi^0(u) \equiv 0 , \quad u \in S^1 . \tag{3.2}$$

3.1.2 Nonlinear analytic semi-flows

In this section we recall basic facts from the theory of nonlinear analytic semi-flows, which can be used in order to prove local in time existence of a smooth solution to the fully nonlinear parabolic equation (3.1) subject to the initial condition (3.2). The theory has been developed by S. Angenent in [6] and A. Lunardi in [73].

Equation (3.1) can be rewritten as an abstract evolutionary equation

$$\partial_t\phi = \mathcal{F}(\phi) \tag{3.3}$$

subject to the initial condition

$$\phi(0) = \phi^0 \in E_1, \tag{3.4}$$

where $\mathcal{F}$ is a C^1 smooth mapping between two Banach spaces E_1, E_0, i.e. $\mathcal{F} \in C^1(E_1, E_0)$. For example, if we take

$$E_0 = h^\varrho(S^1), \qquad E_1 = h^{2+\varrho}(S^1) ,$$

where $h^{k+\varrho}(S^1), k = 0, 1, \cdots$, is the little Hölder space, i.e. the closure of $C^\infty(S^1)$ in the topology of the Hölder space $C^{k+\sigma}(S^1)$ (see

[6]), then the mapping F defined as in the right-hand side of (3.1) is indeed a C^1 mapping from E_1 into E_0. Its Frechét derivative $d\mathcal{F}(\phi^0)$ is given by the linear operator

$$d\mathcal{F}(\phi^0)\phi = a^0\partial_u^2\phi + b^0\partial_u\phi + c^0\phi,$$

where

$$a^0 = F'_q(\partial_u^2\phi^0, \partial_u\phi^0, \phi^0, u) = \frac{\beta'_k}{(g^0)^2}, \quad b^0 = F'_p(\partial_u^2\phi^0, \partial_u\phi^0, \phi^0, u),$$

$$c^0 = F'_\phi(\partial_u^2\phi^0, \partial_u\phi^0, \phi^0, u)\,.$$

Suppose that the initial curve $\Gamma^0 = \mathrm{Img}(x^0)$ is sufficiently smooth, $x^0 \in (h^{2+\varrho}(S^1))^2$ and regular, i.e. $g^0(u) = |\partial_u x^0(u)| > 0$ for any $u \in S^1$. Then $a^0 \in h^{1+\varrho}(S^1)$. A standard result from the theory of analytic semigroups (cf. [54]) enables us to conclude that the principal part $A := a^0\partial_u^2$ of the linearization $d\mathcal{F}(\phi^0)$ is a generator of a analytic semigroup $\{\exp(tA), t \geq 0\}$, in the Banach space $E_0 = h^\varrho(S^1)$.

Maximal regularity theory

In order to proceed with the proof of local in time existence of a classical solution to the abstract nonlinear equation (3.3) we have to recall a notion of a maximal regularity pair of Banach spaces.

Assume that (E_1, E_0) is a pair of Banach spaces with E_1 densely included into E_0. By $L(E_1, E_0)$ we will denote the Banach space of all linear bounded operators from E_1 into E_0. An operator $A \in L(E_1, E_0)$ can be considered as an unbounded operator in the Banach space E_0 with a dense domain $D(A) = E_1$. By $Hol(E_1, E_0)$ we will denote a subset of $L(E_1, E_0)$ consisting of all generators A of an analytic semigroup $\{\exp(tA), t \geq 0\}$, of linear operators in the Banach space E_0 (cf. [54]).

Neither the theory of C^0 semigroups (cf. Pazy [100]) nor the theory of analytic semigroups (cf. Henry [54]) can treat fully nonlinear parabolic equations. This is mainly due to the methodology based on the solution of an integral equation, which is suitable for semilinear equations only. The second reason why these methods cannot provide a local existence result is due to the fact that semigroup theories are working with function spaces, which are fractional powers of the domain of a generator of an analytic semigroup (see [54]).

Therefore we need a more robust theory capable of handling fully nonlinear parabolic equations. This theory is due to Angenent and Lunardi [5, 73] and it is based on abstract results by Da Prato and Grisvard [29, 30]. The basic idea is the linearization technique where one can linearize the fully nonlinear equation at the initial condition ϕ^0. Then one sets up a linearized semi-linear equation with the right hand side, which is of the second order with respect to deviation from the initial condition. In what follows, we will present key steps of this method. First, we need to introduce the maximal regularity class, which will enable us to construct an inversion operator to a non-homogeneous semi-linear equation.

Let $E = (E_1, E_0)$ be a pair of Banach spaces for which E_1 is densely included in E_0. Let us define the following function spaces

$$X = C([0,1], E_0), \qquad Y = C([0,1], E_1) \cap C^1([0,1], E_0)\,.$$

We will identify ∂_t with the bounded differentiation operator from Y to X defined by $(\partial_t \phi)(t) = \phi'(t)$. For a given linear bounded operator $A \in L(E_1, E_0)$ we define the extended operator $\mathcal{A} : Y \to X \times E_1$ defined by $\mathcal{A}\phi = (\partial_t \phi - A\phi, \phi(0))$. Next we define a class $\mathcal{M}_1(E)$ as follows:

$$\mathcal{M}_1(E) = \{A \in Hol(E),\ \mathcal{A} \text{ is an isomorphism between } Y \text{ and } X \times E_1\}\,.$$

It means that the class $\mathcal{M}_1(E)$ consists of all generators of analytic semigroups A such that the initial value problem for the semi-linear evolution equation

$$\partial_t \phi - A\phi = f(t), \qquad \phi(0) = \phi^0,$$

has a unique solution $\phi \in Y$ for any right-hand side $f \in X$ and the initial condition $\phi^0 \in E_1$ (cf. [5]). For such an operator A we obtain boundedness of the inverse of the operator $\phi \mapsto (\partial_t - A)\phi$ mapping the Banach space $Y^{(0)} = \{\phi \in Y, \phi(0) = 0\}$ onto the Banach space X, i.e.

$$\|(\partial_t - A)^{-1}\|_{L(X, Y^{(0)})} \le C < \infty\,.$$

The class $\mathcal{M}_1(E)$ is refereed to as the maximal regularity class for the pair of Banach spaces $E = (E_1, E_0)$.

The following useful perturbation result has been proved by Angenent.

Definition 3.1 *We say that the linear bounded operator $B : E_1 \to E_0$ has a relative zero norm if for any $\varepsilon > 0$ there is a constant $k_\varepsilon > 0$ such that*

$$\|Bx\|_{E_0} \leq \varepsilon \|x\|_{E_1} + k_\varepsilon \|x\|_{E_0}$$

for any $x \in E_1$.

Lemma 3.2 *[5, Lemma 2.5] The set $\mathcal{M}_1(E_1, E_0)$ is closed with respect to perturbations by linear operators with zero relative norm.*

Using properties of the class $\mathcal{M}_1(E)$ we can recall the result due to Angenent [5] on local existence of a smooth solution to the abstract fully nonlinear evolutionary problem (3.3)–(3.4).

Theorem 3.3 *[5, Theorem 2.7] Assume that $\mathcal{F}$ is a C^1 mapping from some open subset $\mathcal{O} \subset E_1$ of the Banach space E_1 into the Banach space E_0. If the Frechét derivative $A = d\mathcal{F}(\phi)$ belongs to $\mathcal{M}_1(E)$ for any $\phi \in \mathcal{O}$ and the initial condition ϕ^0 belongs to $\mathcal{O}$ then the abstract fully nonlinear evolutionary problem (3.3)–(3.4) has a unique solution $\phi \in C^1([0,T], E_0) \cap C([0,T], E_1)$ on some small time interval $[0,T], T > 0$.*

Application of the abstract result for the fully nonlinear parabolic equation for the distance function

Now we are in position to apply the abstract result contained in Theorem 3.3 to the fully nonlinear parabolic equation (3.1) for the distance function ϕ subject to a zero initial condition $\phi^0 = 0$. Notice that one has to carefully choose function spaces to work with. Baillon in [8] showed that, if we exclude the trivial case $E_1 = E_0$, the class $\mathcal{M}_1(E_1, E_0)$ is nonempty only if the Banach space E_0 contains a closed subspace isomorphic to the sequence space (c_0). As a consequence of this criterion we conclude that $\mathcal{M}_1(E_1, E_0)$ is empty for any reflexive Banach space E_0. Therefore the space E_0 cannot be reflexive. On the other hand, one needs to prove that the linearization $A = d\mathcal{F}(\phi) : E_1 \to E_0$ generates an analytic semigroup in E_0. Therefore it is convenient to work with little Hölder spaces satisfying these structural assumptions.

Applying the abstract result from Theorem 3.3 we are able to state the following theorem, which is a special case of a more general result by Angenent [6, Theorem 3.1] to the evolution of planar curves.

Theorem 3.4 *[6, Theorem 3.1] Assume that the normal velocity $\beta = \beta(k,\nu)$ is a $C^{1,1}$ smooth function such that $\beta'_k > 0$ for all $k \in \mathbb{R}$ and $\nu \in [0, 2\pi]$. Let Γ^0 be an embedded smooth curve with Hölder continuous curvature. Then there exists a unique maximal solution $\Gamma^t, t \in [0, T_{max})$, consisting of curves evolving with the normal velocity equal to $\beta(k,\nu)$.*

Remark. Verification of non-emptiness of the set $\mathcal{M}_1(E_1, E_0)$ might be difficult for a particular choice of Banach pair (E_1, E_0). There is however a general construction of the Banach pair (E_1, E_0) such that a given linear operator A belongs to $\mathcal{M}_1(E_1, E_0)$. Let $F = (F_1, F_0)$ be a Banach pair. Assume that $A \in Hol(F_1, F_0)$. We define the Banach space $F_2 = \{\phi \in F_1, A\phi \in F_1\}$ equipped with the graph norm $\|\phi\|_{F_2} = \|\phi\|_{F_1} + \|A\phi\|_{F_1}$. For a fixed $\sigma \in (0,1)$ we introduce the continuous interpolation spaces $E_0 = F_\sigma = (F_1, F_0)_\sigma$ and $E_1 = F_{1+\sigma} = (F_2, F_1)_\sigma$. Then, by result due to Da Prato and Grisvard [29, 30] we have $A \in \mathcal{M}_1(E_1, E_0)$.

3.1.3 Local existence, uniqueness and continuation of classical solutions for the direct Lagrangian approach

In this section we present another approach for the proof of local existence of a classical solution, which is based on analysis of the governing system of equations describing the direct Lagrangian approach. Now we put our attention to the solution of the system of parabolic-ordinary differential equations (2.9) – (2.12). Let a regular smooth initial curve $\Gamma^0 = \mathrm{Img}(x_0)$ be given. Recall that a family of planar curves $\{\Gamma^t = \mathrm{Img}(x(\cdot,t)),\ t \in [0,T)\}$, satisfying (1.1) can be represented by a solution $x = x(u,t)$ to the position vector equation (2.4). Notice that $\beta = \beta(k,\nu,x)$ depends on x, k, ν and this is why we have to provide and analyze a closed system of equations for the variables k, ν as well as the local length $g = |\partial_u x|$ and the position vector x. In the case of a nontrivial tangential velocity functional α the system of parabolic–ordinary governing equations has the follow-

ing form:

$$\partial_t k = \partial_s^2 \beta + \alpha \partial_s k + k^2 \beta \,, \tag{3.5}$$

$$\partial_t \nu = \beta_k' \partial_s^2 \nu + (\alpha + \beta_\nu') \partial_s \nu + \nabla_x \beta \cdot \vec{T} \,, \tag{3.6}$$

$$\partial_t g = -gk\beta + \partial_u \alpha \,, \tag{3.7}$$

$$\partial_t x = \beta \vec{N} + \alpha \vec{T}, \tag{3.8}$$

where $(u,t) \in Q_T = [0,1] \times (0,T)$, $ds = g\,du$, $\vec{T} = \partial_s x = (\cos\nu, \sin\nu)^T$, $\vec{N} = \vec{T}^\perp = (-\sin\nu,\, \cos\nu)^T$, $\beta = \beta(k,\nu,x)$. A solution (k,ν,g,x) to (3.5) – (3.8) is subject to initial conditions

$$k(\cdot,0) = k_0 \,,\ \nu(\cdot,0) = \nu_0 \,,\ g(\cdot,0) = g_0 \,,\ x(\cdot,0) = x_0(.)$$

and periodic boundary conditions at $u = 0, 1$ except of ν for which we require the boundary condition $\nu(1,t) \equiv \nu(0,t) \bmod(2\pi)$. The initial conditions for k_0, ν_0, g_0 and x_0 have to satisfy natural compatibility constraints: $g_0 = |\partial_u x_0| > 0\,,\ k_0 = \det(g_0^{-3} \partial_u x_0, \partial_u^2 x_0)\,,\ \partial_u \nu_0 = g_0 k_0$ following from the equation $k = \det(\partial_s x, \partial_s^2 x)$ and Frenét's formulae applied to the initial curve $\Gamma_0 = \mathrm{Img}(x_0)$. Notice that the system of governing equations consists of coupled parabolic-ordinary differential equations.

Since α enters the governing equations a solution k, ν, g, x to (3.5) – (3.8) does depend on α. On the other hand, the family of planar curves $\{\Gamma^t = \mathrm{Img}(x(\cdot,t)), t \in [0,T)\}$, is independent of a particular choice of the tangential velocity α as it does not change the shape of a curve. The tangential velocity α can be therefore considered as a free parameter to be suitably determined later. For example, in the Euclidean curve shortening equation $\beta = k$ we can write equation (2.4) in the form $\partial_t x = \partial_s^2 x = g^{-1}\partial_u(g^{-1}\partial_u x) + \alpha g^{-1}\partial_u x$ where $g = |\partial_u x|$. Epstein and Gage [36] showed how this degenerate parabolic equation (g needs not to be smooth enough) can be turned into the strictly parabolic equation $\partial_t x = g^{-2}\partial_u^2 x$ by choosing the tangential term α in the form $\alpha = g^{-1}\partial_u(g^{-1})\partial_u x$. This trick is known as "De Turck's trick" named after De Turck who uses this approach to prove short time existence for the Ricci flow (see [32]). Numerical aspects of this "trick" have been discussed by Dziuk and Deckelnick in [34, 35, 31]. In general, we allow the tangential velocity functional α appearing in (3.5) – (3.8) to be dependent on k, ν, g, x in various ways including non-local dependence, in particular (see the next chapter for details).

Let us denote $\Phi = (k, \nu, g, x)$. Let $0 < \varrho < 1$ be fixed. By E_k we

denote the following scale of Banach spaces (manifolds)

$$E_k = h^{2k+\varrho} \times h_*^{2k+\varrho} \times h^{1+\varrho} \times (h^{2+\varrho})^2, \tag{3.9}$$

where $k = 0, \frac{1}{2}, 1,$ and $h^{2k+\varrho} = h^{2k+\varrho}(S^1)$ is the "little" Hölder space (see [5]). By $h_*^{2k+\varrho}(S^1)$ we have denoted the Banach manifold $h_*^{2k+\varrho}(S^1) = \{\nu : \mathbb{R} \to \mathbb{R}\,, \vec{N} = (-\sin\nu, \cos\nu)^T \in (h^{2k+\varrho}(S^1))^2\}$. [1]

Concerning the tangential velocity α we will make a general regularity assumption:

$$\alpha \in C^1(\mathcal{O}_{\frac{1}{2}}, h^{2+\varrho}(S^1)) \tag{3.10}$$

for any bounded open subset $\mathcal{O}_{\frac{1}{2}} \subset E_{\frac{1}{2}}$ such that $g > 0$ for any $(k, \nu, g, x) \in \mathcal{O}_{\frac{1}{2}}$.

In the rest of this section we recall a general result on local existence and uniqueness a classical solution of the governing system of equations (3.5) – (3.8). The normal velocity β depending on k, x, ν belongs to a wide class of normal velocities for which local existence of classical solutions has been shown by Mikula and Ševčovič in [86, 87]. This result is based on the abstract theory of nonlinear analytic semigroups developed by Angenent in [5] an it utilizes the so-called maximal regularity theory for abstract parabolic equations.

Theorem 3.5 *[86, Theorem 3.1] Assume $\Phi_0 = (k_0, \nu_0, g_0, x_0) \in E_1$ where k_0 is the curvature, ν_0 is the tangential vector, $g_0 = |\partial_u x_0| > 0$ is the local length element of an initial regular closed curve $\Gamma_0 = Img(x_0)$ and the Banach space E_k is defined as in (3.9). Assume $\beta = \beta(k, \nu, x)$ is a C^4 smooth and 2π-periodic function in the ν variable such that $\min_{\Gamma_0} \beta_k'(x_0, k_0, \nu_0) > 0$ and α satisfies (3.10). Then there exists a unique solution $\Phi = (k, \nu, g, x) \in C([0,T], E_1) \cap C^1([0,T], E_0)$ of the governing system of equations (3.5) – (3.8) defined on some small time interval $[0,T]\,,\ T > 0$. Moreover, if Φ is a maximal solution defined on $[0, T_{max})$ then we have either*

- *either $T_{max} = +\infty$,*
- *or $\liminf_{t \to T_{max}^-} \min_{\Gamma^t} \beta_k'(x, k, \nu) = 0$,*

[1] Alternatively, one may consider the normal velocity β depending directly on the unit inward normal vector $\vec{N}$ belonging to the linear vector space $(h^{2k+\varrho}(S^1))^2$, i.e. $\beta = \beta(k, x, \vec{N})$.

- *or* $T_{max} < +\infty$ *and* $\max_{\Gamma^t} |k| \to \infty$ *as* $t \to T_{max}$.

Remark. The structural condition (3.10) has been relaxed for the case of the curvature adjusted tangential velocity by Ševčovič and Yazaki in [110]. In Chapter 4 we present a generalization of Theorem 3.5 to the case of the so-called curvature adjusted tangential velocity (see Theorem 4.1). It extends Theorem 3.5 for curvature driven flows whose normal velocity may contain non-local terms.

Remark. In a general case where the normal velocity may depend on the position vector x, the maximal time of existence of a solution can be either finite or infinite. Indeed, as an example one can consider the unit ball $B = \{|x| < 1\}$ and function $\delta(x) = (|x| - 1)^\gamma$ for $x \notin B$, $\gamma > 0$. Suppose that $\Gamma_0 = \{|x| = R_0\}$ is a circle with a radius $R_0 > 1$ and the family $\Gamma^t, t \in [0, T)$, evolves according to the normal velocity function $\beta(x, k) = \delta(x)k$. Then, it is an easy calculus to verify that the family Γ^t approaches the boundary $\partial B = \{|x| = 1\}$ in a finite time $T_{max} < \infty$ provided that $0 < \gamma < 1$ whereas $T_{max} = +\infty$ in the case $\gamma = 1$.

At the end of this section we recall result due to Mikula and Ševčovič [85] on existence and uniqueness of solution to curvature driven flow with degenerate normal velocity. We will assume that the normal velocity function $v = \beta(k, \nu)$ has the form

$$\beta(k, \nu) = \gamma(\nu)|k|^{m-1}k,$$

where $m > 0$ and $\gamma : \mathbb{R} \to \mathbb{R}^+$ is a strictly positive and bounded C^∞ smooth anisotropy function. The proof of the following theorem is based on iterative boot-strap estimates of Nash-Moser type.

Theorem 3.6 *[85, Theorems 5.6 and 6.3] Suppose that* $\beta(k, \nu) = \gamma(\nu)|k|^{m-1}k$, *where* $0 < m \le 2$. *Let* $\Gamma^0 = Img(x^0)$ *be a smooth regular plane curve such that* $(k^0, \nu^0, g^0)^T \in \mathcal{O}_1 \subset E_1 = h^{2+\varrho} \times h^{2+\varrho}_* \times h^{1+\varrho}$. *We also suppose that* Γ^0 *satisfies the condition* $\int_{\Gamma^0} |k^0|^{1-m}\, ds < \infty$.

Then there exists $T > 0$ *and a family of regular plane curves* $\Gamma^t = Img(x(., t)), t \in [0, T]$ *such that*

1) $x, \partial_u x \in (C(\overline{Q_T}))^2$, $\partial_u^2 x,\ \partial_t x,\ \partial_u \partial_t x \in (L^\infty(Q_T))^2$;

2) *the flow* $\Gamma^t = Img(x(., t)), t \in [0, T]$ *of regular plane curves satisfies the geometric equation*

$$\partial_t x = \beta \vec{N} + \alpha \vec{T},$$

where $\beta = \beta(k, \nu)$ and α is the tangential velocity preserving the relative local length, i.e.,

$$\frac{|\partial_u x(u,t)|}{L^t} = \frac{|\partial_u x^0(u)|}{L^0}$$

for any $t \in [0, T]$ and $u \in [0, 1]$.

The assumption $\int_{\Gamma^0} |k^0|^{1-m}\, ds < \infty$ might seem to be restrictive. But it is fulfilled in the case when the initial curve Γ^0 is strictly convex or in the case of a non-convex smooth curve whose inflection points have at most $(2+1/(m-1))$-order contact with their tangents. As an example one can consider the Bernoulli lemniscate $(x^2 + y^2)^2 = 4xy$ having the third-order contact with its tangents at the origin so this condition is satisfied iff $1 < m < 2$.

Chapter 4

Numerical methods for the direct approach

Analytical methods for mathematical treatment of the geometric equation (1.1) are strongly related to numerical techniques for computing curve evolutions. In the *direct approach* one seeks for a parametrization of the evolving family of curves. By solving the so-called *intrinsic heat equation*

$$\partial_t x = \beta \vec{N} + \alpha \vec{T}$$

one can directly find a position vector of a curve (see, e.g. Deckelnick [33, 34, 35], Mikula and Ševčovič [84, 85, 86, 87, 88]). There are also other direct methods based on the solution of a porous medium–like equation for curvature of a curve (see Mikula and Kačur [83, 82]), a crystalline curvature approximation due to Girão and Kohn [46, 47], Ushijima and Yazaki [122], special finite difference schemes by Kimura [65, 66], motion of polygonal curves in an equivalent class by Beneš, Kimura, Tagami and Yazaki [16, 15, 67], and a method based on erosion of polygons in the affine invariant scale case due to Moissan [93].

The direct approach for solving (1.1) can be accompanied by a suitable choice of a tangential velocity α significantly improving and stabilizing numerical computations. It was documented by many authors (see, e.g. Deckelnick [31], Hou, Lowengrub and Shelley [56, 55], Mikula and Ševčovič [84, 85, 86, 87]). We show that tangential velocity stabilizes semi-implicit scheme. The tangential redistribution is related to an integral average of $k\beta$ along the curve

and not to point-wise values of $k\beta$. The point-wise influence of this term would lead to severe time step restriction in a neighborhood of corners while our approach benefits from an overall smoothness of the curve. Thus the method allows for choosing of larger time steps without loss of stability.

In this chapter we discuss a fully discrete numerical scheme for the direct approach for solving the geometric equation (1.1). It is based on numerical approximation of a solution to the system of governing equations (2.9)–(2.12). The numerical scheme is semi-implicit in time, i.e. all nonlinearities are treated from the previous time step and linear terms are discretized at the current time level. Then we solve tridiagonal systems in every time step in a fast and simple way by means of the Thomas algorithm.

We remind ourselves that other popular techniques, like, e.g. level-set method due to Osher and Sethian [116, 98] or phase-field approximations (see e.g. Caginalp, Elliott *et al.* or Beneš [23, 37, 12, 14]) treat the geometric equation (1.1) by means of a solution to a higher dimensional parabolic problem. In comparison to these methods, in the direct approach one space dimensional evolutionary problems are solved only.

4.1 A role of the choice of a suitable tangential velocity

The main purpose of this section is to discuss various possible choices of the tangential velocity functional α appearing in the system of governing equations (2.9)–(2.12). In this system α can be viewed as a free parameter, which has to be determined in an appropriate way. Recall that k, ν, g, x do depend on α but the family $\{\Gamma^t = \mathrm{Img}(x(\cdot,t)), t \in [0,T)\}$, itself is independent of a particular choice of α.

To motivate further discussion, we recall some computational examples in which the usual choice $\alpha = 0$ fails and may lead to serious numerical instabilities like, e.g. formation of the so-called swallow tails. In Fig. 4.1 and 4.2 we computed the mean curvature flow of two initial curves (bold faced curves). We chose $\alpha = 0$ in the experiment shown in Fig. 4.1. It should be obvious that numerically computed grid points merge in some parts of the curve Γ^t preventing thus numerical approximation of $\Gamma^t, t \in [0,T)$, to be continued beyond some

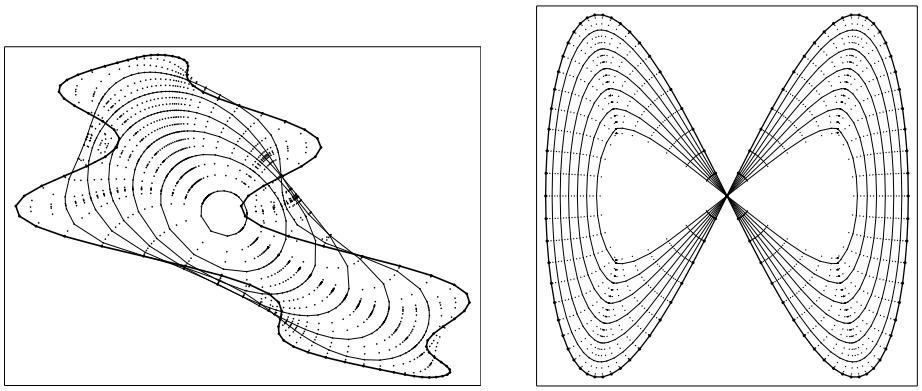

Figure 4.1: Merging of numerically computed grid points in the case of the vanishing tangential velocity functional $\alpha = 0$. Source: Mikula and Ševčovič [85].

time T, which is still far away from the maximal time of existence T_{max}. These examples also showed that a suitable grid points redistribution governed by a nontrivial tangential velocity functional α is needed in order to compute the solution on its maximal time of existence.

The idea behind the construction of a suitable tangential velocity functional α is rather simple and consists in the analysis of the quantity θ defined as follows:

$$\theta = \ln(g/L),$$

where $g = |\partial_u x|$ is a local length and L is a total length of a curve $\Gamma = \mathrm{Img}(x)$. The quantity θ can be viewed as the logarithm of the relative local length g/L. Taking into account equations (2.11) and (2.13) we have

$$\partial_t \theta + k\beta - \langle k\beta \rangle_\Gamma = \partial_s \alpha \,. \tag{4.1}$$

By appropriate choice of $\partial_s \alpha$ in the right hand side of (4.1) we can therefore control behavior of θ. Equation (4.1) can be also viewed as a kind of a constitutive relation determining redistribution of grid points along a curve.

4.1.1 Non-locally dependent tangential velocity functional

We first analyze the case when $\partial_s\alpha$ (and so does α) depends on other geometric quantities k, β and g in a non-local way. The simplest possible choice of $\partial_s\alpha$ is:

$$\partial_s\alpha = k\beta - \langle k\beta\rangle_\Gamma \tag{4.2}$$

yielding $\partial_t\theta = 0$ in (4.1). Consequently,

$$\frac{g(u,t)}{L^t} = \frac{g(u,0)}{L^0} \quad \text{for any } u \in S^1,\ t \in [0, T_{max})\,.$$

Recall that in Theorem 3.6 we proved local existence and uniqueness of solution to the governing system of equations.

Notice that α can be uniquely computed from (4.2) under the additional renormalization constraint: $\alpha(0,t) = 0$, i.e. one point $x_0 = x(0,t)$ is not moved in the tangential direction. In the sequel, tangential redistribution driven by a solution α to (4.2) will be refereed to as *a parametrization preserving relative local length*. It has been first discovered and utilized by Hou *et al.* in [56, 55] and independently by Mikula and Ševčovič in [84, 85, 86, 87].

A general choice of α is based on the following setup:

$$\partial_s\alpha = k\beta - \langle k\beta\rangle_\Gamma + \left(e^{-\theta} - 1\right)\omega(t), \tag{4.3}$$

where $\omega \in L^1_{loc}([0, T_{max}))$ is an auxiliary positive redistribution function. If we additionally suppose

$$\int_0^{T_{max}} \omega(\tau)\, d\tau = +\infty \tag{4.4}$$

then, after insertion of (4.3) into (4.1) and solving the ODE $\partial_t\theta = \left(e^{-\theta} - 1\right)\omega(t)$, we obtain $\theta(u,t) \to 0$ as $t \to T_{max}$ and hence

$$\frac{g(u,t)}{L^t} \to 1 \quad \text{as } t \to T_{max} \quad \text{uniformly w.r. to } u \in S^1.$$

In this case, redistribution of grid points along a curve becomes uniform as t approaches the maximal time of existence T_{max}. We will refer to the parametrization based on (4.3) to as *an asymptotically uniform parametrization*. The impact of the tangential velocity functional defined as in (4.2) on enhancement of redistribution of grid

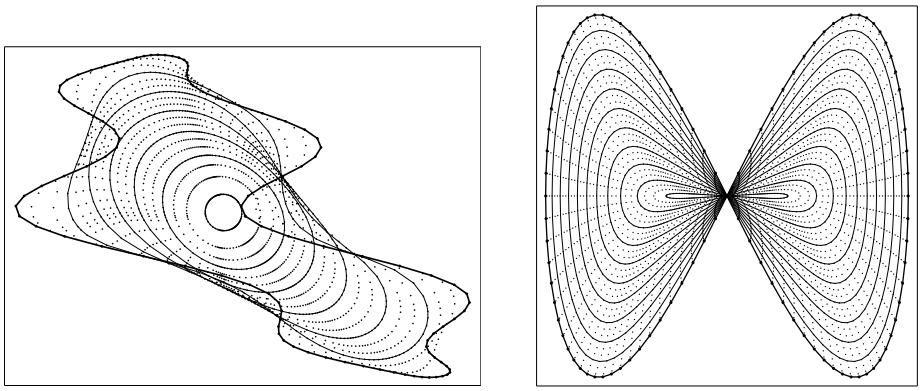

Figure 4.2: Effect of asymptotically uniform tangential redistribution velocity α on enhancement of spatial grids redistribution. Source: Mikula and Ševčovič [85].

points can be observed from two examples shown in Fig. 4.2 computed by Mikula and Ševčovič in [85].

Asymptotically uniform redistribution of grid points is of a particular interest in the case when the family $\{\Gamma^t, t \in [0,T)\}$ shrinks to a point as $t \to T_{max}$, i.e. $\lim_{t\to T_{max}} L^t = 0$. Then one can choose $\omega(t) = \kappa_2 \langle k\beta \rangle_{\Gamma^t}$ where $\kappa_2 > 0$ is a positive constant. By (2.13), $\int_0^t \omega(\tau)\, d\tau = -\kappa_2 \int_0^t \ln L^\tau d\tau = \kappa_2(\ln L^0 - \ln L^t) \to +\infty \quad$ as $t \to T_{max}$. On the other hand, if the length L^t is away from zero and $T_{max} = +\infty$ one can choose $\omega(t) = \kappa_1$, where $\kappa_1 > 0$ is a positive constant in order to fulfill assumption (4.4).

Summarizing, in both types of grid points redistributions discussed above, a suitable choice of the tangential velocity functional α is given by a solution to the equation:

$$\partial_s \alpha = k\beta - \langle k\beta \rangle_\Gamma + (L/g - 1)\,\omega\,,\ \alpha(0) = 0\,, \tag{4.5}$$

where $\omega = \kappa_1 + \kappa_2 \langle k\beta \rangle_\Gamma$ and $\kappa_1, \kappa_2 \geq 0$ are given constants.

If we insert the tangential velocity functional α computed from (4.5) into (2.9)–(2.12) and make use of the identity $\alpha \partial_s k = \partial_s(\alpha k) - k\partial_s \alpha$ then the system of governing equations can be rewritten as fol-

lows:

$$\partial_t k = \partial_s^2 \beta + \partial_s(\alpha k) + k\langle k\beta\rangle_\Gamma + (1 - L/g)\, k\omega\,, \tag{4.6}$$

$$\partial_t \nu = \beta'_k \partial_s^2 \nu + (\alpha + \beta'_\nu)\partial_s \nu + \nabla_x \beta \cdot \vec{T}\,, \tag{4.7}$$

$$\partial_t g = -g\langle k\beta\rangle_\Gamma + (L - g)\omega\,, \tag{4.8}$$

$$\partial_t x = \beta \vec{N} + \alpha \vec{T}\,. \tag{4.9}$$

It is worth to note that the strong reaction term $k^2\beta$ in (2.9) has been replaced by the averaged term $k\langle k\beta\rangle_\Gamma$ in (4.6). A similar phenomenon can be observed in (4.8). This is a very important feature of non-local tangential velocity as it allows for construction of an efficient and stable numerical scheme.

4.1.2 Locally dependent tangential velocity functional

Another possibility for grid points redistribution along evolved curves is based on a tangential velocity functional defined locally. If we take $\alpha = \partial_s \theta$, i.e. $\partial_s \alpha = \partial_s^2 \theta$ then the constitutive equation (4.1) reads as follows: $\partial_t \theta + k\beta - \langle k\beta\rangle_\Gamma = \partial_s^2 \theta$. Since this equation has a parabolic nature one can expect that variations in θ are decreasing during evolution and θ tends to a constant value along the curve Γ due to the diffusion process. The advantage of the particular choice

$$\alpha = \partial_s \theta = \partial_s \ln(g/L) = \partial_s \ln g \tag{4.10}$$

has been already indirectly observed by Deckelnick in [31]. He analyzed the mean curvature flow of planar curves (i.e. $\beta = k$) by means of a solution to the intrinsic heat equation

$$\partial_t x = \frac{\partial_u^2 x}{|\partial_u x|^2}\,, \quad u \in S^1, t \in (0, T),$$

describing the evolution of the position vector x of a curve $\Gamma^t = \mathrm{Img}(x(\cdot, t))$. By using Frenét's formulae we obtain $\partial_t x = k\vec{N} + \alpha\vec{T}$ where $\alpha = \partial_s \ln g = \partial_s \ln(g/L) = \partial_s \theta$.

Inserting the tangential velocity functional $\alpha = \partial_s \theta = \partial_s(\ln g)$ into (2.9)–(2.12) we obtain the following system of governing equations:

$$\partial_t k = \partial_s^2 \beta + \alpha \partial_s k + k^2 \beta, \tag{4.11}$$

$$\partial_t \nu = \beta'_k \partial_s^2 \nu + (\alpha + \beta'_\nu)\partial_s \nu + \nabla_x \beta \cdot \vec{T}, \tag{4.12}$$

$$\partial_t g = -gk\beta + g\partial_s^2(\ln g), \tag{4.13}$$

$$\partial_t x = \beta \vec{N} + \alpha \vec{T}\,. \tag{4.14}$$

Notice that equation (4.13) is a nonlinear parabolic equation whereas (4.8) is a non-local ODE for the local length g.

4.1.3 Curvature adjusted tangential velocity

Besides these uniform or asymptotically uniform redistribution methods, in the so-called crystalline curvature flow, the grid points are distributed densely (sparsely) in those part of the curve where the absolute value of the curvature is large (small). Although this redistribution is far from being uniform, numerical computation is quite stable. One of the reasons for such behavior is that polygonal curves are restricted to a class of admissible facet directions. In order to extract essence of the crystalline curvature flow of polygonal curves and generalize it to a wide class of plane curve evolution, Yazaki [124] showed that the tangential velocity $\alpha = -\partial_s \beta / k$ is implicitly involved in the crystalline curvature flow of planar curves.

Our aim is to design the relative local length ratio and, subsequently, α such that redistribution takes into account the shape of the limiting curve. In other words, how to densely (sparsely) redistribute grid points on those parts of a curve where the modulus of the curvature is large (small).

The modulus $|k|$ of curvature will be measured by the shape function $\varphi(k)$. As an example of a shape function one can consider $\varphi(k) \equiv 1$ or $\varphi(k) = |k|$. Now, let us introduce a generalized relative local length adopted to the shape function φ as follows:

$$r_\varphi(u,t) = \frac{g(u,t)}{L^t} \frac{\varphi(k(u,t))}{\langle \varphi(k(\cdot,t)) \rangle}, \quad u \in [0,1], \quad t \in [0,T). \tag{4.15}$$

Here, the bracket $\langle F \rangle$ denotes the average of function F over the curve Γ.

Next we explain the role of the generalized ratio r_φ. Suppose, for a moment, that $r_\varphi(u,t) \equiv 1$ for all u at a time t. Hence, if $|k|$

is above/below the average in the sense that $\varphi(k) \gtrless \langle\varphi(k)\rangle$, then $g \lesseqgtr L$ holds, respectively. Therefore the distribution of grid points on corresponding sub-arcs is dense/sparse, respectively.

In [109] Yazaki and Ševčovič constructed the tangential velocity α with the property that the generalized ratio r_φ tends to unity as $t \to T_{max}$ (see also [19]). Using the expression (4.15) and following similar ideas as in Section 4.1.1 the curvature adjusted tangential velocity α is given by the equation:

$$\partial_s(\varphi(k)\alpha) = f - \frac{\langle f\rangle}{\langle\varphi(k)\rangle}\varphi(k) + \omega(t)\varphi(k)(r_\varphi^{-1} - 1). \tag{4.16}$$

where $f = \varphi(k)k\beta - \varphi'(k)\left(\partial_s^2\beta + k^2\beta\right)$ and ω is a redistribution function. In order to construct a unique solution α, we assume the following renormalization condition for α:

$$\langle\varphi(k)\alpha\rangle = 0. \tag{4.17}$$

We refer to the paper by Yazaki and Ševčovič [109] for details on the derivation of the curvature adjusted tangential velocity. The approach can be applied to the motion of open curves (cf. Osaki, Satoh, and Yazaki [97]) or the Hele-Shaw or combined with the boundary element method (cf. Yazaki [125]).

Clearly, if $\varphi(k) \equiv 1$ we obtain the uniform (if $\omega = 0$) or asymptotically uniform tangential redistribution (if $\int_0^{T_{max}} \omega(\tau)d\tau = \infty$) introduced in Section 4.1.1.

Suppose that the evolving curve Γ^t is convex. If we consider the shape function $\varphi(k) = |k|$ and $\omega(t) \equiv 0$, then, with regard to (4.16) we have $\partial_s(k\alpha) = -\partial_s^2\beta$. Taking into account the renormalization constraint $\langle\varphi(k)\alpha\rangle = 0$ we end up with $\alpha = -\partial_s\beta/k$. This is exactly the same tangential velocity as it was derived by Yazaki in the continuous limit of the crystalline curvature flow (see [124]).

Minimization of the length and area discrepancy and curvature adjusted tangential redistribution

In [109] we studied an interesting question what is the optimal redistribution of a finite number of vertices $\{x^1, x^2, \cdots, x^N\}$ belonging to a given smooth closed curve Γ such that the discrepancy between the length or area of Γ and that of a polygon spanned by those vertices is minimal. Using the Lagrange multipliers method (cf., e.g. Hamala

Figure 4.3: Various redistributions of $N = 12$ grid points along the ellipse: (left) the length discrepancy minimizing curvature adjusted redistribution with $\varphi(k) = |k|^{2/3}$, and (right) the area discrepancy minimizing curvature adjusted redistribution with $\varphi(k) = |k|^{1/3}$. Source: Ševčovič and Yazaki [109].

and Trnovská [52, Chapter 1]) we found optimal solutions to the discrete optimization problems:

$$\min_{X\subset\Gamma}(L(\Gamma) - \mathcal{L}(X)), \qquad \min_{X\subset\Gamma}(A(\Gamma) - \mathcal{A}(X)), \tag{4.18}$$

for the minimization of the length approximation discrepancy and area approximation discrepancy, respectively. Here, $X = \{x^1, x^2, \cdots, x^N\}$ are discrete points belonging to a given curve Γ, $\mathcal{L}(X)$ and $\mathcal{A}(X)$ are the length and area of the polygon $poly(X)$. We proved that, in the limit $N \to \infty$, the length/area discrepancy minimizing redistribution of $X = \{x^1, x^2, \cdots, x^N\}$, is related to the curvature adjusted redistribution discussed in previous section with the shape functions

$$\begin{aligned} \varphi(k) &= |k|^{2/3} \quad \text{for the length discrepancy,} \\ \varphi(k) &= |k|^{1/3} \quad \text{for the area discrepancy.} \end{aligned}$$

Local existence, uniqueness and continuation of solutions

Unfortunately, except of the case $\varphi(k) \equiv 1$ the local existence result Theorem 3.5 from Chapter 3 cannot be applied directly because the structural condition (3.10) is not satisfied. This is due to the fact that the right-hand side of the equation (4.16) contains the second derivative of $\beta = \beta(k, \nu, x)$ and, as a consequence we obtain

$$\alpha \in C^1(\mathcal{O}_{\frac{1}{2}}, h^\varrho(S^1)) \tag{4.19}$$

(see [110, Lemma 1]). Hence $\partial_s\alpha$ entering the governing equation for the local length (3.7) need not exist. But this drawback can be

overcome by a simple "trick" developed in our paper [110]. Instead of g we will consider the equation for the relative ratio r_φ. With regard to the construction of the curvature adjusted tangential velocity we obtain

$$\partial_t k = \partial_s^2 \beta + \alpha \partial_s k + k^2 \beta, \tag{4.20}$$

$$\partial_t \nu = \beta'_k \partial_s^2 \nu + (\alpha + \beta'_\nu)\partial_s \nu + \nabla_x \beta . \vec{T}, \tag{4.21}$$

$$\partial_t r_\varphi = (r_\varphi - 1)(\kappa_1 + \kappa_2 \langle k\beta \rangle), \tag{4.22}$$

$$\partial_t x = w \partial_s^2 x + \alpha \partial_s x + F\vec{N}, \tag{4.23}$$

which is equivalent to the system (3.5)–(3.8) for the case when the normal velocity is rewritten in the form:

$$\beta(k, \nu, x) = w(k, \nu, x)k + F(\nu, x)$$

and $\omega \equiv \kappa_1 + \kappa_2 \langle k\beta \rangle$. Indeed, we can express the differential

$$ds = g^{-1} du = \frac{L\langle \varphi(k) \rangle}{\varphi(k)} r_\varphi du$$

and consequently the derivative ∂_s in terms of r_φ, k and the derivative ∂_u.

A solution $\Phi = (k, \nu, r_\varphi, x)$ to the system of PDEs (4.20)–(4.23) is subject to the initial condition $\Phi(\cdot, 0) = \Phi_0$ corresponding to the initial curve $\Gamma^0 = \mathrm{Img}(x_0)$.

Similarly as in Theorem 3.5 (see Chapter 3) we define the following scale of Banach space

$$E_\mu = h^{2\mu+\varrho} \times h_*^{2\mu+\varrho} \times h^{1+\varrho} \times (h^{2\mu+\varrho})^2 \quad \text{for } \mu = 0,\ 1/2,\ 1.$$

By $h_*^{2\mu+\varrho}(S^1)$ we denoted the Banach manifold $h_*^{2\mu+\varrho}(S^1) = \{\nu : \mathbb{R} \to \mathbb{R}, \vec{N} = (-\sin\nu, \cos\nu)^T \in (h^{2\mu+\varrho}(S^1))^2\}$. Here, $h^{2\mu+\varrho}$ is the little Hölder space (see Chapter 3).

Assuming $\varphi = \varphi(k)$ and $\beta = \beta(k, \nu, x)$ are at least C^3 smooth functions such that $\varphi(k) > 0$ and β is a 2π-periodic function in the ν variable. Furthermore, by $\mathcal{O}_{\frac{1}{2}} \subset E_{\frac{1}{2}}$ we will denote a bounded open subset such that $r_\varphi > 0$ for any $(k, \nu, r_\varphi, x) \in \mathcal{O}_{\frac{1}{2}}$. Following similar techniques as in the proof of Theorem 3.5, in [110] Ševčovič and Yazaki proved the following local existence and uniqueness result:

Theorem 4.1 *[110, Theorem 1] Assume $\Phi_0 = (k_0, \nu_0, r_{\varphi 0}, x_0) \in E_1$ where k_0 is the curvature, ν_0 is the tangential vector, $r_{\varphi 0} > 0$ is the φ-adjusted relative local length of an initial regular curve $\Gamma^0 = Img(x_0)$. Assume $\varphi(k) > 0$ and $\beta \equiv \tilde{\beta}(k, \nu, x) + F_\Gamma$ where $\tilde{\beta} : \mathbb{R}^2 \times \mathbb{R} \times \mathbb{R} \to \mathbb{R}$ and $\varphi : \mathbb{R} \to \mathbb{R}$ are C^3 smooth functions of their arguments such that $\tilde{\beta}$ is a 2π-periodic function in the ν variable and $\min_{\Gamma_0} \tilde{\beta}'_k(k_0, \nu_0, x_0) > 0$. The non-local part of the normal velocity F_Γ is assumed to be a C^1 smooth function from a neighborhood $\mathcal{O}_{\frac{1}{2}} \subset E_{\frac{1}{2}}$ of Φ_0 into $\mathbb{R}$, i.e. $F_\Gamma \in C^1(\mathcal{O}_{\frac{1}{2}}, \mathbb{R})$.*

Then there exists a unique solution $\Phi = (k, \nu, r_\varphi, x) \in C([0, T], E_1) \cap C^1([0, T], E_0)$ of the governing system of equations (4.20)–(4.23) defined on some time interval $[0, T]\,,\ T > 0$.

Furthermore, in [110] we showed the following global existence and continuation result:

Theorem 4.2 *[110, Theorem 2] Let $\{\Gamma^t, t \geq 0\}$, be a family of planar curves evolving in the normal direction with the velocity β for which short time existence of smooth solutions is guaranteed by Theorem* 4.1. *Suppose that $\Gamma^t, 0 \leq t < T_{max}$, is a maximal solution defined on the maximal time interval $[0, T_{max})$. If $T_{max} < +\infty$ then*

- *either $\|k\|_{0,\Gamma^t} + \|\beta\|_{0,\Gamma^t} \to \infty$ as $t \to T_{max}$,*
- *or $\sup_{0 \leq t < T_{max}} (\|k\|_{0,\Gamma^t} + \|\beta\|_{0,\Gamma^t}) < \infty$ and, in this case, $\liminf_{t \to T^-_{max}} \min_{\Gamma^t} \tilde{\beta}'_k(k, \nu, x) = 0$.*

Here $\|F\|_{0,\Gamma} = \max_\Gamma |F|$ and $\|F\|_{1,\Gamma} = \max_\Gamma (|F| + |\partial_s F|)$ are C^0 and C^1 norms of a quantity $F : \Gamma \to \mathbb{R}$.

4.2 Flowing finite volume approximation scheme

The aim of this part is to review numerical methods for solving the system of equations (2.9)–(2.12). We begin with a simple case in which we assume the normal velocity to be an affine function of the curvature with coefficients depending on the tangent angle only. Next we consider a slightly generalized form of the normal velocity in which coefficients may also depend on the position vector x.

In our computational method a solution of the evolution equation (1.1) is represented by discrete plane points $x_i^j, i = 0, \cdots, n,\ j = 0, \cdots, m$, where index i represents space discretization and index j a discrete time stepping. Since we only consider closed initial curves the periodicity condition $x_0^0 = x_n^0$ is required at the beginning. If we take a uniform division of the time interval $[0, T]$ with a time step $\tau = T/m$ and a uniform division of the fixed parametrization interval $[0, 1]$ with a step $h = 1/n$, a point x_i^j corresponds to $x(ih, j\tau)$. Difference equations will be given for discrete quantities $k_i^j,\ \nu_i^j,\ r_i^j,$ $i = 1, \cdots, n,\ j = 1, \cdots, m$ representing piecewise constant approximations of the curvature, tangent angle and element length for the segment $\left[x_{i-1}^j, x_i^j\right]$ and for α_i^j representing tangential velocity of the flowing node x_i^{j-1}.

Then, at the j-th discrete time level, $j = 1, \cdots, m$, the approximation of the curve is given by a discrete version of the position vector reconstruction formula

$$x_i^j = x_0^j + \sum_{l=1}^{i} r_l^j (\cos(\nu_l^j), \sin(\nu_l^j))^T, \quad i = 1, \cdots, n. \tag{4.24}$$

Using the Newton-Leibniz formula and constant approximation of the quantities inside flowing control volumes, at any time t we get

$$\alpha_i - \alpha_{i-1} = r_i k_i \beta(k_i, \nu_i) - r_i B - \omega \left(r_i - \frac{L}{n} \right).$$

By taking discrete time stepping, for *values of the tangential velocity* α_i^j we obtain

$$\alpha_i^j = \alpha_{i-1}^j + r_i^{j-1} k_i^{j-1} \beta(k_i^{j-1}, \nu_i^{j-1}) - r_i^{j-1} B^{j-1} - \omega(r_i^{j-1} - M^{j-1}), \tag{4.25}$$

$i = 1, \cdots, n$, with $\alpha_0^j = 0$ (x_0^j is moving only in the normal direction) where

$$M^{j-1} = \frac{1}{n} L^{j-1},\ L^{j-1} = \sum_{l=1}^{n} r_l^{j-1},\ B^{j-1} = \frac{1}{L^{j-1}} \sum_{l=1}^{n} r_l^{j-1} k_l^{j-1} \beta(k_l^{j-1}, \nu_l^{j-1})$$

and $\omega = \kappa_1 + \kappa_2 B^{j-1}$, κ_1, κ_2 are redistribution parameters.

Using the similar approach as above, we obtain

$$\frac{dr_i}{dt} + r_i B + r_i \omega = \omega \frac{L}{n},$$

where r_i is the approximation of the local length $g = |\partial_u x|$ at x_i. By taking a backward time difference we obtain an update for local lengths

$$r_i^j = \frac{r_i^{j-1} + \tau\omega M^{j-1}}{1 + \tau(B^{j-1} + \omega)}, \quad i = 1, \cdots, n, \quad r_0^j = r_n^j, \quad r_{n+1}^j = r_1^j. \tag{4.26}$$

Local lengths are used for approximation of intrinsic derivatives in (2.9) – (2.12). Integrating the equation for the curvature (2.9) in flowing control volume $[x_{i-1}, x_i]$ we obtain

$$r_i \frac{dk_i}{dt} = [\partial_s \beta(k, \nu)]_{x_{i-1}}^{x_i} + [\alpha k]_{x_{i-1}}^{x_i} + k_i(r_i(B + \omega) - \omega\frac{L}{n}).$$

Now, by replacing the time derivative by the time difference, approximating k in nodal points by the average value of neighboring segments, and using the semi-implicit approach we obtain a *tridiagonal system* with periodic boundary conditions imposed for new discrete values of the curvature

$$a_i^j k_{i-1}^j + b_i^j k_i^j + c_i^j k_{i+1}^j = d_i^j, \quad i = 1, \cdots, n, \quad k_0^j = k_n^j, \quad k_{n+1}^j = k_1^j. \tag{4.27}$$

A similar tridiagonal system of discrete equations can be obtained for the discrete values of the tangent angle ν_i^j. Solving tridiagonal equations for the curvature and tangent angle is fast and efficient because we can apply the fast Thomas algorithm. The point x_0^{j-1} is moved in the normal direction by $\beta^j \vec{N}^j$ only due to the zero tangential velocity $\alpha_0^j = 0$.

Normal velocity depending on the tangent angle and the position vector

Next we consider a more general motion of the curves with explicit dependence of the flow on position x and suggest numerical scheme for such a situation. We consider (1.1) with a linear dependence of β on the curvature, i.e.

$$\beta(k, \nu, x) = \delta(x, \nu)k + c(x, \nu),$$

where $\delta(x, \nu) > 0$. By using Frenét's formulae one can rewrite the position vector equation (2.12) as an intrinsic convection-diffusion

equation for the vector x and we get the system

$$\partial_t k = \partial_s^2 \beta + \partial_s(\alpha k) + k\frac{1}{L}\int_\Gamma k\beta ds + k\omega(1 - \frac{L}{g}), \quad (4.28)$$

$$\partial_t \nu = \beta'_k \partial_s^2 \nu + (\alpha + \beta'_\nu)\partial_s \nu + \nabla_x \beta \cdot \vec{T}, \quad (4.29)$$

$$\partial_t g = -g\frac{1}{L}\int_\Gamma k\beta ds - \omega(g - L), \quad (4.30)$$

$$\partial_t x = \delta(x,\nu)\partial_s^2 x + \alpha\partial_s x + \vec{C}(x,\nu), \quad (4.31)$$

where $\vec{C}(x,\nu) = c(x,\nu)\vec{N} = c(x,\nu)(-\sin\nu, \cos\nu)^T$. In comparison to the scheme given above, two new tridiagonal systems have to be solved at each time level in order to update the curve position vector x.

4.3 Tangential redistribution for the mean curvature driven flow of surfaces

In this section we present the key steps of derivation of construction of the tangential velocity for the mean curvature flow of surfaces driven in the normal direction by the geometric equation (1.2), i.e. $v = H + F$, where H is the mean curvature and F is a given external force.

We will consider a flow of immersed n-dimensional manifolds $\{\mathcal{M}^t, t \geq 0\}$ driven by (1.2). We will assume that an immersed manifold $\mathcal{M}$ is parametrized by a mapping

$$X : \mathcal{U} \subset \mathbb{R}^n \to \mathbb{R}^{n+1},$$

where X is a differentiable immersion, i.e. its derivative $X'(u) \in T_{X(u)}(\mathcal{M})$ is injective for all $u \in \mathcal{U}$. For simplicity, we will consider a manifold without boundary, i.e. $\partial\mathcal{M} = \emptyset$. This assumption simplifies derivation of the tangential velocity vector. A general case when $\partial\mathcal{M} \neq \emptyset$ is discussed in a detail in the paper [102] by Remešíková, Mikula, Sarkoci and Ševčovič.

First, we recall necessary definitions and notion from differential geometry. Let us proceed with definition of the corresponding Riemannian metric, which is an $n \times n$ matrix $g = (g_{ij})_{i,j=1,\cdots,n}$, where

$$g_{ij} = \partial_{u_i} X \cdot \partial_{u_i} X.$$

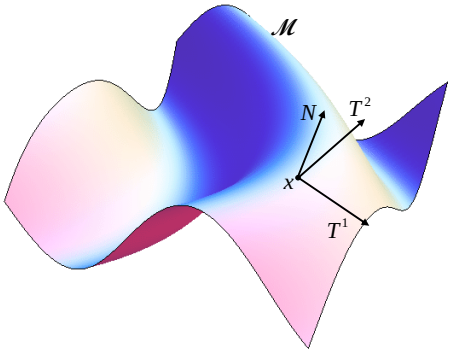

Figure 4.4: A manifold $\mathcal{M}$, its unit normal vector N and tangential vectors $T^1, T^2 \in T_X(\mathcal{M})$ at a point $X \in \mathcal{M}$.

Here, "$\cdot$" stands for the Euclidean inner product in $\mathbb{R}^{n+1}$. Let us denote by $g^{-1} = (g^{ij})_{i,j=1,\cdots,n}$ the inverse matrix of g. Let $A = (h_{ij})_{i,j=1,\cdots,n}$, be the second fundamental form, h_{ij} being defined as: $h_{ij} = \partial^2_{u_i u_j} X \cdot \vec{N}$, where $\vec{N}$ is the unit normal vector to $\mathcal{M}$ at the point X. Now the mean curvature H is just the trace of the second fundamental form, i.e.

$$H = trace(g^{-1}A) = g^{ij}h_{ij},$$

where we have used the Einstein convention for summation of repeating indices. For example, the N dimensional sphere of the radius $r > 0$ has the mean curvature $H = N/r$.

Let $\beta : \mathcal{M} \to \mathbb{R}^m$ be a function (scalar or vector valued). The Laplace-Beltrami operator of β is defined as

$$\Delta_{\mathcal{M}}\beta = g^{ij}\left(\partial^2_{u_i u_j}\beta(X(u)) - \Gamma^k_{ij}\partial_{u_k}\beta(X(u))\right),$$

where $\Gamma^k_{ij} = \frac{1}{2}g^{kl}(\partial_{u_i}g_{lj} + \partial_{u_j}g_{il} - \partial_{u_l}g_{ij})$ are the Christoffel symbols of the second kind. For example, if $\beta(X) = X$ is the position vector then

$$\Delta_{\mathcal{M}}X = H\vec{N}.$$

The position vector equation for time evolving family $\{\mathcal{M}^t = \text{Img}X(\cdot,t), t \geq 0\}$, has the general form

$$\partial_t X = \beta\vec{N} + \alpha^k\partial_{u_k}X,$$

where $\partial_{u_k} X, k = 1, \cdots, n$, are tangent vectors (not necessarily of the unit length) and $\alpha^k, k = 1, \cdots, n$, are components of the tangential velocity vector. The unit tangent vectors are then given by $\vec{T}^k = \partial_{u_k} X / |\partial_{u_k} X|$ (see Fig. 4.4). Similarly as in the previous section, derivation of a suitable tangential velocity relies on the equations for the entries g_{ij} of the Riemannian metrics g. After long but straightforward calculations Ševčovič in 2001 in unpublished note showed that

$$\partial_t g_{ij} = -2\beta h_{ij} + \alpha^k \partial_{u_k} g_{ij} + \partial_{u_i} \alpha^k g_{kj} + \partial_{u_j} \alpha^k g_{ik}.$$

Therefore for $G = \sqrt{\det g}$ we have

$$\partial_t G = -\beta H G + \partial_{u_k}(G\alpha^k).$$

This formula has been also derived by Bauer *et al.* [10].

Recall that for the total area $\mathcal{A}$ of the manifold $\mathcal{M}$ we have the expression

$$\mathcal{A} = \int_{\mathcal{M}} d\chi^n = \int_{\mathcal{U}} G du,$$

where $d\chi^n = G du$ is the n-dimensional Hausdorff measure.

Similarly, as in the one dimensional case of evolution of curves our aim is to control the ratio $G/\mathcal{A}$ of the local area G with respect to total area $\mathcal{A}$ of the surface $\mathcal{M}$. Using expression for the time derivative of G we conclude

$$\frac{d}{dt}\frac{G}{\mathcal{A}} = \frac{G}{\mathcal{A}} \left(-\beta H + \langle \beta H \rangle_{\mathcal{M}} + \frac{1}{G} \partial_{u_k}(G\alpha^k) \right),$$

where $\langle \beta H \rangle_{\mathcal{M}} = \frac{1}{\mathcal{A}} \int_{\mathcal{M}} \beta H d\chi^n$ is the average of βH over the manifold $\mathcal{M}$. Here, we have used the assumption that the manifold $\mathcal{M}$ has no boundary and so integration of the term $\frac{1}{G}\partial_{u_k}(G\alpha^k)$ over $\mathcal{M}$ yields zero.

Now, if we choose the tangential velocities $\alpha^k, k = 1, \cdots, n$, such that

$$\frac{1}{G}\partial_{u_k}(G\alpha^k) = \beta H - \langle \beta H \rangle_{\mathcal{M}} \tag{4.32}$$

we obtain

$$\frac{d}{dt}\frac{G}{\mathcal{A}} = 0 \quad \text{and so} \quad \frac{G(u,t)}{\mathcal{A}^t} = \frac{G(u,0)}{\mathcal{A}^0}$$

uniformly with respect to $u \in \mathcal{U}$. Therefore it yields uniform redistribution. On the other hand, if we choose the tangential velocities

$\alpha^k, k = 1, \cdots, n$, such that

$$\frac{1}{G}\partial_{u_k}(G\alpha^k) = \beta H - \langle \beta H \rangle_{\mathcal{M}} + \big(\frac{\mathcal{A}}{G} - 1\big)\omega, \tag{4.33}$$

where ω is a non-negative function such that $\int_0^{T_{max}} \omega(\tau)d\tau = \infty$ then our tangential velocities yield

$$\lim_{t \to T_{max}} \frac{G(u,t)}{\mathcal{A}^t} = 1 \quad \text{uniformly w.r. to } u \in \mathcal{U},$$

resulting thus in the asymptotically uniform redistribution, which was derived by Remešíková, Mikula, Sarkoci and Ševčovič in [102].

The tangential velocity vector $\alpha^k, k = 1, \cdots, n$, can be chosen as a gradient of a scalar tangential velocity potential ψ such that

$$\alpha = \nabla_{\mathcal{M}}\psi, \quad \text{and so} \quad \frac{1}{G}\partial_{u_k}(G\alpha^k) = \text{div}_{\mathcal{M}}(\alpha) = \Delta_{\mathcal{M}}\psi. \tag{4.34}$$

This form of tangential velocity simplifies computation of α. The uniform redistribution with scalar tangential velocity potential (4.34) has been used in practical computations of mean curvature evolving surfaces by Morigi in [94].

In Fig. 4.5 we present the comparison of the evolution of the initial surface with and without tangential redistribution. It was evolved in the normal direction by the mean curvature. The left column depicts evolution without consideration of a tangential redistribution whereas the right column illustrates its evolution when asymptotically uniform redistribution was applied. We can observe significantly better redistribution of discretization triangles when compared to those obtained without redistribution. The results were obtained by Remešíková, Mikula, Sarkoci and Ševčovič in [102].

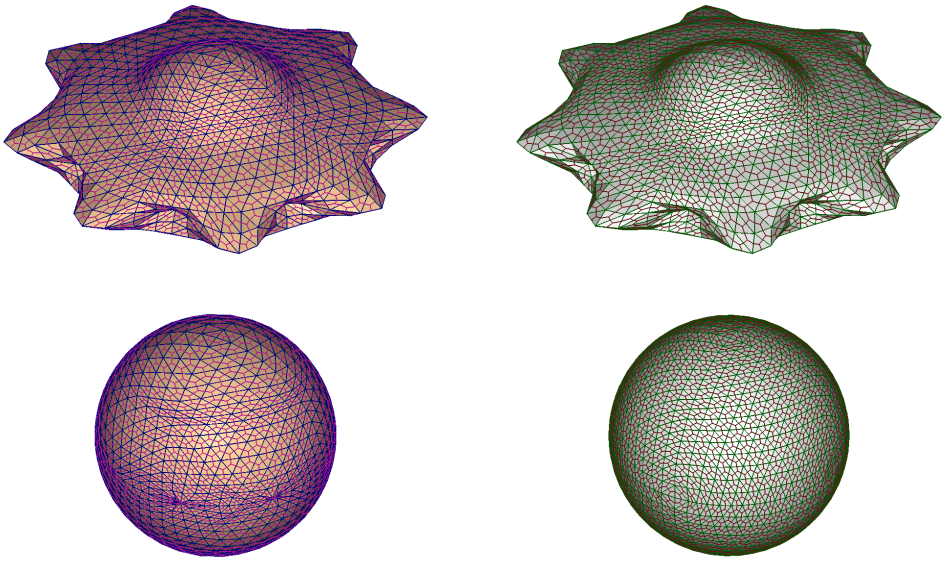

Figure 4.5: Mean curvature driven evolution of an initial closed surface without tangential redistribution (left) and with the asymptotically uniform tangential redistribution (right). Source: Remešíková, Mikula, Sarkoci and Ševčovič [102].

Chapter 5

Applications of the direct Lagrangian approach in curvature driven flows

The purpose of this chapter is to present results dealing with applications of the direct Lagrangian approach in various applied fields. We first review numerical results of the flowing finite volume numerical scheme described in Sections 4.2 and 4.3. Then we derive the governing equation for the evolution of curves driven by the geodesic curvature on a given surface and we present applications to construction of closed geodesic curves on a given surface. the following section is devoted to results of edge detection in image segmentation. We present a model for edge detection in static images as well as a model for tracking moving boundaries. Next we discuss theoretical results on nonlinear stability of a triple junction of a network of plane curves describing phase interfaces. Final sections are devoted to the study of non-local flows with special attention to gradient flows minimizing the isoperimetric ratio in the relative Finsler geometry and the inverse Wulff problem.

5.1 Computation of curvature driven evolution of planar curves with external force

In the following figures we present numerical solutions computed by the scheme discussed in Section 4.2. Initial curves are plotted

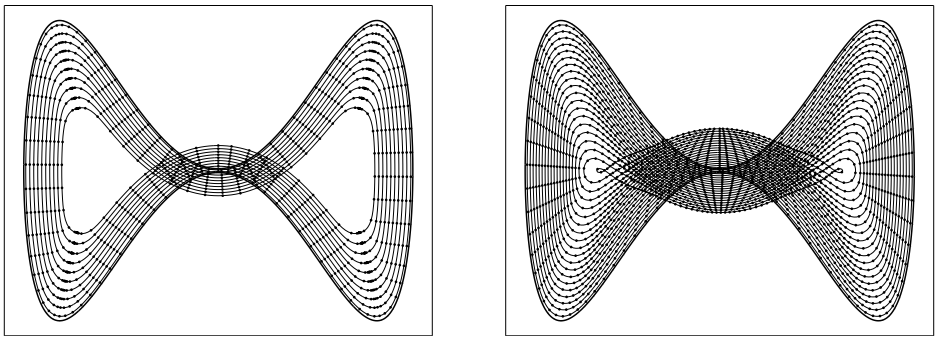

Figure 5.1: Isotropic curvature driven motion, $\beta(k,\nu) = \varepsilon k + F$, with $\varepsilon = 1$, $F = 10$, without (left) and with (right) uniform tangential redistribution of grid points. Source: Mikula and Ševčovič [86].

with a thick line and the numerical solution is given by solid lines with points representing the motion of grid points during the curve evolution. In Fig. 5.1 we compare computations with and without tangential redistribution for a large driving force F. As an initial curve we chose $x_1(u) = \cos(2\pi u)$, $x_2(u) = 2\sin(2\pi u) - 1.99\sin^3(2\pi u)$, $u \in [0,1]$. Without redistribution, the computations are collapsing soon because of the degeneracy in local element lengths in parts of a curve with high curvature leading to a merging of the corresponding grid points. Using the redistribution the evolution can be successfully handled. We used $\tau = 0.00001$, 400 discrete grid points and we plotted every $150th$ time step.

In Fig. 5.2 we present experiments with a three-fold anisotropy starting with unit circle. We used $\tau = 0.001$, 300 grid points and we plotted every $50th$ time step (left) and every $750th$ time step (right). In all experiments we chose redistribution parameters $\kappa_1 = \kappa_2 = 10$.

5.2 Flows of curves on a surface driven by the geodesic curvature

The purpose of this section is to analytically and numerically investigate a flow of closed curves on a given graph surface $\mathcal{M}$ driven by the geodesic curvature $\mathcal{K}_g$. We show how such a flow can be reduced to a flow of vertically projected planar curves governed by a solution of a fully nonlinear system of parabolic differential equa-

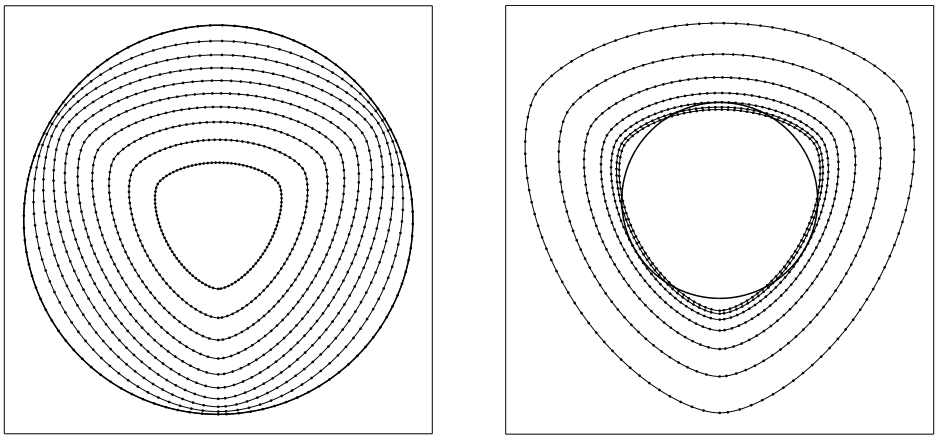

Figure 5.2: Anisotropic curvature driven motion of the initial unit circle including uniform tangential redistribution of grid points; $\beta(k,\nu) = \gamma(\nu)k + F$, with $\gamma(\nu) = 1 - \frac{7}{9}\cos(3\nu)$, $F = 0$ (left) and $\gamma(\nu) = 1 - \frac{7}{9}\cos(3\nu)$, $F = -1$ (right). Source: Mikula and Ševčovič [86].

tions. We present various computational examples of evolution of surface curves driven by the geodesic curvature are presented in this part. The normal velocity $\mathcal{V}$ of the evolving family of surface curves $\{\mathcal{G}^t, t \geq 0\}$, is proportional to the geodesic curvature $\mathcal{K}_g$ of $\mathcal{G}^t$, i.e.

$$\mathcal{V} = \delta \mathcal{K}_g, \tag{5.1}$$

where $\delta = \delta(X, \vec{\mathcal{N}}) > 0$ is a smooth positive coefficient describing anisotropy depending on the position X and the orientation of the unit inward normal vector $\vec{\mathcal{N}}$ to the curve on a surface.

The idea how to analyze and compute numerically such a flow is based on the so-called direct approach method applied to a flow of vertically projected family of planar curves. Vertical projection of surface curves on a simple surface $\mathcal{M}$ into the plane $\mathbb{R}^2$. It allows for reducing the problem to the analysis of evolution of planar curves $\Gamma^t : S^1 \to \mathbb{R}^2$, $t \geq 0$ driven by the normal velocity v given as a nonlinear function of the position vector x, tangent angle ν and as an affine function of the curvature k of Γ^t, i.e.

$$v = \beta(x, \nu, k) \equiv= a(x, \nu)k + c(x, \nu), \tag{5.2}$$

where $a(x,\nu) > 0, c(x,\nu)$ are bounded smooth coefficients.

5.2.1 Planar projection of the flow on a graph surface

Throughout this section we will always assume that the surface $\mathcal{M} = \{(x,z)) \in \mathbb{R}^3,\, z = \phi(x),\ x \in \Omega\}$ is a smooth graph of a function $\phi : \Omega \subset \mathbb{R}^2 \to \mathbb{R}$ defined in a domain $\Omega \subset \mathbb{R}^2$. Hereafter, the symbol (x,z) stands for a vector $(x_1,x_2,z) \in \mathbb{R}^3$, where $x = (x_1,x_2) \in \mathbb{R}^2$. In such a case any smooth closed curve $\mathcal{G}$ on the surface $\mathcal{M}$ can be then represented by its vertical projection to the plane, i.e. $\mathcal{G} = \{(x,z) \in \mathbb{R}^3,\, x \in \Gamma,\ z = \phi(x)\}$ where Γ is a closed planar curve in $\mathbb{R}^2$.

In [87, 88] Mikula and Ševčovič showed, that for a curve $\mathcal{G} = \{(x,\phi(x)) \in \mathbb{R}^3,\, x \in \Gamma\}$ on a surface $\mathcal{M} = \{(x_1,x_2,\phi(x_1,x_2)) \in \mathbb{R}^3,\ (x_1,x_2) \in \Omega\}$ the geodesic curvature $\mathcal{K}_g$ is given by

$$\mathcal{K}_g = \frac{1}{\Big(1+(\nabla\phi\cdot\vec{T})^2\Big)^{\frac{3}{2}}}\left(\big(1+|\nabla\phi|^2\big)^{\frac{1}{2}}\ k + \frac{\vec{T}^T\nabla^2\phi\,\vec{T}}{(1+|\nabla\phi|^2)^{\frac{1}{2}}}\nabla\phi\cdot\vec{N}\right) \tag{5.3}$$

(see [87]). Moreover, the unit inward normal vector $\vec{\mathcal{N}} \perp T_x(\mathcal{M})$ to a surface curve $\mathcal{G} \subset \mathcal{M}$ relative to $\mathcal{M}$ can be expressed as

$$\vec{\mathcal{N}} = \frac{\Big((1+(\nabla\phi\cdot\vec{T})^2)\vec{N} - (\nabla\phi.\vec{T})(\nabla\phi\cdot\vec{N})\vec{T},\ \nabla\phi\cdot\vec{N}\Big)}{\Big((1+|\nabla\phi|^2)(1+(\nabla\phi.\vec{T})^2)\Big)^{\frac{1}{2}}}$$

(see also [87]). Hence for the normal velocity $\mathcal{V}$ of $\mathcal{G}^t = \{(x,\phi(x)),\, x \in \Gamma^t\}$ we have

$$\mathcal{V} = \partial_t(x,\phi(x))\cdot\vec{\mathcal{N}} = (\vec{N},\nabla\phi\cdot\vec{N}).\beta\vec{\mathcal{N}} = \left(\frac{1+|\nabla\phi|^2}{1+(\nabla\phi\cdot\vec{T})^2}\right)^{\frac{1}{2}}\beta,$$

where β is the normal velocity of the vertically projected planar curve Γ^t having the unit inward normal $\vec{N}$ and tangent vector $\vec{T}$. Following the so-called direct approach discussed in Chapter 2 (see also [31, 34, 35, 56, 82, 84, 85, 86, 87, 88]) the evolution of planar curves $\Gamma^t, t \geq 0$, can be described by a solution $x = x(\cdot,t) \in \mathbb{R}^2$ to the position vector equation $\partial_t x = \beta\vec{N} + \alpha\vec{T}$ where β and α are normal and tangential velocities of Γ^t, respectively. Assuming the family of surface curves $\mathcal{G}_t$ satisfies (5.1) it has been shown in [87] that the geometric equation $v = \beta(k,\nu,x)$ for the normal velocity v of the

vertically projected planar curve Γ^t can be written in the following form:

$$v = \beta(k, \nu, x) \equiv a(x, \nu)\, k - b(x, \nu)\, \nabla\phi(x) \cdot \vec{N}, \tag{5.4}$$

where $a = a(x, \nu) > 0$ and $b = b(x, \nu)$ are smooth functions given by

$$a(x, \nu) = \frac{\delta}{1 + (\nabla\phi \cdot \vec{T})^2}\,, \quad b(x, \nu) = -a(x, \nu)\frac{\vec{T}^T \nabla^2\phi\, \vec{T}}{1 + |\nabla\phi|^2}\,, \tag{5.5}$$

where $\delta(X, \vec{\mathcal{N}}) > 0, X = (x, \phi(x)), \phi = \phi(x)$, k is the curvature of Γ^t, and $\vec{N} = (-\sin\nu, \cos\nu)^T$ and $\vec{T} = (\cos\nu, \sin\nu)^T$ are the unit inward normal and tangent vectors to a curve Γ^t.

We can also consider a more general flow of curves on a given surface driven by the normal velocity

$$\mathcal{V} = \mathcal{K}_g + \mathcal{F}, \tag{5.6}$$

where $\mathcal{F}$ is the normal component of a given external force $\vec{G}$, i.e. $\mathcal{F} = \vec{G} \cdot \vec{\mathcal{N}}$. The external vector field $\vec{G}$ is assumed to be perpendicular to the plane $\mathbb{R}^2$ and it may depend on the vertical coordinate $z = \phi(x)$ only, i.e.

$$\vec{G}(x) = -(0, 0, \gamma),$$

where $\gamma = \gamma(z) = \gamma(\phi(x))$ is a given scalar "gravity" functional.

Assuming the family of surface curves $\mathcal{G}^t$ satisfies (5.6) it has been shown in [87] that the geometric equation $v = \beta(k, \nu, x)$ for the normal velocity v of the vertically projected planar curve Γ^t can be written in the following form:

$$v = \beta(k, \nu, x) \equiv a(x, \nu)\, k - b(x, \nu)\, \nabla\phi(x) \cdot \vec{N},$$

where $a = a(x, \nu) > 0$ and $b = b(x, \nu)$ are smooth functions given by

$$a(x, \nu) = \frac{1}{1 + (\nabla\phi \cdot \vec{T})^2}\,, \quad b(x, \nu) = a(x, \nu)\left(\gamma(\phi) - \frac{\vec{T}^T \nabla^2\phi\, \vec{T}}{1 + (\nabla\phi \cdot \vec{T})^2}.\right), \tag{5.7}$$

In order to compute the evolution of surface curves driven by the geodesic curvature and external force we can use the numerical approximation scheme developed in Chapter 4 for the flow of vertically projected planar curves driven by the normal velocity given as in (5.4).

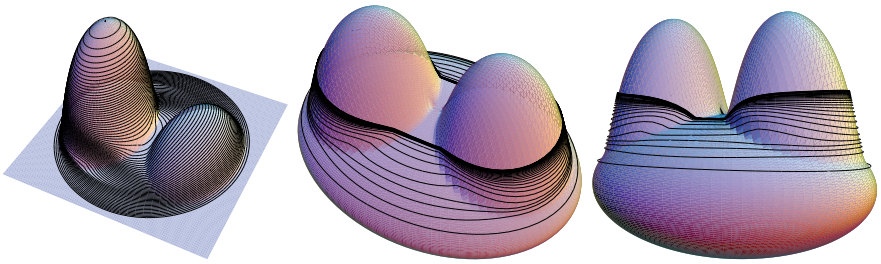

Figure 5.3: (Left) a geodesic flow $\mathcal{V} = \mathcal{K}_g$ on a surface with two humps having different heights, (middle, right) a geodesic flow on a surface with two sufficiently high humps. The evolving family of surface curves approaches a closed geodesic as $t \to \infty$. Source: Mikula and Ševčovič [88].

The next couple of examples illustrate a geodesic flow $\mathcal{V} = \mathcal{K}_g$ on a surface with two humps. In Fig. 5.3 (left) we show an example of an evolving family of surface curves shrinking to a point in finite time. In this example the behavior of evolution of surface curve is similar to that of planar curves for which Grayson's theorem holds. On the other hand, in Fig. 5.3 (middle, right) we present the case when the surface has two sufficiently high humps preventing evolved curve to pass through them. As it can be seen from Fig. 5.3 (middle, right) the evolving family of surface curves approaches a closed geodesic curve $\bar{\mathcal{G}}$ as $t \to \infty$.

The initial curve with large variations in the curvature is evolved according to the normal velocity $\mathcal{V} = \mathcal{K}_g + \mathcal{F}$ where the external force $\mathcal{F} = \vec{G} \cdot \vec{\mathcal{N}}$ is the normal projection of $\vec{G} = -(0, 0, \gamma)$ (see Fig. 5.4). In the numerical experiment we considered a strong external force coefficient $\gamma = 30$. The evolving family of surface curves approaches a stationary curve $\bar{\Gamma}$ lying in the bottom of the sharp narrow valley. In the next section we will show how this flow can be applied to the edge detection problem.

5.2.2 Stability of stationary curves

In this section we focus our attention on the analysis of closed stationary surface curves. We present sufficient conditions for their dynamic stability. A stationary curve is a surface curve $\bar{\Gamma}$ satisfying $\mathcal{K}_g + \mathcal{F} = 0$. Since there is a one-to-one correspondence between the flow of curves on a given surface and the flow of vertically projected

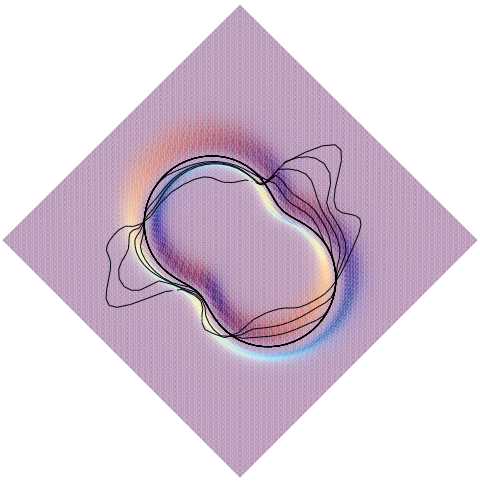

Figure 5.4: A geodesic flow on a flat surface with a sharp narrow valley. Source: Mikula and Ševčovič [88].

planar curves we will be concerned with stationary planar curves satisfying $\beta(k, \nu, x) = 0$, where β is given by (5.4). Linearized stability of stationary curves including, in particular, those arising from vertical projections of curves on surfaces has been investigated by Mikula and Ševčovič. We present the main result on linearized stability and show how the linearized stability criterion can be verified on concrete examples.

Definition 5.1 *A closed smooth planar curve $\bar{\Gamma} = Img(\bar{x})$ is called a stationary curve with respect to the normal velocity β iff $\bar{\beta} \equiv \beta(\bar{x}, \bar{k}, \bar{\nu}) = 0$ on $\bar{\Gamma}$ where $\bar{x}, \bar{k}$ and $\bar{\nu}$ are the position vector, curvature and tangential angle of the curve $\bar{\Gamma}$.*

Before stating the main result we need to introduce the following weight function $w : [0, 1] \to \mathbb{R}$, which plays an important role in the stability criterion. Let us define the function w as follows:

$$w(u) = \frac{\bar{g}}{\bar{\beta}'_k} \exp\left(\int_0^u \frac{\bar{\beta}'_\nu}{\bar{\beta}'_k} \bar{g}\, du \right). \tag{5.8}$$

It has been shown in [88, Proposition 3.2] that the weight function w is 1-periodic in the u-variable provided that the normal velocity β has one of the following forms:

a) $\beta(x,k) = a(x)k + c(x)$ where $a(x) > 0, c(x)$ are C^1 smooth functions;

b) $\beta(k,\nu,x) = a(\phi(x))k - b(\phi(x))\nabla\phi \cdot \vec{N}$ where $a(\phi) > 0, b(\phi)$ are C^1 smooth functions and $\phi(x)$ is C^2 smooth;

c) $\beta(k,\nu,x) = a(x,\nu)k - b(x,\nu)\nabla\phi \cdot \vec{N}$ where a, b are defined as in (5.5) and $\phi(x)$ is a C^2 smooth function.

The main result on linearized stability can be stated as follows:

Theorem 5.2 *[88, Theorem 3.1, Corollary 3.2] t A stationary curve $\bar{\Gamma}$ is linearly stable if $\sup_{\bar{\Gamma}} Q < 0$ and it is linearly unstable if $\int_0^1 Qw\,du > 0$ where $Q = \bar{\beta}'_{\bar{k}}\bar{k}^2 + \nabla_x\bar{\beta} \cdot \vec{\bar{N}}$ and w is the weight defined as in (5.8).*

In the examples shown in Fig. 5.5 we present numerical results of simulations of a surface flow driven by the geodesic curvature and gravitational like external force, $\mathcal{V} = \mathcal{K}_g + \mathcal{F}$, on a wave-let surface given by the graph of the function $\phi(x) = f(|x|)$ where $f(r) = \sin(r)/r$ and $\gamma = 2$. In the first example shown in Fig. 5.5 (left) we started from the initial surface curve having large variations in the geodesic curvature. The evolving family converges to the stable stationary curve $\bar{\Gamma} = \{x, |x| = \bar{r}\}$ with the second smallest stable radius. Vertical projections of evolving surface curves are shown in Fig. 5.5 (right).

5.3 Applications in the theory of image segmentation

5.3.1 Edge detection in static images

A similar equation to (1.1) arises from the theory of image segmentation in which detection of object boundaries occurring in the analyzed image plays an important role. A given black and white image can be represented by its intensity function $I : \mathbb{R}^2 \to [0, 255]$. The aim is to detect edges of the image, i.e. closed planar curves on which the gradient ∇I is large (see [62]). The method of the so-called active contour models is to construct an evolving family of plane curves converging to an edge (see [63]).

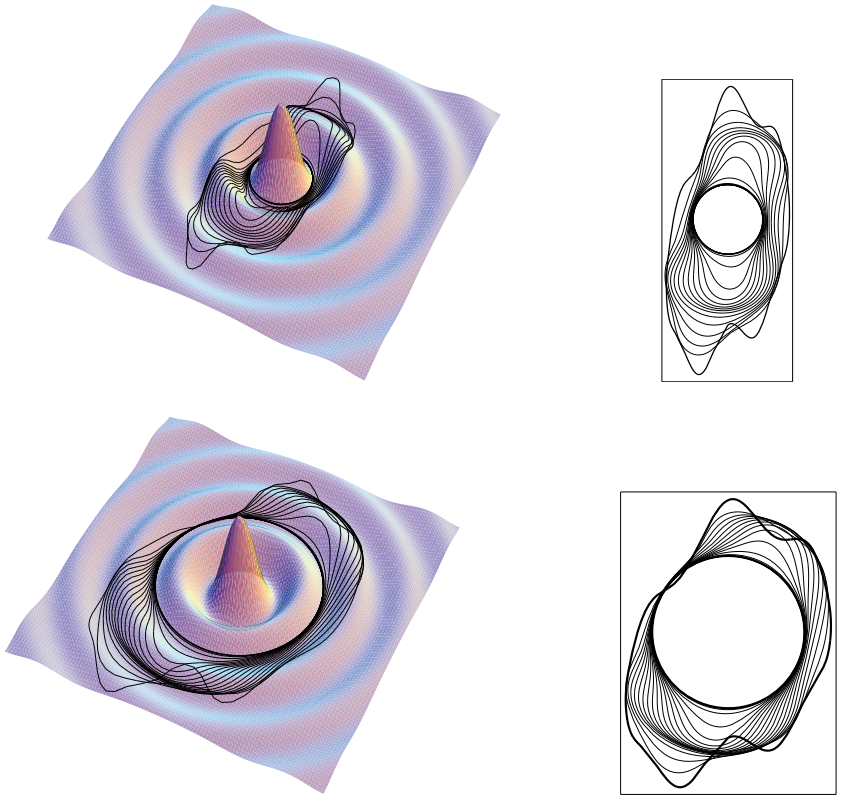

Figure 5.5: A surface flow on a wavelet like surface (left) and its vertical projection to the plane (right). (Top) Surface curves converge to the stable stationary circular curve $\bar{\Gamma} = \{x, |x| = \bar{r}\}$ with the smallest radius. Starting from a different initial curve they converge to the stationary circle with the second smallest radius (bottom). Source: Mikula and Ševčovič [88].

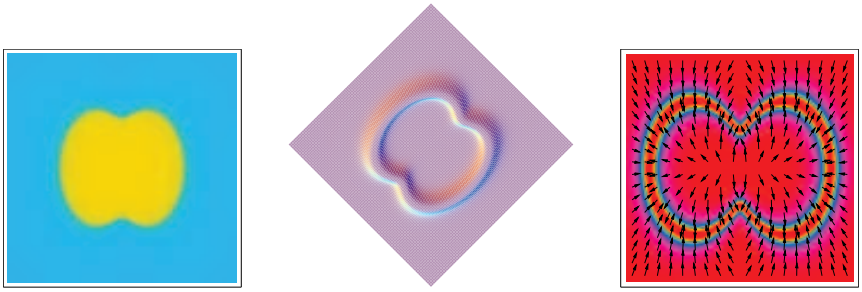

Figure 5.6: A "dumb-bell" image (left), the corresponding function ϕ (middle) and and corresponding vector field $-\nabla\phi(x)$ (right). Source: Mikula and Ševčovič [87].

One can construct a family of curves evolving by the normal velocity $v = \beta(k, \nu, x)$ of the form

$$\beta(k, \nu, x) = \delta(x, \nu)k + c(x, \nu),$$

where $c(x, \nu)$ is a driving force and $\delta(x, \nu) > 0$ is a smoothing coefficient. These functions depend on the position vector x as well as the orientation angle ν of a curve. Evolution starts from an initial curve, which is a suitable approximation of the edge and then it converges to the edge. If $c > 0$ then the driving force shrinks the curve whereas the impact of c is reversed in the case $c < 0$. Let us consider an auxiliary function $\phi(x) = h(|\nabla I(x)|)$ where h is a smooth edge detector function like, e.g. $h(s) = 1/(1 + s^2)$. The gradient $-\nabla\phi(x)$ has an important geometric property: it points towards regions where the norm of the gradient ∇I is large (see Fig. 5.6 right). Let us therefore take $c(x, \nu) = -b(\phi(x))\nabla\phi(x) \cdot \vec{N}$ and $\delta(x, \nu) = a(\phi(x))$ where $a, b > 0$ are given smooth functions. Now, if an initial curve belongs to a neighborhood of an edge of the image and it is evolved according to the geometric equation

$$v = \beta(k, \nu, x) \equiv a(\phi(x))k - b(\phi(x))\nabla\phi \cdot \vec{N}$$

then it is driven towards this edge. In the context of level set methods, edge detection techniques based on this idea were first discussed by Caselles et al. and Malladi *et al.* in [25, 75] (see also [26, 27, 64]).

We apply our computational method to the image segmentation problem. First, numerical experiment is shown in Fig. 5.7. We look for an edge in a 2D slice of a real 3D echocardiography, which was

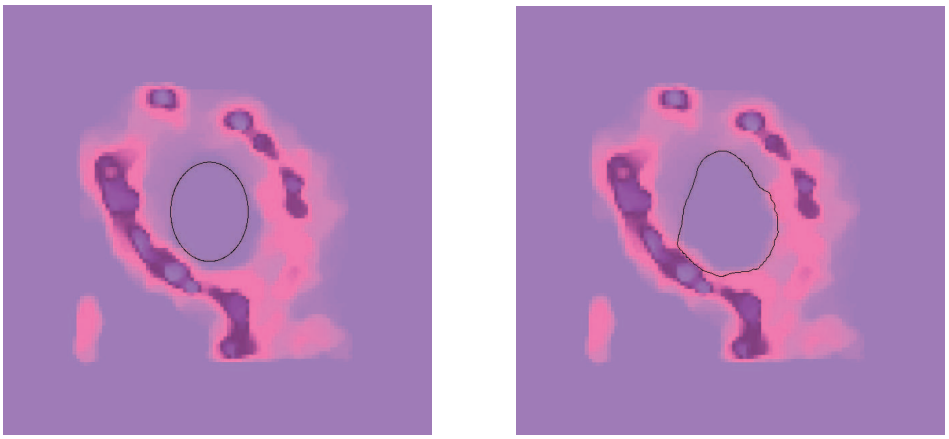

Figure 5.7: An initial ellipse is inserted into the 2D slice of a prefiltered 3D echocardiography (left), the slice together with the limiting curve representing the edge (right). Source: Mikula and Ševčovič [87]. The testing data set (the image function I) is a courtesy of Prof. Claudio Lamberti, DEIS, University of Bologna.

prefiltered by the method of [105]. We have inserted an initial ellipse into the slice close to an expected edge (Fig. 5.7 left). Then it was evolved according to the normal velocity described above using the time stepping $\tau = 0.0001$ and non-local redistribution strategy from Chapter 4 with parameters $\kappa_1 = 20$, $\kappa_2 = 1$ until the limiting curve has been formed (400 time steps). The final curve representing the edge in the slice can be seen in Fig. 5.7 right.

Next we present results for the image segmentation problem computed by means of a geodesic flow with external force discussed in the previous section. We consider an artificial dumb-bell image from Fig. 5.6. If we take $\phi(x) = 1/(1 + |\nabla I(x)|^2)$ then the surface $\mathcal{M}$ defined as a graph of ϕ has a sharp narrow valley corresponding to points of the image in which the gradient $|\nabla I(x)|$ is very large representing an edge in the image. In contrast to the previous example shown in Fig. 5.7 we will make use of the flow of curves on a surface $\mathcal{M}$ driven by the geodesic curvature and the strong "gravitational-like" external force $\mathcal{F}$. According to the previous section such surface flow can be represented by a family of vertically projected plane curves driven by the normal velocity

$$v = a(x,\nu)k - b(x,\nu)\nabla\phi(x)\cdot\vec{N},$$

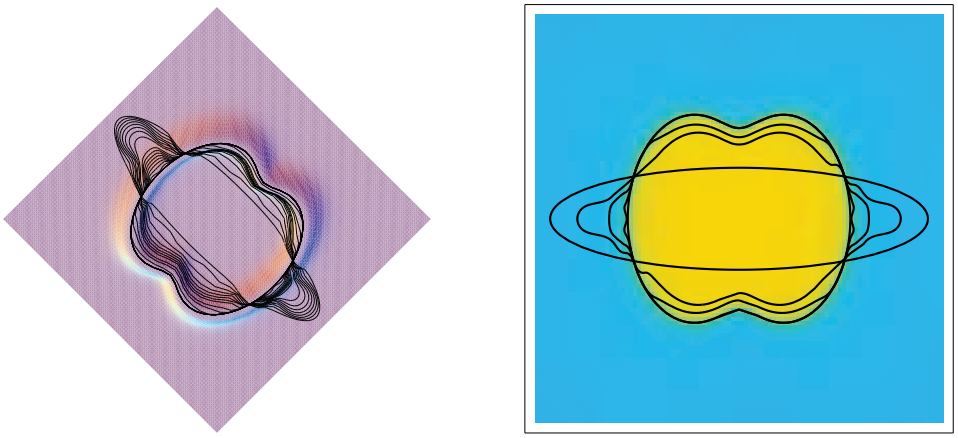

Figure 5.8: A geodesic flow on a flat surface with a sharp narrow valley (left) and its vertical projection to the plane with density plot of the image intensity function $I(x)$ (right). Source: Mikula and Ševčovič [87].

where coefficients a, b are defined as in (5.5) with the strong external force coefficient $\gamma = 100$. The results of computation are presented in Fig. 5.8.

In [109] Yazaki and Ševčovič (see also Beneš *et al.* [19]) applied the curvature adjusted tangential velocity to the edge detection problem. In Fig. 5.9 and 5.10 we show results of edge detection, especially in Fig. 5.10 the curvature adjusted tangential redistribution was very useful due to sharp corners in the segmented image, even if the number of points is not enough.

5.3.2 Tracking moving boundaries

In this section we describe a model for tracking boundaries in a sequence of moving images. Similarly as in the previous section the model is based on curvature driven flow with an external force depending on the position vector x.

Parametric active contours have been used extensively in computer vision for different tasks like segmentation and tracking. However, all parametric contours are known to suffer from the problem of frequent bunching and spacing out of curve points locally during the curve evolution. In this part, we discuss the mathematical basis for selecting such a suitable tangential component for stabilization. We demonstrate the usefulness of the proposed choice of a tangen-

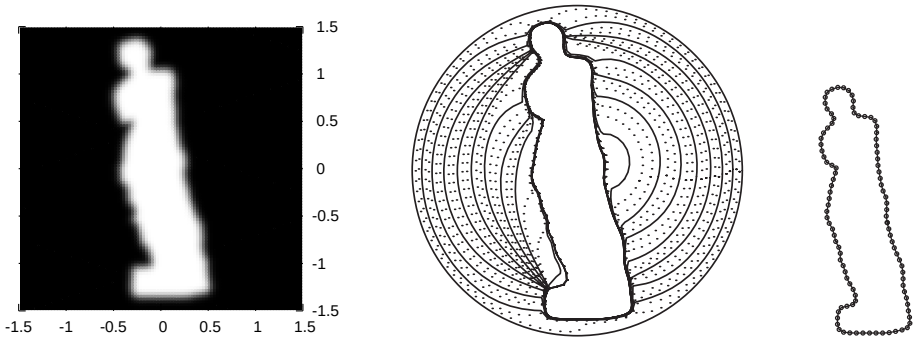

Figure 5.9: (left) indicates the original bitmap image faded shadow "Venus" (middle) indicates evolving curves starting from circle with radius 1.5, and the final segmented curve (right). Source: Ševčovič and Yazaki [109].

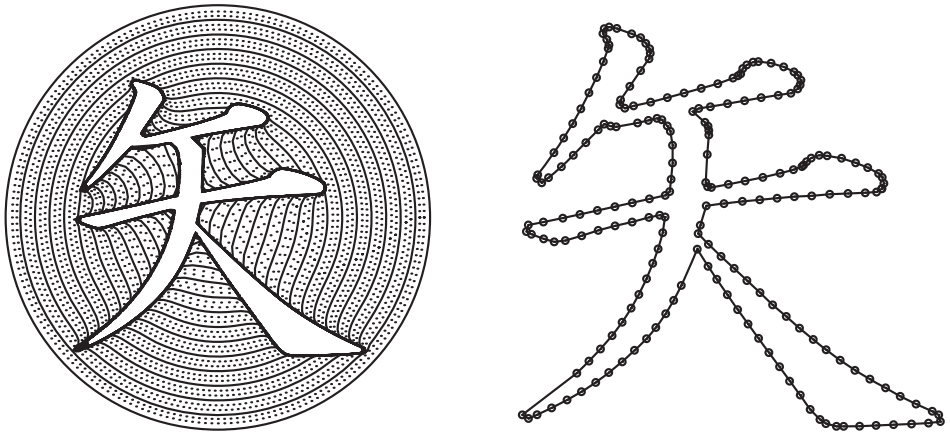

Figure 5.10: (left) indicates the original bitmap image "ya" (it is the Chinese character for arrow) evolving curves starting from circle with radius 2, and the final curve (right). Source: Ševčovič and Yazaki [109].

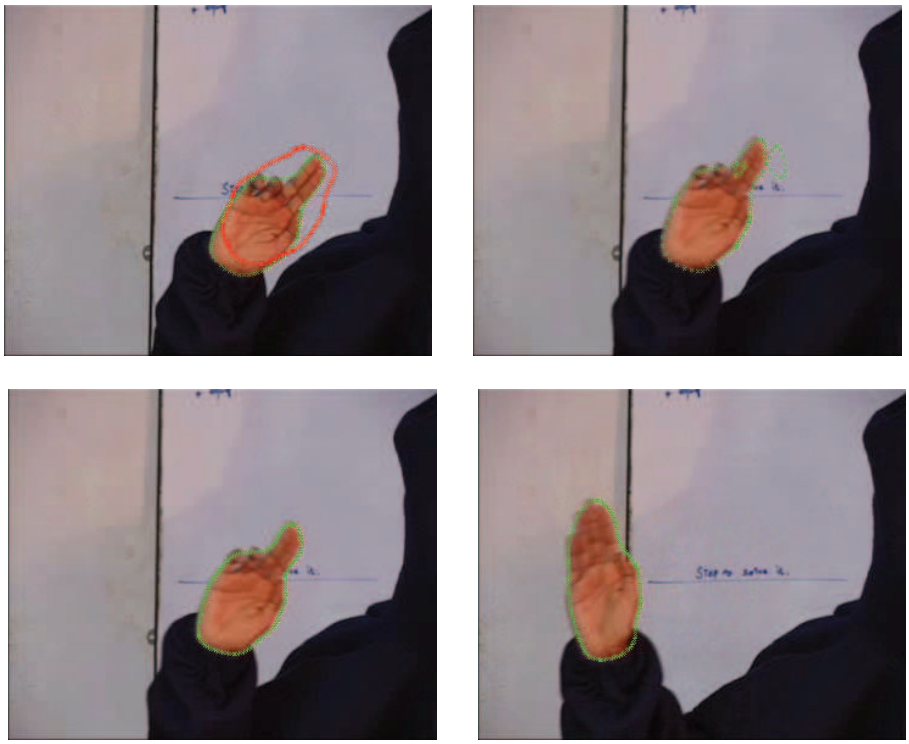

Figure 5.11: Illustration of curve degeneration. (Left) the initial curve in red, (right) bunching of points (in red) starts due to target motion leading to a loop formation. Tracking results for the same sequence as in Fig. 5.11 using a nontrivial tangential redistribution. Source: Srikrishnan, Chaudhuri, Dutta Roy and Ševčovič [119].

tial velocity method with a number of experiments. The results in this section can be found in the recent papers by Srikrishnan *et al.* [118, 119].

The force at each point on the curve can be resolved into two components: along the local tangent and normal denoted by α and β, respectively. This is written as:

$$\frac{\partial x}{\partial t} = \beta \vec{N} + \alpha \vec{T}\,. \tag{5.9}$$

In this application, the normal velocity β has the form: $\beta = \mu k + f(x)$ where f is a bounded function depending on the position of a curve point x. For the purpose of tracking we use the function $f(x) = \log\left(\frac{Prob_B(I(x))}{Prob_T(I(x))}\right)$ and we smoothly cut-off this function if ei-

ther $Prob_B(I(x))$ or $Prob_B(I(x))$ are less than a prescribed tolerance. Here, $Prob_B(I(x))$ stands for the probability that the point x belongs to a background of the image represented by the image intensity function I whereas $Prob_T(I(x))$ represents the probability that the point x belongs to a target in the image to be tracked. Both probabilities can be calculated from the image histogram (see [118, 119] for details).

In this field of application of a curvature driven flow of planar curves representing tracked boundaries in moving images it is very important to propose a suitable tangential redistribution of numerically computed grid points. Let us demonstrate the importance of tangential velocity by the following motivational example. In Fig. 5.11, we show two frames from a tracking sequence of a hand. Without any tangential velocity (i.e. $\alpha = 0$) one can observe formation of small loops in the right picture, which is the very next frame to the initial left one. These loops blow up and the curve becomes unstable within the next few frames.

In [119] we proposed a suitable tangential velocity functional α capable of preventing evolved family of curves (image contours) from formation such undesirable loops like in Fig. 5.11 (right-top). Using a tangential velocity satisfying

$$\frac{\partial \alpha}{\partial u} = K - g + gk\beta,$$

where $K = L(\Gamma) - \int_\Gamma k\beta \, ds$ we are able to significantly improve the results of tracking boundaries in moving images. This tangential velocity is a variant of asymptotically uniform redistribution discussed in Chapter 4. Indeed, it can rewritten as follows:

$$\partial_s \alpha = k\beta - 1 - \frac{L}{g}(\langle k\beta \rangle - 1).$$

If we compare tracking results in Fig. 5.11 (bottom) and those from Fig. 5.11 (top) we can conclude that the presence of a nontrivial suitably chosen tangential velocity α significantly improved tracking results.

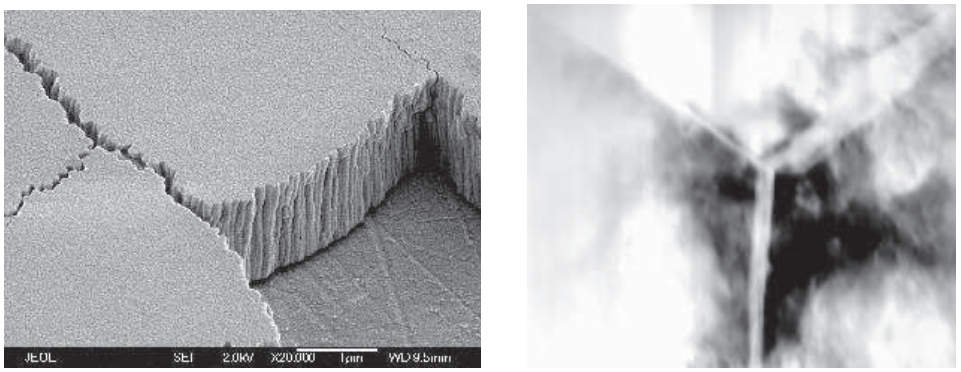

Figure 5.12: Triple junctions in Cu - Fe sulfide.

5.4 Evolution of a network of curves, triple junction stability

The motion of curves under the curvature flow has been widely studied in the past (see e.g. [40, 50] and references mentioned in Chapters 1 and 2. However, less is known about the evolution of networks under the curvature flow [22, 58]. In this case, the arcs in the network evolve in the normal direction with a speed proportional to the curvature of the arcs. At intersections with an outer boundary and at triple junctions boundary conditions have to hold. At the outer boundary one can prescribe the position (see [68, 76]), or the angle with the outer boundary [22, 58]. At the triple junction Young's law, a force balance, leads to angle conditions. An example of the stationary triple junction in Cu - Fe sulfide is shown in Fig. 5.12.

In this section we review results on existence and uniqueness of classical solutions to the moving triple junction problem and we present a result on nonlinear stability of stationary triple junction. We are interested in the stability of stationary solutions to the curvature flow with a triple junction when we prescribe the natural angle condition of 90° at the outer boundary. For this case a linear stability criterion has been derived by Ikota and Yanagida [58] (see also [59]). In [42] we rigorously proved that this criterion also leads to nonlinear stability.

We now specify the problem in detail. Let Ω be a bounded domain in $\mathbb{R}^2$ with C^3-boundary $\partial\Omega$. We search families of curves Γ_t^1, Γ_t^2, and Γ_t^3 which are parametrized by time t and which are contained in Ω.

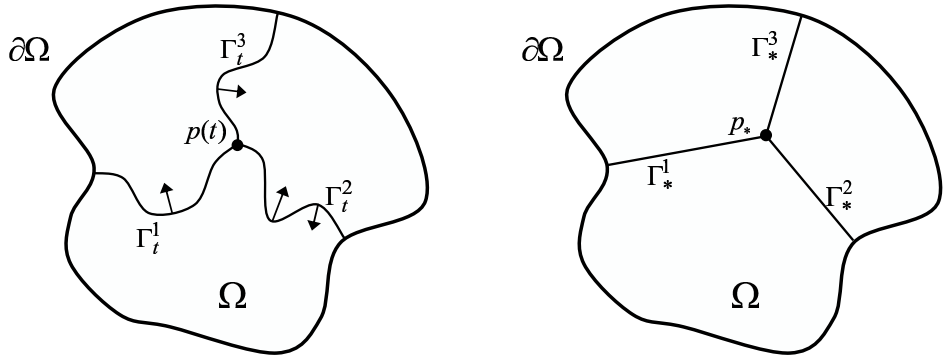

Figure 5.13: Evolution of network of curves $\Gamma_t^i \to \Gamma_*^i$ and triple junction position $p(t) \to p_*$ for $t \to \infty$. Source: Garcke, Kohsaka and Ševčovič [42].

The three curves are supposed to meet at a triple junction $p(t) \in \Omega$ at their one end point and at the other end point they are required to intersect with $\partial\Omega$, see Fig. 5.13. We require for $i = 1, 2, 3$

$$\begin{aligned} &\delta^i v^i = \gamma^i k^i \quad \text{on} \quad \Gamma_t^i\,, \\ &\sum_{i=1}^{3} \gamma^i T^i = 0 \quad \text{at} \quad p(t), \\ &\Gamma_t^i \perp \partial\Omega \quad \text{at} \quad \Gamma_t^i \cap \partial\Omega. \end{aligned} \tag{5.10}$$

Here, v^i and k^i are the normal velocity and curvature of Γ_t^i, respectively. The constants β^i and γ^i are given physical parameters and T^i are unit tangents to the curve which are chosen such that they point away from the triple junction.

In the following we assume strict inequalities and an argument as in Bronsard and Reitich [22] gives that the angles θ^i between the tangents T^j and T^k fulfill

$$\frac{\sin\theta^1}{\gamma^1} = \frac{\sin\theta^2}{\gamma^2} = \frac{\sin\theta^3}{\gamma^3}$$

with $0 < \theta^i < \pi$ $(i = 1, 2, 3)$ and $\theta^1 + \theta^2 + \theta^3 = 2\pi$.

The flow of triple junction curves is a gradient flow for the total length energy functional

$$E(\Gamma) = \sum_{i=1}^{3} \gamma^i L(\Gamma^i)\,,$$

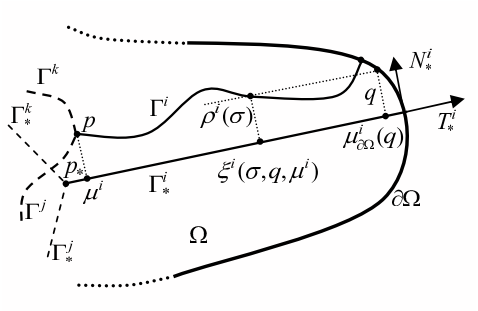

Figure 5.14: Description of the local parametrization of the curve Γ^i meeting Γ^j and Γ^k at the triple junction point p. Source: Garcke, Kohsaka and Ševčovič [42].

where $\Gamma = \bigcup_{i=1}^{3} \Gamma^i$ and $L(\Gamma^i)$ is the length of Γ^i.

Existence of solutions to the evolution problem (5.10) has been shown by Bronsard and Reitich [22]. In our approach of proving full nonlinear stability of triple junction we however needed higher regularity of solutions. In [42] Garcke, Kohsaka and Ševčovič proved the existence of classical solutions via optimal regularity theory on C^β spaces due to Lunardi [73]. In order to state the main result on existence we have to introduce a suitable parametrization of the evolving family on network curves in tubular neighborhood of the stationary triple junction. The parametrization ρ^i defined over a time independent domain $I^i = [0, L(\Gamma^i_*]$ corresponds to a distance of Γ^i_t from Γ^i_* and μ^i are shifts of the triple junction position $p = p(t)$ from its stationary position p_* for $i = 1, 2, 3$. The parametrization is depicted in Fig. 5.14.

Theorem 5.3 *[42, Theorem 2.3] Let $\alpha \in (0,1)$ and let us assume that $\rho^i_0 \in C^{2+\alpha}(I^i)$ and μ^i_0 ($i = 1,2,3$) with sufficiently small $\|\rho^i_0\|_{C^{2+\alpha}(I^i)}$ and $|\mu^i_0|$ fulfill the compatibility conditions. Then there exists a*

$$T_0 = T_0\Big(1/\|\rho_0\|_{C^{2+\alpha}}\Big) > 0$$

such that the problem with $(\rho^i(\cdot,0), \mu^i(0)) = (\rho^i_0, \mu^i_0)$ ($i = 1,2,3$) has a unique solution (ρ, μ) such that $\rho^i \in C^{2+\alpha,1}(I^i \times [0,T_0))$ and $\mu^i \in C^1[0,T_0]$.

Our main result on nonlinear stability of the triple junction now reads as follows:

Theorem 5.4 *[42, Theorems 7.1 and 7.3]*

The stationary triple junction position p_* and the stationary facets $\Gamma_*^i, i = 1, 2, 3,$ are stable if one of the following conditions is satisfied:

a) either all $h_*^1, h_*^2, h_*^3 > 0$ are positive,

b) or, at most one of them is non-positive, and

$$\gamma^1(1 + l^1 h_*^1)h_*^2 h_*^3 + \gamma^2(1 + l^2 h_*^2)h_*^1 h_*^3 + \gamma^3(1 + l^3 h_*^3)h_*^1 h_*^2 > 0\,.$$

Here, $h_*^i, i = 1, 2, 3,$ is the curvature of the outer boundary $\partial\Omega$ at contact points $x_i^* \in \partial\Omega$ of the stationary facets Γ_*^i with length l_*^i.

More precisely, under the aforementioned assumptions there exist constants $C, \omega, \delta > 0$ such that

$$\sum_{i=1}^{3} \|\rho^i(\cdot, t)\|_{H^2} \le Ce^{-\omega t} \sum_{i=1}^{3} \|\kappa^i(\cdot, 0)\|_{L^2}$$

for any $t \ge 0$ and $\sum_{i=1}^{3} \|\kappa^i(\cdot, 0)\|_{L^2} < \delta$. Moreover,

$$\sum_{i=1}^{3} \|\rho^i(\cdot, t)\|_{C^{1+\alpha}} \le Ce^{-\omega t} \sum_{i=1}^{3} \|\rho^i(\cdot, 0)\|_{C^{2+\alpha}}$$

for any $t \ge 0$ and $\sum_{i=1}^{3} \|\rho^i(\cdot, 0)\|_{C^{2+\alpha}} < \delta$.

5.5 Nonlocal geometric flows and variational problems

5.5.1 Geometric flows with constraints

In Section 1.1.5 we discussed the role of the curvature driven flows with the normal velocity non-locally dependent on the entire curve. As a first example we mentioned the area preserving flow investigated by Gage in [41]. In the context of volume preserving modification of the Allen-Cahn system of equations it was investigated by Rubinstein and Sternberg in [103] and Beneš *et al.* [20] for the anisotropic case.

The normal velocity for the area preserving flow is given by

$$\beta = k - \frac{2\pi}{L}.$$

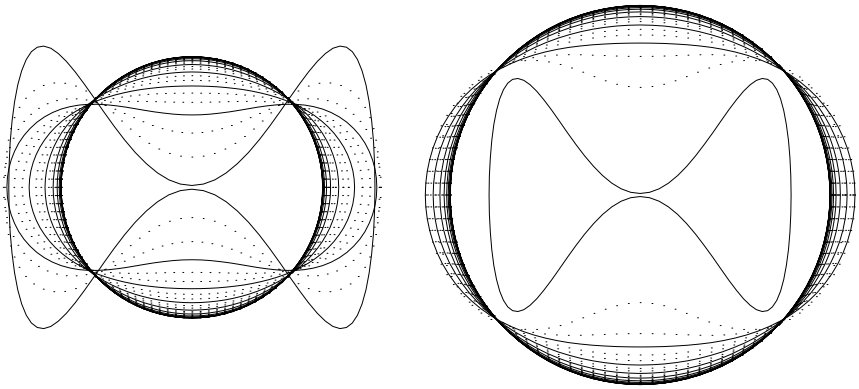

Figure 5.15: Evolution of the initial curve by the area-preserving flow (left) and the total length-preserving flow. Source: Ševčovič and Yazaki [110].

Indeed, using the area equation (2.14) we obtain

$$\frac{d}{dt}A = -\int_\Gamma \beta ds = \int_\Gamma k - \frac{2\pi}{L} ds = 2\pi - \frac{2\pi}{L} L = 0$$

and so the enclosed area is preserved. The area preserving flow is length decreasing, i.e. $\frac{d}{dt}L \leq 0$ so it preserves the enclosed area but it decreases the total length (see Ševčovič and Yazaki [110, Section 5.1]). In the example depicted in Fig. 5.15 (left) we show evolution of a dumb-bell initial curve driven in the normal direction by the area preserving flow. The asymptotic profile is circle enclosing the same area as the initial curve.

The area preserving flow can be considered as the gradient flow for the length subject to area constraint, i.e.

$$\begin{aligned} &\min_\Gamma L(\Gamma) \\ &\text{s.t. } A(\Gamma) = A(\Gamma^0). \end{aligned} \tag{5.11}$$

The second non-local constrained geometric flow is related to the total length preservation. Following the same idea as before and using the equation for the total length evolution (2.13) one can show that the geometric flow evolving curves with the normal velocity

$$\beta = k - \frac{\mathcal{E}}{2\pi} \qquad \text{where } \mathcal{E} = \int_\Gamma k^2 ds$$

preserves their total length $L(\Gamma^t) = L(\Gamma^0)$. The second example shown in Fig. 5.15 (right) depicts evolution of the same initial curve

driven by the length preserving flow. The asymptotic profile is again a circle having the same length as the initial curve.

An interesting property of the length preserving flow is the fact that it increases the enclosed area. By using the arc-length parametrization Ševčovič and Yazaki [110]) proved that $\frac{d}{dt}A \geq 0$. The total length preserving flow of convex curves was also investigated recently by Mu and Zhu in [74]. However, in their analysis they employed the Gauss parametrization allowing only for description of evolution of convex curves.

Similarly, as in the case of the area preserving flow, the length preserving flow can be viewed as the gradient flow for the area subject to length constraint, i.e.

$$\begin{aligned} &\max_{\Gamma} A(\Gamma) \\ &\text{s.t. } L(\Gamma) = L(\Gamma^0). \end{aligned} \tag{5.12}$$

In fact, it can be considered as a dual nonlinear optimization problem to (5.11) (cf. [52]).

5.5.2 Gradient flows for the isoperimetric ratio in the Euclidean and Finsler geometry

Gradient flow for isoperimetric ratio in the Euclidean geometry

In this part we focus our attention to the gradient for the isoperimetric ratio for Jordan curves. The isoperimetric ratio can defined as follows:

$$\Pi(\Gamma) = \frac{L(\Gamma)^2}{4\pi A(\Gamma)}.$$

It is well known that the $\Pi \geq 1$ and equality $\Pi = 1$ is attained by circles only. It can be shown that the gradient flow of curves minimizing the isoperimetric ratio has the normal velocity of the following form:

$$\beta = k - \frac{L}{2A}$$

(cf. [61] and [110]). Such a flow was first investigated by Jiang and Pan in [61]. Similarly as Mu and Zhu in [74], they employed the Gauss parametrization for evolution of convex curves and so results of [61] can be applied to convex curves. In [110] Ševčovič and Yazaki investigated qualitative properties of the gradient flow for the

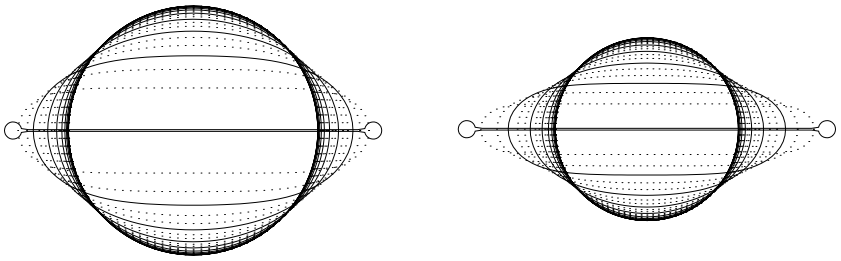

Figure 5.16: Evolution of a thin dumb-bell initial curve by the total length-preserving flow (left). Evolution of the same initial curve driven by the isoperimetric ratio gradient flow. Source: Ševčovič and Yazaki [110].

isoperimetric ratio. We showed that some of their results (e.g. area increasing property) can be directly generalized to the case of evolution of Jordan curves by using the arc-length parametrization. We proved the following result:

Theorem 5.5 *[110, Proposition 1] A flow of planar embedded closed curves driven in the normal direction by the velocity $\beta = k - \frac{L}{2A}$ is a gradient flow minimizing the isoperimetric ratio $\Pi = L^2/(4\pi A)$. It is a convexity-preserving flow. It is the enclosed area increasing flow. Finally, it represents the total length decreasing flow for convex curves.*

The gradient flow for the isoperimetric ratio can be used to find the minimizer of the problem

$$\max_{\Gamma} \frac{L(\Gamma)^2}{4\pi A(\Gamma)}.$$

Clearly, the solution to (5.13) is a circle.

In Fig. 5.16 (right) we show the evolution of a very thin dumb-bell initial curve by the isoperimetric gradient flow. The limiting curve is again a circle. It is a smaller circle when compared to the limiting circle corresponding to the length preserving flow, which is shown in Fig. 5.16 (left). Due to the application of the curvature adjusted tangential velocity we obtained a fine and accurate resolution of parts of the evolved curve having large modulus of the curvature and we could compute its evolution preserving the enclosed area over sufficiently large time interval until it became convex. The limiting curve is again a circle but neither its enclosed area nor the total length are related to those of the initial curve.

Gradient flow for isoperimetric ratio in the relative Finsler geometry

A natural generalization of the classical Euclidean geometry is the so-called relative Finsler geometry. Notice that in the classical Euclidean geometry all distances or lengths are isotropic, i.e. they are independent on orientation in the space. In the relative Finsler geometry we may prescribe certain directions and measure distances in different directions differently. The key concept in the relative Finsler geometry is played by the so-called Wulff shape. The Wulff shape is the intersection of all hyperplanes whose distance from the origin depends on their orientation. In the plane $\mathbb{R}^2$ the Wulff shape can be defined as the set

$$W_\sigma = \bigcap_{\nu\in[0,2\pi]} \left\{ x \in \mathbb{R}^2,\ -x\cdot\vec{N} \le \sigma(\nu) \right\},$$

where $\sigma(\nu)$ is the so-called anisotropy function depending on the angle ν. It is assumed to be a 2π-periodic function. The boundary of the Wulff shape can be expressed as follows:

$$\partial W_\sigma = \left\{ x \in \mathbb{R}^2,\ x = -\sigma(\nu)\vec{N} + \sigma'(\nu)\vec{T},\ \nu \in [0,2\pi] \right\},$$

where $\vec{N} = (-\sin\nu, \cos\nu)^T, \vec{T} = (\cos\nu, \sin\nu)^T$. As a consequence the curvature of the boundary of the Wulff shape is given by $k = [\sigma(\nu)+\sigma''(\nu)]^{-1}$ on ∂W_σ. If we introduce the notion of the anisotropic curvature

$$k_\sigma := [\sigma(\nu) + \sigma''(\nu)]k$$

then $k_\sigma \equiv 1$ on ∂W_σ. In Fig. 5.18 we present typical examples of Wulff shapes corresponding to m-fold anisotropy functions σ for $m = 3, 4, 5, 6$.

In material science the typical anisotropy is hexagonal. Nevertheless, other types of anisotropies can be observed in material science. For instance, in Fig. 5.17 we show results of preparation of (111) facet of plumbum (lead) equilibrated on copper (cf. [120]).

The surface energy associated with the anisotropy function σ can be defined as the weighted integral

$$L_\sigma(\Gamma) = \int_\Gamma \sigma(\nu)\, ds.$$

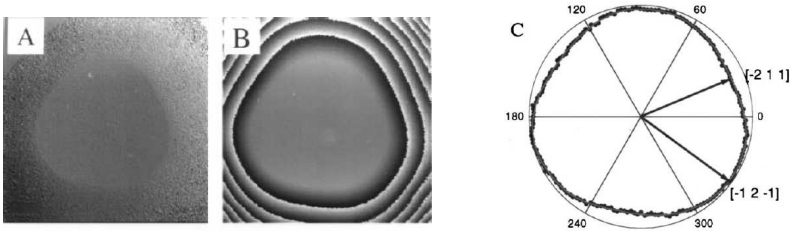

Figure 5.17: A three-fold anisotropy function can be found as a shape of the (111) facet of Pb particles, prepared and equilibrated on Cu(111) under ultrahigh vacuum conditions. Source: Surnev *et al.* [120].

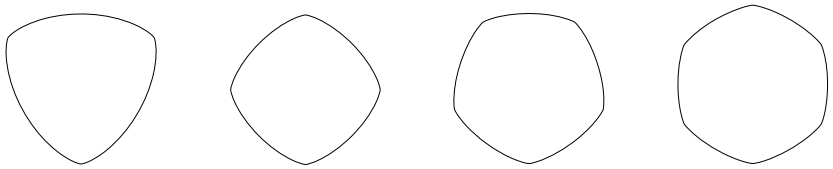

Figure 5.18: Wulff shapes corresponding to the anisotropy function $\sigma(\nu) = 1 + \varepsilon\cos(m\nu)$ and $\varepsilon = 0.99/(m^2-1)$ for $m = 3, 4, 5, 6$. Source: Ševčovič and Yazaki [114].

Notice that, for $\sigma \equiv 1$ the Wulff shape is just the unit disc in the plane and $L_\sigma(\Gamma) = L(\Gamma)$ is the Euclidean length of Γ.

In 1901 crystallographer G. Wulff stated his famous theorem: *"The minimum surface energy for a given volume of a polyhedron will be achieved if the distances of its faces from one given point are proportional to their capillary constants"* (cf. [123]). It can be rephrased as follows: Given an anisotropy function σ, what is the minimizing Jordan curve Γ for the surface energy $L_\sigma(\Gamma)$ for a given area $A(\Gamma)$? In [123] Wulff gave the answer to this question. The minimizer is just the boundary ∂W_σ of the Wulff shape or any of its homothetic images. Moreover, he proved the following isoperimetric inequality in the relative Finsler geometry:

$$\Pi_\sigma(\Gamma) := \frac{L_\sigma(\Gamma)^2}{4|W_\sigma|A(\Gamma)} \geq 1 \tag{5.13}$$

and the equality $\Pi_\sigma(\Gamma) = 1$ is attained for any curve Γ homothetically similar to the boundary of the Wulff shape. Here, $|W_\sigma| = A(\partial W_\sigma)$ is the area of the Wulff shape W_σ. It can be expressed in terms of the

anisotropy function σ as follows:

$$|W_\sigma| = \frac{1}{2}\int_0^{2\pi} |\sigma(\nu)|^2 - |\sigma'(\nu)|^2 d\nu \tag{5.14}$$

(cf. [114]).

The anisoperimetric inequality (5.13) has been generalized by Ševčovič and Yazaki in [114]. Following the method of Lagrange multipliers (cf., e.g. Hamala and Trnovská [52, Chapter 1]) we proved the following mixed anisoperimetric inequality:

Theorem 5.6 *[114, Theorem 2] Let Γ be a C^2 smooth Jordan curve in the plane. Then*

$$\frac{L_\sigma(\Gamma) L_\mu(\Gamma)}{A(\Gamma)} \geq K_{\sigma,\mu}, \tag{5.15}$$

where $K_{\sigma,\mu} = 2\sqrt{|W_\sigma||W_\mu|} + L_\sigma(\partial W_\mu)$. The equality in (5.15) holds if and only if the curve Γ is homothetically similar to the boundary $\partial W_{\widetilde{\sigma}}$ of a Wulff shape corresponding to the mixed anisotropy function $\widetilde{\sigma} = \sqrt{|W_\mu|}\,\sigma + \sqrt{|W_\sigma|}\,\mu$. In particular, if $\sigma = \mu$ then $K_{\sigma,\sigma} = 4|W_\sigma|$ and the anisoperimetric inequality (5.13) holds true.

Furthermore, in [114] we showed that the gradient flow minimizing the anisoperimetric ratio (5.13) is driven by the normal velocity given by:

$$\beta = k_\sigma - \frac{L_\sigma}{2A}.$$

There are several interesting facts about this non-local geometric flow distinguishing it from the isoperimetric ratio gradient flow in the isotropic Euclidean geometry. In summary, we have shown the following result. The proof of the temporal length increasing and area decreasing property differing it thus from the isoperimetric ratio flow is based on the mixed anisoperimetric inequality stated in Theorem 5.6.

The evolution of the initial dumb-bell curve driven by the gradient flow minimizing anisoperimetric ratio with respect to the three fold anisotropy function σ is shown in Fig. 5.19. The asymptotic profile is a curve homothetically similar to the boundary ∂W_σ of the underlying Wulff shape.

The gradient flow for the isoperimetric ratio in the relative Finsler geometry can be used in order to find the minimizer of the problem

$$\min_\Gamma \frac{L_\sigma(\Gamma)^2}{4|W_\sigma| A(\Gamma)}.$$

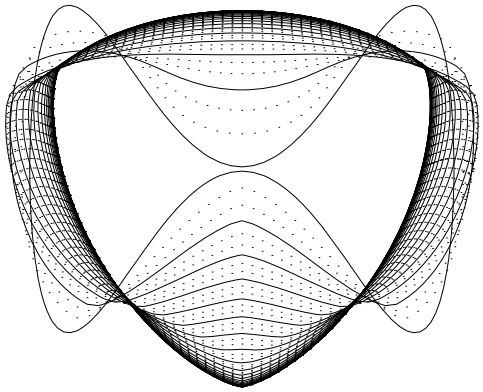

Figure 5.19: Evolution of a curve starting from the initial dumb-bell curves with a three fold anisotropy σ. Source: Ševčovič and Yazaki [114].

According to Wulff's theorem, the solution to (5.13) is a curve homothetically similar to the boundary ∂W_σ of the underlying Wulff shape.

Theorem 5.7 *[114, Theorem 4] If $\sigma \equiv 1$ then the isoperimetric ratio gradient flow with the normal velocity $\beta = k - L/(2A)$ is area non-decreasing and length non-increasing flow of smooth Jordan curves $\Gamma^t, t \in [0, T_{max})$ in the plane provided that Γ^0 is a convex curve.*

Assume the anisotropy function σ is not constant and such that $\sigma + \sigma'' > 0$. Let Γ^0 be an initial curve, which is homothetically similar to the boundary $\partial W_{\bar\sigma}$ of a Wulff shape with the modified anisotropy density function $\bar\sigma = a\sigma + b$ where a, b are constants, $a, b > 0$. Then, for the anisoperimetric ratio gradient flow $\Gamma^t, t \in [0, T_{max})$, evolving in the normal direction by the velocity $\beta = k_\sigma - \frac{L_\sigma}{2A}$, we have $\frac{d}{dt}L(\Gamma^t) > 0$ at $t = 0$. If, moreover, $a/b = \sqrt{\pi}/\sqrt{|W_\sigma|}$ then $\frac{d}{dt}A(\Gamma^t) < 0$ at $t = 0$.

5.6 Inverse Wulff problem

In the previous section we investigated the gradient flow for the following minimization problem: given the anisotropy function σ find the minimizer - a Jordan curve Γ such that

$$\min_{\Gamma} \frac{L_\sigma(\Gamma)^2}{4|W_\sigma|A(\Gamma)}. \tag{5.16}$$

The purpose of this section is to review recent advances on the inverse Wulff problem. In a series of papers [111, 112, 121], Ševčovič and Trnovská investigated the inverse Wulff problem formulated as follows: *given a plane Jordan curve* Γ, *find the optimal anisotropy function* σ *minimizing the anisoperimetric ratio for* Γ, *i.e.*

$$\min_{\sigma} \frac{L_\sigma(\Gamma)^2}{4|W_\sigma|A(\Gamma)} \tag{5.17}$$

under the constraint that the Wulff shape W_σ is convex, i.e. $k > 0$ and so $\sigma + \sigma'' \geq 0$ and $\sigma \geq 0$.

Knowledge of the anisotropy function σ plays an essential role in many applied problems. In particular, it enters the crystal growth models based on solutions of the Allen-Cahn type of nonlinear parabolic partial differential equation (c.f. [18, 11] and other references therein). In [11] Bellettini and Paolini derived the Allen-Cahn parabolic partial differential equation for the gradient flow for the anisotropic Ginzburg-Landau free energy

$$\mathcal{E}(u) = \int_\Omega \frac{\epsilon}{2}\Phi(\nabla u)^2 + \frac{1}{\epsilon} f(u)dx,$$

where Φ is the Finsler metric function related to the anisotropy function σ through the relation: $\Phi(\vec{N}) = \sigma(\nu)$ where $\vec{N} = (-\sin\nu, \cos\nu)^T$. Here, the function $u \in [-1, 1]$ stands for the order parameter characterizing two phases ($u = \pm 1$) of a material. The function f is a double-well potential that gives rise to a phase separation and $\epsilon \ll 1$ is a small parameter representing thickness of the interface (cf. [18, 11]).

Inverse Wulff problem as a non-convex variational problem

Due to the homogeneity of the anisoperimetric ratio Π_σ with respect to scaling of σ, the inverse Wulff problem can be reformulated as follows: given a plane Jordan curve Γ, find the optimal anisotropy function $\sigma(\nu)$ minimizing the anisoperimetric ratio for Γ, i.e.

$$\begin{aligned} &\min_{\sigma} \frac{1}{2}\int_0^{2\pi} |\sigma'(\nu)|^2 - |\sigma(\nu)|^2 d\nu \\ &\text{s.t. } L_\sigma(\Gamma) = 1, \sigma \geq 0, \sigma + \sigma'' \geq 0. \end{aligned} \tag{5.18}$$

In [111] (see also [112, 121]) Ševčovič and Trnovská proposed the method on how to solve the non-convex optimization problem

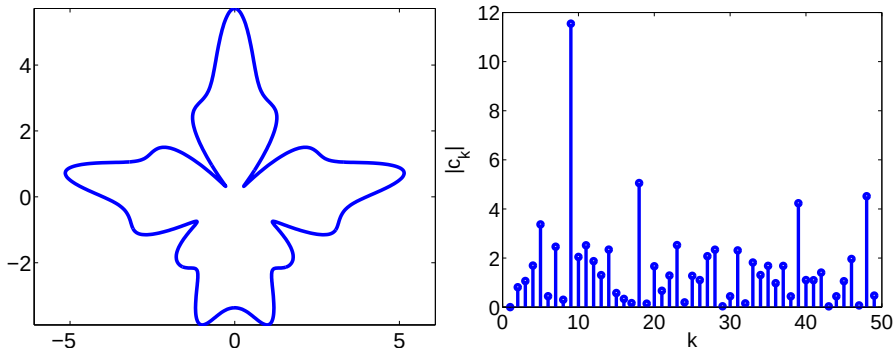

Figure 5.20: (Left) Jordan curve corresponding to the boundary of a dendrite, (right) the spectrum of moduli $|c_k|, k \geq 1$. Source: Ševčovič and Trnovská [112].

(5.18) by means of its reduction to a semidefinite programming problem for Fourier coefficients of the unknown anisotropy function σ.

Fourier series decomposition and Fourier spectrum of a curve

Let $\sigma : \mathbb{R} \to \mathbb{R}$ be a 2π-periodic function, $\sigma \in W^{2,2}_{per}(0, 2\pi)$. It can be represented by its complex Fourier series

$$\sigma(\nu) = \sum_{k=-\infty}^{\infty} \sigma_k e^{ik\nu}, \quad \text{where } \sigma_k = \frac{1}{2\pi} \int_0^{2\pi} e^{-ik\nu} \sigma(\nu) d\nu \qquad (5.19)$$

are complex Fourier coefficients. Since $\sigma(\nu)$ is assumed to be a real function we have $\sigma_{-k} = \bar{\sigma}_k$ for any $k \in \mathbb{Z}$ and $\sigma_0 \in \mathbb{R}$. Notice that for $\sigma \in W^{2,2}_{per}(0, 2\pi)$ we have $\sigma(\nu) + \sigma''(\nu) = \sum_{k=-\infty}^{\infty} (1 - k^2)\sigma_k e^{ik\nu}$ in the norm of the Lebesgue space $L^2(0, 2\pi) = W^{0,2}_{per}(0, 2\pi)$.

The objective function in (5.18) can be expressed in terms of the Fourier coefficients as follows:

$$-|W_\sigma| = \frac{1}{2} \int_0^{2\pi} |\sigma'(\nu)|^2 - |\sigma(\nu)|^2 d\nu = \pi \sum_{k=-\infty}^{\infty} (k^2 - 1)|\sigma_k|^2. \qquad (5.20)$$

Similarly, we can express the interface energy $L_\sigma(\Gamma)$:

$$L_\sigma(\Gamma) = \int_\Gamma \sigma(\nu) ds = \sum_{k=-\infty}^{\infty} \sigma_k \int_\Gamma e^{ik\nu} ds = \sum_{k=-\infty}^{\infty} \bar{c}_k \sigma_k \equiv c^T \sigma, \qquad (5.21)$$

where the complex coefficients

$$c_k = \int_\Gamma e^{-ik\nu} ds, k \in \mathbb{Z},$$

form the so-called Fourier length spectrum of the curve Γ introduced by Ševčovič and Trnovská in [111]. In Fig. 5.20 we show a dendrite-like Jordan curve and its Fourier length spectrum. We can observe that ninth mode c_9 is dominant for this curve. In [111] we proved the following theorem:

Theorem 5.8 *[111, Propositions 4.1 and 4.2] Let Γ be a C^1 smooth curve in the plane. Then the complex Fourier length spectrum $\{c_p, p \in \mathbb{Z}\}$ satisfies:*

1. $c_0 = L(\Gamma) > 0$ *and* $\bar{c}_p = c_{-p}$. *If Γ is a closed (Jordan) curve then* $c_{\pm 1} = 0$.
2. *For any $N \in \mathbb{N}$, the Toeplitz circulant matrix $R = Toep(c_0, c_1, \ldots, c_{N-1})$, i. e. $R_{pq} = c_{p-q}$, is a positive semidefinite* [1] *complex Hermitian matrix.*
3. $|c_k| \le c_0$ *for any* $k \in \mathbb{Z}$.
4. *If, in addition,* $c_1 = 0$ *then* $|c_{2k}|^2 + |c_{2k+1}|^2 \le c_0^2$ *for any* $k \le N/2 - 1$, *and*
$$\sum_{p=2}^{N-1} \frac{|c_p|^2}{p^2 - 1} \le \frac{c_0^2}{2} \left(1 - \frac{1}{N}\right).$$

In [79] McLean and Woardeman derived a useful criterion for non-negativity of a partial finite Fourier series sum. This criterion is a consequence of the classical Riesz-Fejer factorization theorem it reads as follows:

Theorem 5.9 *[79, Proposition 2.3] Let $\sigma_0 \in \mathbb{R}, \sigma_k = \bar{\sigma}_{-k} \in \mathbb{C}$ for $k = 1, \cdots, N-1$. Then the finite Fourier series expansion $\sigma(\nu) = \sum_{k=-N+1}^{N-1} \sigma_k e^{ik\nu}$ is a non-negative function $\sigma(\nu) \ge 0$ for $\nu \in \mathbb{R}$, if and only if there exists a complex Hermitian matrix F such that F is positive semidefinite ($F \succeq 0$) and $\sum_{p=k+1}^{N} F_{p,p-k} = \sigma_k$ for each $k = 0, 1, \cdots, N-1$.*

[1] A Hermitian matrix F is positive semidefinite ($F \succeq 0$) iff $x^* F x \ge 0$ for all vectors x, where $x^* = \bar{x}^T$.

Semidefinite representation of the inverse Wulff problem

The non-convex optimization problem (5.18) can be approximated by a finite Fourier series expansion of the anisotropy function σ, i.e. $\sigma(\nu) \approx \sigma^N(\nu) = \sum_{k=-N+1}^{N-1} \sigma_k e^{ik\nu}$. Taking into account the criterion for positiveness of partial Fourier series Theorem 5.9 and making use of realification of the problem for complex vector $\sigma = (\sigma_0, \sigma_1, \cdots, \sigma_{N-1})^T \in \mathbb{C}^N$, $x = [\Re(\sigma); \Im(\sigma)] \in \mathbb{R}^{2N}$ then (5.18) can be formulated as the non-convex semidefinite optimization problem:

$$
\begin{aligned}
&\min_x \quad x^T P_0 x \\
&\text{s.t.} \quad Ax = b, \\
&\qquad \sum_{p=k+1}^{N} F_{p,p-k} = x_k^R + i x_k^I, \quad k = 1, \cdots, N-1, \\
&\qquad \sum_{p=k+1}^{N} G_{p,p-k} = (1-k^2)(x_k^R + i x_k^I), \quad k = 1, \cdots, N-1, \\
&F, G \succeq 0.
\end{aligned}
\tag{5.22}
$$

Here, P_0 is a symmetric real matrix representing the indefinite quadratic form $\sum_{k=-N+1}^{N-1}(k^2-1)|\sigma_k|^2$ and A is a $1 \times 2N$ matrix representing the constraint $c^T\sigma = 1$.

It is well known that non-convex quadratic optimization programs are NP hard in general. However, there is a systematic way how to deal with such problems, which is based on the so-called semidefinite relaxation (cf. Boyd and Vanderberghe [21]). The idea is rather simple and consists in replacing the quadratic objective function $x^T P_0 x$ by the trace $trace(P_0 X)$ where $X = xx^T$ and subsequent relaxing this non-convex constraint $X = xx^T$ and $Axx^T = bx^T$ by a convex semidefinite constraint $X \succeq xx^T$ and enhanced constraint $AX = bx^T$. In [111] we showed that the so-called enhanced semidefinite relaxation of (5.22) can be represented by the following convex semidefinite optimization program:

$$
\begin{aligned}
&\min_{x,X} \quad trace(P_0 X) \\
&\text{s.t.} \quad Ax = b, AX = bx^T, X \succeq xx^T, \\
&\qquad \sum_{p=k+1}^{N} F_{p,p-k} = x_k^R + i x_k^I, \quad k = 1, \cdots, N-1, \\
&\qquad \sum_{p=k+1}^{N} G_{p,p-k} = (1-k^2)(x_k^R + i x_k^I), \quad k = 1, \cdots, N-1, \\
&F, G \succeq 0.
\end{aligned}
\tag{5.23}
$$

Moreover, we rigorously proved that (5.22) and its relaxation (5.23) yield the same optimum value and so they are equivalent. The key role in the proof of equivalence is played by the structural condition:

$$P_0 + V^T A + A^T V \succeq 0$$

for some matrix V (cf. [111, 112, 121]). With help of Theorem 5.8 we proved that the aforementioned condition is satisfied and so the problems (5.22) and (5.23) yield the same optimum value. Concerning the limit $N \to \infty$ we showed the following result:

Theorem 5.10 *[111, Theorem 6.1] Let $\sigma^N \in \mathcal{K}$ be a minimizer to optimization problem* (5.22) *in the dimension $N \in \mathbb{N}$. Then $1 \leq \lim_{N\to\infty} \Pi_{\sigma^N}(\Gamma) = \inf_{\sigma\in\mathcal{K}} \Pi_\sigma(\Gamma)$. Here, $\mathcal{K}$ is the cone $\mathcal{K} = \{\sigma \in W^{2,2}_{per}(0, 2\pi) \mid \sigma(\nu) \geq 0, \sigma(\nu)+\sigma''(\nu) \geq 0,$ for a.e. $\nu \in [0, 2\pi]\}$. Moreover, $\tilde{\sigma}^N \to \sigma$ as $N \to \infty$ in the norm of the Sobolev space $W^{1,2}_{per}(0, 2\pi)$.*

To solve problem (5.23) we used CVX, a package for specifying and solving convex programs [49, 48] and semidefinite programming solver due to J. Sturm [108]. Numerical results of construction of the optimal anisotropy function σ are shown in Fig. 5.21 and Fig. 5.22.

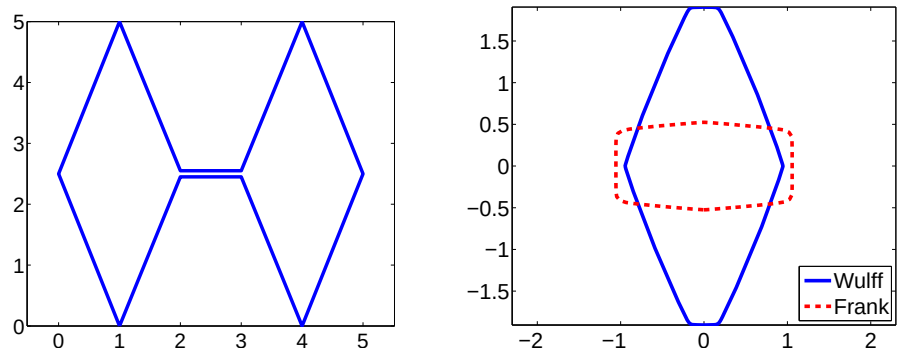

Figure 5.21: Nonconvex polygonal curves (left) and their corresponding optimal Wulff shapes and Frank diagrams (right). Source: Ševčovič and Trnovská [111].

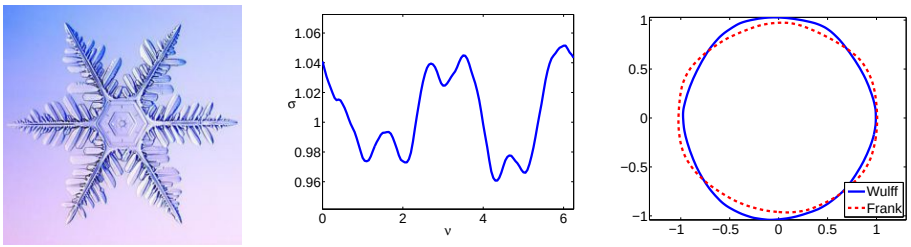

Figure 5.22: (Left) the curve representing a boundary of a snowflake, (middle) the optimal anisotropy function σ, (right) the Wulff shape and Frank diagram. Source: Ševčovič and Trnovská [111].

Chapter 6

Synopsis of the selected papers

The last chapter contains nine selected papers of the author written in collaboration with Karol Mikula, Shigetoshi Yazaki, Harald Garcke, Yoshihito Kohsaka and Mária Trnovská.[1]

6.1 Evolution of plane curves driven by a nonlinear function of curvature and anisotropy

In the joint paper with Karol Mikula[2] included in this section we studied anisotropic flows with the normal velocity nonlinearly depending on the curvature and satisfying a geometric equation $v = \beta(k, \nu)$, where v is the normal velocity and k and ν are the curvature and tangential angle of a plane curve Γ. We followed the direct approach and we analyze the so-called intrinsic heat equation governing the motion of plane curves obeying such a geometric equation. The intrinsic heat equation is modified to include an appropriate nontrivial tangential velocity functional α. We showed how the presence of a nontrivial tangential velocity can prevent numerical solutions from forming various instabilities. From an analytical point of view we presented some new results on short time existence of a regular family of evolving curves in the degenerate case when $\beta(k, \nu) = \gamma(\nu)k^m$, $0 < m \leq 2$, and the governing system of equations includes a non-

[1] The full versions of the papers can be downloaded from:
`www.iam.fmph.uniba.sk/institute/sevcovic/drsc`

[2] K.Mikula and D. Ševčovič: Evolution of plane curves driven by a nonlinear function of curvature and anisotropy, SIAM Journal on Applied Mathematics, 61(5) (2001), 1473-1501.

trivial tangential velocity functional. In this paper we proved Theorem 3.6 ([85, Theorems 5.6 and 6.3]) on local existence, uniqueness and continuation of solutions to the anisotropic geometric flow.

6.2 A direct method for solving an anisotropic mean curvature flow of plane curves with an external force

The purpose of this section written jointly with Karol Mikula[3] was to propose and analyze a new method for solving the evolution of plane curves satisfying the geometric equation $v = \beta(x, k, \nu)$ where v is the normal velocity, k and ν are the curvature and tangential angle of a plane curve $\Gamma \subset \mathbb{R}^2$ at the point $x \in \Gamma$ is proposed. We derived a governing system of partial differential equations for the curvature, tangential angle, local length and position vector of an evolving family of plane curves and prove local in time existence of a classical solution. These equations include a nontrivial tangential velocity functional governing a uniform redistribution of grid points and thus preventing numerically computed solutions from forming various instabilities. We discretized the governing system of equations in order to find a numerical solution for 2D anisotropic interface motions and image segmentation problems. In this paper we proved Theorem 3.5 on local existence, uniqueness and continuation of classical solutions to geometric flows with normal velocity depending on the curvature, tangent angle and position vector (cf. [86, Theorem 3.1]).

6.3 Evolution of plane curves with a curvature adjusted tangential velocity

We studied evolution of a closed embedded plane curve with the normal velocity depending on the curvature, the orientation and the position of the curve. Together with Shigetoshi Yazaki[4] we proposed a new method of tangential redistribution of points by curvature adjusted control in the tangential motion of evolving curves. The tan-

[3] K. Mikula and D. Ševčovič: A direct method for solving an anisotropic mean curvature flow of plane curves with an external force, Math. Methods in the Appl. Sci., 27 (2004), 1545-1565.

[4] D. Ševčovič and S.Yazaki: Evolution of plane curves with a curvature adjusted tangential velocity, Japan J. Indust. Appl. Math., 28(3) (2011), 413-442.

gential velocity may not only distribute grid points uniformly along the curve but also produce a suitable concentration and/or dispersion depending on the curvature. Our study is based on solutions to the governing system of nonlinear parabolic equations for the position vector, tangent angle and curvature of a curve. We furthermore presented a semi-implicit numerical discretization scheme based on the flowing finite volume method. Several numerical examples illustrating capability of the new tangential redistribution method are also presented in this paper.

6.4 Computational and qualitative aspects of motion of plane curves with a curvature adjusted tangential velocity

In this section we present the joint paper with Shigetoshi Yazaki.[5] We investigated a time dependent family of plane closed Jordan curves evolving in the normal direction with a velocity which is assumed to be a function of the curvature, tangential angle and position vector of a curve. We followed the direct approach and analyzed the system of governing PDEs for relevant geometric quantities. We focused on a class of the so-called curvature adjusted tangential velocities for computation of the curvature driven flow of plane closed curves. Such a curvature adjusted tangential velocity depends on the modulus of the curvature and its curve average. Using the theory of abstract parabolic equations we proved local existence, uniqueness and continuation of classical solutions to the system of governing equations. We furthermore analyzed geometric flows for which normal velocity may depend on global curve quantities like the length, enclosed area or total elastic energy of a curve. We also proposed a stable numerical approximation scheme based on the flowing finite volume method. Several computational examples of various non-local geometric flows are also presented in this paper. In this paper we proved Theorems 4.1 and 4.2 and local existence, uniqueness and limiting behavior of solution to the system of equations describing the curvature adjusted tangential velocity driven flow (cf. [110, Theorem 1] and [110, Theorem 2]).

[5] D. Ševčovič and S.Yazaki: Computational and qualitative aspects of motion of plane curves with a curvature adjusted tangential velocity, Mathematical Methods in the Applied Sciences, 35(15) (2012), 1784-1798.

6.5 Computational and qualitative aspects of evolution of curves driven by curvature and external force

In this section written jointly with Karol Mikula[6] we proposed a direct method for solving the evolution of plane curves satisfying the geometric equation $v = \beta(x, k, \nu)$ where v is the normal velocity, k and ν are the curvature and tangential angle of a plane curve $\Gamma \subset R^2$ at a point $x \in \Gamma$. We derived and analyzed the governing system of partial differential equations for the curvature, tangential angle, local length and position vector of an evolving family of plane curves. The governing equations include a nontrivial tangential velocity functional yielding the uniform redistribution of grid points along the evolving family of curves preventing thus numerically computed solutions from forming various instabilities. We also proposed a full space-time discretization of the governing system of equations and study its experimental order of convergence. Several computational examples of the evolution of plane curves driven by curvature and external force as well as the geodesic curvatures driven evolution of curves on various complex surfaces are presented in this paper.

6.6 Evolution of curves on a surface driven by the geodesic curvature and external force

The purpose of this section was to study a flow of closed curves on a given graph surface driven by the geodesic curvature and external force. It is a joint work with Karol Mikula.[7] Using the vertical projection of surface curves to the plane we show how the geodesic curvature driven flow can be reduced to a solution of a fully nonlinear system of parabolic differential equations. We showed that the flow of surface curves is gradient like, i.e. there exists a Lyapunov functional non-increasing along trajectories. Special attention is put on the analysis of closed stationary surface curves. We presented sufficient conditions for their dynamic stability. Several computational

[6] K. Mikula and D. Ševčovič: Computational and qualitative aspects of evolution of curves driven by curvature and external force, Computing and Visualization in Science, 6 (2004), 211-225.

[7] K. Mikula and D. Ševčovič: Evolution of curves on a surface driven by the geodesic curvature and external force, Applicable Analysis, 85(4) (2006), 345-362.

examples of evolution of surface curves driven by the geodesic curvature and external force on various surfaces are presented in this paper. We also discussed a link between the geodesic flow and the edge detection problem arising from the image segmentation theory. We showed Theorem 5.2 on stability of stationary curves (cf. [88, Theorem 3.1, Corollary 3.2]).

6.7 Nonlinear stability of stationary solutions for curvature flow with triple junction

This section contains the joint paper with Harald Garcke and Yoshihito Kohsaka. [8] We analyzed the motion of a network of three planar curves with a speed proportional to the curvature of the arcs, having perpendicular intersections with the outer boundary and a common intersection at a triple junction. As a main result we showed that a linear stability criterion due to Ikota and Yanagida is also sufficient for nonlinear stability. We also proved local and global existence of classical smooth solutions as well as various energy estimates. We proved exponential stabilization of an evolving network starting from the vicinity of a linearly stable stationary network. In Theorems 5.3 and 5.4 we established local existence of classical solutions and proved the nonlinear stability of a stationary triple junction. (cf. [42, Theorem 2.3] and [42, Theorems 7.1 and 7.3]).

6.8 On a gradient flow of plane curves minimizing the anisoperimetric ratio

In this section we present the joint paper with Shigetoshi Yazaki[9] in which we studied the gradient flow for the isoperimetric ratio in the relative Finsler geometry characterized by a given anisotropy function. We showed that for such a flow the normal velocity is a function of the anisotropic curvature and it also depends on the total interfacial energy and enclosed area of the curve. In Theorem 5.7, in con-

[8] H. Garcke, Y. Kohsaka and D. Ševčovič: Nonlinear stability of stationary solutions for curvature flow with triple junction, Hokkaido Mathematical Journal, 38(4) (2009), 721-769.

[9] D. Ševčovič and S.Yazaki: On a gradient flow of plane curves minimizing the anisoperimetric ratio, IAENG International Journal of Applied Mathematics, 43(3) (2013), 160-171.

trast to the gradient flow for the isoperimetric ratio, we showed existence of initial curves for which the enclosed area is decreasing with respect to time. In Theorem 5.6 we derived a mixed anisoperimetric inequality for the product of total interfacial energies corresponding to different anisotropy functions.

6.9 Solution to the inverse Wulff problem by means of the enhanced semidefinite relaxation method

In this section writen jointly with Mária Trnovská[10] we investigated the inverse Wulff problem which can be interpreted as a dual problem to minimization of the isoperimetric ratio in the relative Finsler geometry. We proposed a novel method of resolving the optimal anisotropy function. The idea is to construct the optimal anisotropy function as a solution to the inverse Wulff problem, i. e. as a minimizer for the anisoperimetric ratio for a given Jordan curve in the plane. It leads to a non-convex quadratic optimization problem with linear matrix inequalities. In order to solve it we proposed the so-called enhanced semidefinite relaxation method which is based on a solution to a convex semidefinite problem obtained by a semidefinite relaxation of the original problem augmented by quadratic-linear constraints. We showed that the sequence of finite dimensional approximations of the optimal anisoperimetric ratio converges to the optimal anisoperimetric ratio which is a solution to the inverse Wulff problem. Several computational examples, including those corresponding to boundaries of real snowflakes and discussion on the rate of convergence of numerical method are also presented in this paper. In this paper we furthermore introduced the Fourier spectrum of a curve. In Theorem 5.8 we proved some useful properties of the spectrum (cf. [111, Propositions 4.1 and 4.2]). In Theorem 5.10 we also showed convergence of the discrete approximations to the solution of the inverse Wulff problem (cf. [111, Theorem 6.1]).

[10] D. Ševčovič and M. Trnovská: Solution to the inverse Wulff problem by means of the enhanced semidefinite relaxation method, Journal of Inverse and III-posed Problems, 23(3) (2015), 263-285.

Conclusions

In this survey paper we investigated the direct Lagrangian method for solving the mean curvature flow of curves and surfaces. We showed how this geometric flow can be analyzed from qualitative and numerical point of view. We provided several results on local in time existence, uniqueness and continuation of classical solutions to the governing system of fully nonlinear parabolic equation describing evolution of the curvature, position vector and other relevant geometric quantities. We furthermore presented several results concerning the stability of stationary curves. Special attention was put on the construction of a stable numerical scheme for computing various mean curvature driven flows. We emphasized the role of a suitably chosen tangential velocity, which enhances stability and accuracy of the numerical scheme based on the flowing finite volume method. Various applications arising from phase interface dynamics, edge detection, nonlocal geometric flows, nonlinear variational and optimization problems were presented in this paper.

Bibliography

[1] S. Angenent, and M. Gurtin, *Multiphase thermomechanics with interfacial structure. II: Evolution of an isothermal interface*, Arch. Rat. Mech. Anal. **108**(4) (1989), 323–391.

[2] S. Angenent, and M. Gurtin, *Anisotropic motion of a phase interface. Well-posedness of the initial value problem and qualitative properties of the interface*, J. Reine Angew. Math. **446** (1994), 1–47.

[3] S. Angenent, and M. Gurtin, *General contact-angle conditions with and without kinetics*, Quart. Appl. Math. **54**(3) (1996), 557–569.

[4] U. Abresch, and J. Langer, *The normalized curve shortening flow and homothetic solutions*, J. Differ. Geom. **23** (1986), 175–196.

[5] S. Angenent, *Nonlinear analytic semiflows*, Proc. R. Soc. Edinb., Sect. A **115** (1990), 91–107.

[6] S. Angenent, *Parabolic equations for curves on surfaces. I: Curves with p-integrable curvature*, Annals of Math. **132**(2) (1990), 451–483.

[7] S. Angenent, G. Sapiro, and A. Tannenbaum, *On the affine heat equation for non-convex curves*, J. Amer. Math. Soc. **11**(3) (1998), 601–634.

[8] J.-B. Baillon, *Caractère borné de certains générateurs de semigroupes linéaires dans les espaces de Banach*, C. R. Acad. Sci. Paris Sér. A-B **290**(16) (1980), A757–A760.

[9] M. Balažovjech, K. Mikula, M. Petrášova, J. Urbán, *Lagrangean method with topological changes for numerical modelling of forest fire propagation*, Proceedings of ALGORITMY 2012, 19th Conference on Scientific Computing, Podbanske, Slovakia, September 9-14, 2012, (Eds. A.Handlovicova, Z.Minarechova, D.Sevcovic), ISBN 978-80-227-3742-5, Publishing House of STU, 2012, 42-52.

[10] M. Bauer, P. Harms, and P. W. Michor, *Sobolev metrics on shape space of surfaces*, J. Geom. Mech. **3** (2011), 389-438.

[11] G. Bellettini, and M. Paolini, *Anisotropic motion by mean curvature in the context of Finsler geometry*, Hokkaido Math. J. **25** (1996), 537–566.

[12] M. Beneš, *Mathematical and computational aspects of solidification of pure substances*, Acta Math. Univ. Comen. **70**(1) (2001), 123–151.

[13] M. Beneš, J. Kratochvíl, J. Křišťan, V. Minárik, and P. Pauš, *A parametric simulation method for discrete dislocation dynamics*, The European Physical Journal ST, **177** (2009), 177-192.

[14] M. Beneš, and K. Mikula, *Simulation of anisotropic motion by mean curvature–comparison of phase field and sharp interface approaches*, Acta Math. Univ. Comenian. **67**(1) (1998), 17–42.

[15] M. Beneš, M. Kimura, and S. Yazaki, *Second order numerical scheme for motion of polygonal curves with constant area speed*, Interfaces and Free Boundaries **11**(4) (2009), 515-536.

[16] M. Beneš, M. Kimura, and S. Yazaki, *Analytical and numerical aspects on motion of polygonal curves with constant area speed*, Proceedings of MAGIA 2007, Conference on Mathematics, Geometry and their Applications, Kocovce 10.-12.9.2007, STU Bratislava 2007, pp. 127-141. ISBN:978-80-227-2796-9.

[17] M. Beneš, K. Mikula, T. Oberhuber, D. Ševčovič, *Comparison study for level set and direct Lagrangian methods for computing Willmore flow of closed planar curves*, Computing and Visualization in Science, **12**(6) (2009), 307-317.

[18] M. Beneš, *Diffuse-interface treatment of the anisotropic mean-curvature flow*, Applications of Mathematics **48** (2003), 437–453.

[19] M. Beneš, M. Kimura, P. Pauš, D. Ševčovič, T. Tsujikawa, S. Yazaki, *Application of a curvature adjusted method in image segmentation*, Bulletin of Inst. of Mathematics, Academia Sinica, New Series, **3**(4) 2008, 509-524.

[20] M.Beneš, S.Yazaki, and M. Kimura, *Computational studies of non-local anisotropic Allen-Cahn equation*, Math. Bohemica **136** (2011), 429-437.

[21] S. Boyd, L. Vandenberghe, *Semidefinite programming*, SIAM Review **38** (1996), 49–95.

[22] L. Bronsard, and F. Reitich, F., *On three-phase boundary motion and the singular limit of a vector valued Ginzburg–Landau equation*, Arch. Rat. Mech., **124** (1993), 355–379.

[23] G. Caginalp, *The dynamics of a conserved phase field system: Stefan-like, Hele-Shaw, and Cahn-Hilliard models as asymptotic limits*, IMA J. Appl. Math. **44**(1) (1990), 77–94.

[24] I. Capuzzo Dolcetta, S. Finzi Vita, and R. March, *Area-preserving curve-shortening flows: From phase separation to image processing*, Interfaces Free Bound. **4** (2002), 325-343. MR

[25] V. Caselles, F. Catté, T. Coll, and F. Dibos, *A geometric model for active contours in image processing*, Numer. Math. **66**(1) (1993), 1–31.

[26] V. Caselles, R. Kimmel, and G. Sapiro, *Geodesic active contours*, International Journal of Computer Vision **22** (1997), 61–79.

[27] V. Caselles, R. Kimmel, G. Sapiro, and C. Sbert, *Minimal surfaces: a geometric three-dimensional segmentation approach*, Numer. Math. **77**(4) (1997), 423–451.

[28] M. Crandall, and P.-L. Lions, *Viscosity solutions of Hamilton–Jacobi equations*, Trans. Amer. Math. Soc. **227** (1983), 1–42.

[29] G. Da Prato, and P. Grisvard, *Sommes d'opérateurs linéaires et équations différentielles opérationnelles*, J. Math. Pures Appl. **54**(3) (1975), 305–387.

[30] G. Da Prato, and P. Grisvard, *Equations d'évolution abstraites non linéaires de type parabolique*, Ann. Mat. Pura Appl. **120** (1979), 329–396.

[31] K. Deckelnick, *Weak solutions of the curve shortening flow*, Calc. Var. Partial Differ. Equations **5**(6) (1997), 489–510.

[32] D. DeTurck, *The Cauchy problem for Lorentz metrics with prescribed Ricci curvature*, Compositio Math. **48**(3) (1983), 327–349.

[33] G. Dziuk, *An algorithm for evolutionary surfaces*, Numer. Math. **58**(6) (1991), 603–611.

[34] G. Dziuk, *Convergence of a semi-discrete scheme for the curve shortening flow*, Math. Models Methods Appl. Sci. **4**(4) (1994), 589–606.

[35] G. Dziuk, *Discrete anisotropic curve shortening flow*, SIAM J. Numer. Anal. **36**(6) (1999), 1808–1830.

[36] C. Epstein, and M. Gage, *The curve shortening flow*, Wave motion: theory, modelling, and computation (Berkeley, Calif., 1986), Math. Sci. Res. Inst. Publ., vol. 7, Springer, New York, 1987, pp. 15–59.

[37] Ch. Elliott, M. Paolini, and R. Schätzle, *Interface estimates for the fully anisotropic Allen-Cahn equation and anisotropic mean-curvature flow*, Math. Models Methods Appl. Sci. **6**(8) (1996), 1103–1118.

[38] S. Esedoglu, S. J. Ruuth, and R. Tsai, *Threshold dynamics for high order geometric motions*, Interfaces Free Bound. **10** (2008), 263-282.

[39] P. Finsler, *Über das Vorkommen definiter und semidefiniter Formen und Scharen quadratischer Formen*, Comment. Math. Helv. **9** (1937), 188–192. ol. 25, Springer-Verlag, New York, 1993.

[40] M. Gage, and R.S. Hamilton, *The heat equation shrinking convex plane curves*, J. Differ. Geom. **23** (1986), 69–96.

[41] M. E. Gage, *On area-preserving evolution equation for plane curves*, Contemporary Mathematics, **51** (1986), 51–62.

[42] H. Garcke, Y. Kohsaka, and D. Ševčovič *Nonlinear stability of stationary solutions for curvature flow with triple junction*, Hokkaido Mathematical Journal, **38**(4) (2009), 721-769.

[43] H. Garcke, K. Ito, and Y. Kohsaka, *Linearized stability analysis of stationary solutions for surface diffusion with boundary conditions*, SIAM J. Math. Anal. **36**(4) (2005), 1031–1056.

[44] H. Garcke, K. Ito, and Y. Kohsaka, *Nonlinear stability of stationary solutions for surface diffusion with boundary conditions*, SIAM J. Math. Anal. **40**(2) (2008), 491-515.

[45] Y. Giga, *Surface evolution equations. A level set approach*, Monographs in Mathematics 99, Birkhäuser Verlag, Basel. 2006.

[46] P. Girão, *Convergence of a crystalline algorithm for the motion of a simple closed convex curve by weighted curvature*, SIAM J. Numer. Anal. **32**(3) (1995), 886–899.

[47] P. Girão, and R. Kohn, *Convergence of a crystalline algorithm for the heat equation in one dimension and for the motion of a graph by weighted curvature*, Numer. Math. **67**(1) (1994), 41–70.

[48] M. Grant, and S. Boyd, *CVX: Matlab software for disciplined convex programming, version 2.0 beta*, http://cvxr.com/cvx, September 2013.

[49] M. Grant, and S. Boyd, *Graph implementations for nonsmooth convex programs*, In: Recent Advances in Learning and Control (a tribute to M. Vidyasagar), V. Blondel, S. Boyd, and H. Kimura, editors, pages 95-110, Lecture Notes in Control and Information Sciences, Springer, 2008.

[50] M. Grayson, *The heat equation shrinks embedded plane curves to round points*, J. Differential Geom. **26** (1987), 285–314.

[51] M. Gurtin, *Thermomechanics of evolving phase boundaries in the plane*, Oxford Mathematical Monographs, The Clarendon Press Oxford University Press, New York, 1993.

[52] M. Hamala, and M. Trnovská, *Nonlinear programming, theory and algorithms*, (in Slovak), Bratislava: Epos. 340 pp. (2013).

[53] A. Handlovičová, K. Mikula, and A. Sarti, *Numerical solution of parabolic equations related to level set formulation of mean curvature flow*, Comput. Visualization Sci. **1** (1998), 179–182.

[54] D. Henry, *Geometric theory of semilinear parabolic equations*, Lecture Notes in Mathematics, vol. 840, Springer-Verlag, Berlin, 1981.

[55] T. Y. Hou, I. Klapper, and H. Si, *Removing the stiffness of curvature in computing 3-D filaments*, J. Comput. Phys. **143**(2) (1998), 628–664.

[56] T. Y. Hou, J. S. Lowengrub, and M. J. Shelley, *Removing the stiffness from interfacial flows with surface tension*, J. Comput. Phys. **114**(2) (1994), 312–338.

[57] G. Huisken, *Asymptotic behavior for singularities of the mean curvature flow*, J. Differ. Geom. **31**(1) (1990), 285–299.

[58] R. Ikota, and E. Yanagida, *A stability criterion for stationary curves to the curvature-driven motion with a triple junction*, Differential Integral Equations, **16** (2003), 707–726.

[59] R. Ikota, and E. Yanagida, *Stability of stationary interfaces of binary-tree type*, Calc. Var. Partial Differ. Equ., **22**(4) (2005), 375–389.

[60] R. Jensen, *Viscosity solutions of hamilton–jacobi equations*, Arch. Rat. Mech. Anal. **101** (1988), 1–27.

[61] L. Jiang, and S. Pan, *On a non-local curve evolution problem in the plane*, Comm. in Analysis and Geometry, **16**(1) (2008), 1–26.

[62] J. Kačur, and K. Mikula, *Solution of nonlinear diffusion appearing in image smoothing and edge detection*, Applied Numer. Math. **17**(1) (1995), 47–59.

[63] M. Kass, A. Witkin, and D. Terzopulos, *Snakes: active contour models*, International Journal of Computer Vision **1** (1987), 321–331.

[64] S. Kichenassamy, A. Kumar, P. Olver, A. Tannenbaum, and A. Yezzi, *Conformal curvature flows: from phase transitions to active vision*, Arch. Rational Mech. Anal. **134**(3) (1996), 275–301.

[65] M. Kimura, *Accurate numerical scheme for the flow by curvature*, Applied Math. Lett. **7**(1) (1994), 69–73.

[66] M. Kimura, *Numerical analysis of moving boundary problems using the boundary tracking method*, Japan J. Indust. Appl. Math. **14**(3) (1997), 373–398.

[67] M. Kimura, D. Tagami, and S. Yazaki, *Polygonal Hele-Shaw problem with surface tension*, Interfaces and Free Boundaries **15**(1) (2013), 77–93.

[68] D. Kinderlehrer, and Ch. Liu, Ch., *Evolution of grain boundaries*, Math. Models Methods Appl. Sci., **11**(4) (2001), 713–729.

[69] V. Klement, T. Oberhuber, and D. Ševčovič *Application of the level-set model with constraints in image segmentation*, to appear in: Numerical Mathematics, Theory, Methods and Applications, 2016.

[70] M. Kolář, M. Beneš, D. Ševčovič, and J. Kratochvíl, *Mathematical model and computational studies of discrete dislocation dynamics*, IAENG International Journal of Applied Mathematics **45**(3) (2015), 198-207.

[71] M. Kolář, M. Beneš, and D. Ševčovič, *Computational studies of conserved mean curvature flow*, Mathematica Bohemica, **139**(4) (2014), 677-684.

[72] J. Kratochvíl, and R. Sedláček, *Statistical foundation of continuum dislocation plasticity*, Physical Review B **77** (2008), 134102.

[73] A. Lunardi, *Analyticity of the maximal solution of an abstract nonlinear parabolic equation*, Nonlinear Analysis **6**(5) (1982), 503–521.

[74] L. Ma, and A. Zhu, *On a length preserving curve flow*, Monatshefte für Mathematik **165**(1) (2012) 57–78.

[75] R. Malladi, J. Sethian, and B. Vemuri, *Shape modeling with front propagation: a level set approach*, IEEE Trans. Pattern Anal. Mach. Intell. **17** (1995), 158–174.

[76] C. Mantegazza, M. Novaga, and V.M. Tortorelli, *Motion by curvature of planar networks*, Ann. Sc. Norm. Super. Pisa Cl. Sci., **3**(2) (2004), 235–324.

[77] H. Matano, *Convergence of solutions of one-dimensional semilinear parabolic equations*, J. Math. Kyoto Univ., **18** (1978), 221–227.

[78] J. McCoy, *The surface area preserving mean curvature flow*, Asian J. Math. **7** (2003), 7-30.

[79] J. W. McLean, and H. J. Woerdeman, *Spectral Factorizations and Sums of Squares Representations via Semidefinite Programming*, SIAM. J. Matrix Anal. Appl. **23** (2001), 646–655.

[80] M. Meyer, M. Desbrun, P. Schroeder, and A. H. Barr, *Discrete differentialgeometry operators for triangulated 2–manifolds*, Visualization and Mathematics III (Hans-Christian Hege and Konrad Polthier, eds.) (2003), pp. 35-–57.

[81] A.S. Mikhailov, V.A. Davydov, and V.S. Zykov, *Complex dynamics of spiral waves and motion of curves*, Physica D: Nonlinear Phenomena, **70** (1994), 1-39.

[82] K. Mikula, *Solution of nonlinear curvature driven evolution of plane convex curves*, Applied Numer. Math. **23**(3) (1997), 347–360.

[83] K. Mikula, and J. Kačur, *Evolution of convex plane curves describing anisotropic motions of phase interfaces*, SIAM J. Sci. Comput. **17**(6) (1996), 1302–1327.

[84] K. Mikula, and D. Ševčovič, *Solution of nonlinearly curvature driven evolution of plane curves*, Applied Numer. Math. **31**(2) (1999), 191–207.

[85] K. Mikula, and D. Ševčovič, *Evolution of plane curves driven by a nonlinear function of curvature and anisotropy*, SIAM Journal on Applied Mathematics **61**(5) (2001), 1473–1501.

[86] K. Mikula, and D. Ševčovič, *A direct method for solving an anisotropic mean curvature flow of plane curves with an external force*, Math. Methods Appl. Sci. **27**(13) (2004), 1545–1565.

[87] K. Mikula, and D. Ševčovič, *Computational and qualitative aspects of evolution of curves driven by curvature and external force*, Comput. and Visualization in Science **6**(4) (2004), 211–225.

[88] K. Mikula, and D. Ševčovič, *Evolution of curves on a surface driven by the geodesic curvature and external force*, Applicable Analysis **85**(4) (2006), 345–362.

[89] K. Mikula, D. Ševčovič, M. Balažovjech, *A simple, fast and stabilized flowing finite volume method for solving general curve evolution equations*, Commun. Comput. Phys. **7**(1) (2010), 195-211.

[90] K. Mikula, and D. Ševčovič, *Tangentially stabilized Lagrangian algorithm for elastic curve evolution driven by intrinsic Laplacian of curvature*. In: Proceedings of Algoritmy 2005, 17th Conference on Scientific Computing, Vysoke Tatry, Podbanske, Slovakia, Eds. A.Handlovičová, Z. Krivá, K. Mikula, D. Ševčovič, (2005), pp. 32-41.

[91] K.Mikula, R.Spir, M.Smisek, E.Faure, N.Peyrieras, *Nonlinear PDE based numerical methods for cell tracking in zebrafish embryogenesis*, Applied Numerical Mathematics, **95** (2015), 250-266.

[92] K.Mikula, J.Urbán, *A new tangentially stabilized 3D curve evolution algorithm and its application in virtual colonoscopy*, Advances in Computational Mathematics, **40**(4) (2014), 819-837.

[93] L. Moissan, *Affine plane curve evolution: A fully consistent scheme*, IEEE Trans. Image Process. **7** (1998), 411–420.

[94] S. Morigi, *Geometric surface evolution with tangential contribution*, J. Comput. Appl. Math. **233** (2010), 1277-1287.

[95] W. W. Mullins, *Two-dimensional motion of idealized grain boundaries*, J. Appl. Phys., **27** (1956), 900–904.

[96] R. Nochetto, M. Paolini, and C. Verdi, *Sharp error analysis for curvature dependent evolving fronts*, Math. Models Methods Appl. Sci. **3**(6) (1993), 711–723.

[97] K. Osaki, H. Satoh, and S. Yazaki, *Towards modelling spiral motion of open plane curves*, Discrete and Continuous Dynamical Systems - Series S, **8**(5) 2015, 1009-1022.

[98] S. Osher, and R. Fedkiw, *Level set methods and dynamic implicit surfaces*, Applied Mathematical Sciences, vol. 153, Springer-Verlag, New York, 2003.

[99] S. Osher, and J. Sethian, *Fronts propagating with curvature-dependent speed: algorithms based on Hamilton-Jacobi formulations*, J. Comput. Phys. **79**(1) (1988), 12–49.

[100] A. Pazy, *Semigroups of linear operators and applications to partial differential equations*, Applied Mathematical Sciences, vol. 44, Springer-Verlag, New York, 1983.

[101] P. Pauš, and S. Yazaki, *Exact solution for dislocation bowing and a posteriori numerical technique for dislocation touching-splitting*, JSIAM Letters (to appear).

[102] M. Remešíková, K. Mikula, P. Sarkoci, and D. Ševčovič, *Manifold evolution with tangential redistribution of points, SIAM J. Sci. Comput.*, **36**(4) (2014), A1384-A1414.

[103] J. Rubinstein, and P. Sternberg, *Nonlocal reaction-diffusion equation and nucleation*, IMA J. Appl. Math. **48** (1992), 249-264.

[104] K. Sakakibara and S. Yazaki, *Structure-preserving numerical scheme for the one-phase Hele-Shaw problems by the method of fundamental solutions*, submitted, 2015.

[105] A. Sarti, K. Mikula, and F. Sgallari, *Nonlinear multiscale analysis of three-dimensional echocardiographi sequences*, IEEE Trans. on Medical Imaging **18** (1999), 453–466.

[106] G. Sapiro, and A. Tannenbaum, *On affine plane curve evolution*, J. Funct. Anal. **119**(1) (1994) 79–120.

[107] G. Sapiro, *Geometric partial differential equations and image analysis*, Cambridge University Press, Cambridge, 2001.

[108] J. F. Sturm, Using SeDuMi 1.02, *A Matlab toolbox for optimization over symmetric cones*, Optimization Methods and Software, **11** (1999), 625–653.

[109] D. Ševčovič, and S.Yazaki, *Evolution of plane curves with a curvature adjusted tangential velocity*, Japan J. Indust. Appl. Math., **28**(3) (2011), 413-442.

[110] D. Ševčovič, and S.Yazaki, *Computational and qualitative aspects of motion of plane curves with a curvature adjusted tangential velocity*, Mathematical Methods in the Applied Sciences, **35**(15) (2012), 1784-1798.

[111] D. Ševčovič, and M. Trnovská, *Solution to the Inverse Wulff Problem by Means of the Enhanced Semidefinite Relaxation Method*, Journal of Inverse and III-posed Problems, **23**(3) (2015), 263-285.

[112] D. Ševčovič, and M. Trnovská, *Application of the Enhanced Semidefinite Relaxation Method to Construction of the Optimal Anisotropy Function*, IAENG International Journal of Applied Mathematics **45**(3) (2015), 227-234.

[113] D. Ševčovič, *Qualitative and quantitative aspects of curvature driven flows of planar curves*. In: Topics on partial differential equations, Jindrich Necas Center for Mathematical Modeling Lecture notes, Vol. 2, MatFyzPress 2007, 55-119. ISBN:978-80-7378-005-0.

[114] D. Ševčovič, and S.Yazaki, *On a gradient flow of plane curves minimizing the anisoperimetric ratio*, IAENG International Journal of Applied Mathematics, **43**(3) 2013, 160-171.

[115] J. A. Sethian, *Numerical algorithms for propagating interfaces: Hamilton-Jacobi equations and conservation laws*, J. Differential Geometry **31**(1) (1990), 131–161.

[116] J. Sethian, *Level set methods*, Cambridge Monographs on Applied and Computational Mathematics, vol. 3, Cambridge University Press, Cambridge, 1996, Evolving interfaces in geometry, fluid mechanics, computer vision and materials science.

[117] J. Sethian, *Adaptive fast marching and level set methods for propagating interfaces*, Acta Math. Univ. Comenian. **67**(1) (1998), 3–15.

[118] V. Srikrishnan, S. Chaudhuri, and S. Dutta Roy, *Stabilisation of active contours using tangential evolution: An application to tracking*, Proceedings of International Conference on Computing: Theory and Applications (ICCTA'07) (2007), 660–664.

[119] V. Srikrishnan, S. Chaudhuri, S. Dutta Roy, and D. Ševčovič, *On stabilisation of parametric active contours*, In: Computer Vision and Pattern Recognition, 2007. CVPR '07. IEEE Conference on Computer Vision and Pattern Recognition (2007), 1–6.

[120] K. Arenhold, S. Surnev, P. Coenen, H.P. Bonzel, and P. Wynblatt, *Scanning tunneling microscopy of equilibrium crystal shape of Pb particles: test of universality*, Surface Science **417** (1998), L1160-L1165.

[121] M. Trnovská, and D. Ševčovič, *Enhanced semidefinite relaxation method with application to optimal anisotropy function construction*, in: Proceedings of the 4th International Symposium & 26th National Conference on Operational Research, June 4-6, 2015, Chania, Greece, M. Doumpos, E. Grigoroudis Eds., 241-245.

[122] T. Ushijima, and S. Yazaki, *Convergence of a crystalline algorithm for the motion of a closed convex curve by a power of curvature $V = K^\alpha$*, SIAM J. Numer. Anal. **37**(2) (2000), 500–522.

[123] G. Wulff, *Zür Frage der Geschwindigkeit des Wachstums und der Auflösung der Kristallfläschen*, Zeitschrift für Kristallographie, **34** (1901), 449–530.

[124] S. Yazaki, *On the tangential velocity arising in a crystalline approximation of evolving plane curves*, Kybernetika, **43**(6) (2007), 913–918.

[125] S. Yazaki, *A numerical scheme for the Hele-Shaw ow with a time-dependent gap by a curvature adjusted method*, Nonlinear Dynamics in Partial Differential Equations, Adv. Stud. Pure Math., **64**, Math. Soc. Japan, Tokyo (2015), 253-261.

[126] C. Zanella, M. Campana, B. Rizzi, C. Melani, G. Sanguinetti, P. Bourgine, K. Mikula, N. Peyrieras, A. Sarti, *Cells Segmentation from 3-D Confocal Images of Early Zebrafish Embryogenesis*, IEEE Transactions on Image Processing, **19** (2010), 770-781.

[127] T. J. Zelenyak, *Stabilization of solutions of boundary value problems for a second order parabolic equation with one space variable*, Differential Equations **4** (1968), 17–22.

About the author

The author of this survey paper is working in the field of applications of partial differential equations in mathematical theory of finance, differential geometry and other applied fields. He published more than seventy scientific papers, has written five books and monographs in the field of applications of differential equations in financial mathematics.

He graduated from Comenius University in 1993. In 2001 he defended habilitation thesis and in 2011 he was appointed full professorship from Comenius University, Bratislava, in the field of Mathematics. He enrolled several long invited stays and visiting professorships at Hitotsubashi University, Tokyo, Charles University in Prague, Czech Technical University in Prague, Masaryk University in Brno, Technical University of Budapest, Vienna Technical University, University of Lisbon, University of La Coruna where he lectured on modern analytical and numerical methods of financial mathematics and methods of solving nonlinear parabolic equations. Currently, he is collaborating with research groups in Czech Technical University (prof. M. Beneš), Slovak Technical University (prof. K. Mikula), University of Regensburg (prof. H. Garcke), Meiji University Tokyo (prof. S. Yazaki), Hitotsubashi University Tokyo (prof. N. Ishimura), University of Lisbon (prof. M. Grossinho), University Woolongong Australia (prof. S.P. Zhu), University of Wuppertal (prof. M. Ehrhardt) and others.

iris-knihy.sk
ISBN 978-80-89726-75-2